# CONSIDERATION FOR SALT MARSH RESTORATION DESIGN IN A HYPERTIDAL ESTUARY

by

Jennifer Graham

A Thesis Submitted to Saint Mary's University, Halifax, Nova Scotia,
in Partial Fulfillment of the Requirements for the
Degree of Master of Science in Applied Science

November 28, 2012, Halifax, Nova Scotia



| | |
|---|---|
| Approved: | Dr. Danika van Proosdij<br>Supervisor<br>Department of Geography |
| Approved: | Dr. David Lieske<br>External Examiner<br>Department of Geography & Environment<br>Mount Allison University |
| Approved: | Dr. Tony Bowron<br>Supervisory Committee Member<br>CB Wetlands and Environmental Specialist |
| Approved: | Dr. Jeremy Lundholm<br>Supervisory Committee Member<br>Department of Biology &<br>Environmental Science |
| Approved: | Dr. Cristian Suteanu<br>Supervisory Committee Member<br>Department of Geography &<br>Environmental Science |
| Approved: | Dr. Hai Wang<br>Graduate Studies Representative |
| Date: | November 28, 2012 |

**Abstract**

**Considerations for Salt Marsh Restoration Design in a Hypertidal Estuary**

By Jennifer Graham

Salt marshes around the world have been seriously impacted by human activities and are in need of restoration more than ever in our changing climate. However, successful restoration requires a better understanding of these systems than available in our region at present. To this end ground surveys and digital terrain data were used to conduct a morphometric analysis of representative tidal channels in the Avon Estuary. Channel morphology was strongly related freshwater discharge and channel order while drainage density, channel length, and sinuosity were related to site history and maturity. Hydraulic geometry exponents were established and used in conjunction with low-altitude photography and survey data to assess channel development at the Cogmagun Salt Marsh Restoration. Although developing on an acceptable trajectory the excavation of a single breach and channel at this site has had a significant effect on site development, and should be taken into consideration in future projects.

November 28, 2012

**Acknowledgements**

I would first like to thank my supervisor Danika van Proosdij and my committee for their excellent guidance in completing this manuscript. I would also like to thank Tony Bowron and Nancy Neatt (CBWES Inc.) and Bob Pett (NSTIR) whose encouragement, support and guidance were key in getting this project off the ground and completed. This project would not have been possible without my class mates Ben Lemieux, Mike Fedak, Casey O'laughlin and many others who came out and got muddy or helped in the lab. Last but not least I would like to thank my friends and family who listened when I needed an ear and provided support and help of all kinds. Thanks everyone!

## Contents

***List of Tables***

**List of Figures**

**Glossary of Symbols, Terms and Formulas**

| | |
|---|---|
| $H_b$ | **Bankfull Elevation (m):** The elevation at which a channel is filled to the top of its banks and at a point where the water begins to overflow onto a floodplain (Leopold et al. 1964). |
| $R_b$ | **Bifurcation Ratio:** Number of stream segments in a given order divided by the number of segments in the next highest order. |
| $L_{tot}$ ; $L_{tide}$; $L_{seg}$ | **Channel Length (m):** $L_{seg}$ is the channel meander length (length along thalweg) of a single channel segment. For $L_{tot}$ all channel segments upstream of a given cross-section (including upland segments) were summed, while for $L_{tide}$ only upstream channel segments lying within the tidal basin below the elevation of HHWLT were used. |
| | **Channel Segment:** A section of a channel network occurring between junctions. |
| $w$ | **Channel Width (m) :** the width of the channel at bankfull elevation. |
| $Q$ | **Characteristic Discharge ($m^3/s$):** volume rate of water flow through a given cross-sectional area |
| $A$ | **Cross-sectional Area ($m^2$):** Cross-sectional area of a channel between the channel bed and the water surface at bankfull elevation. Calculated using a modified trapezoid rule where $A$ = sum of trapezoid areas between *bankfull* elevation and bed elevation between each sample point. |
| $r^2$ | **Coefficient of determination:** Describes how well a regression line fits a set of data. Values approaching 1 indicate that a regression line fits the data well and is the square of the correlation coefficient. |
| $D_{tide}$ | **Contributing Marsh Area; Tidal Drainage Area ($m^2$):** The area lying within the tidal floodplain below the elevation of HHWLT that drains all tidal waters, precipitation received as a runoff or base flow (groundwater sources) into a particular channel. |
| $D_{tot}$ | **Drainage Area ($m^2$):** The area that drains all precipitation received as a runoff or base flow (groundwater sources) into a particular channel. |
| $Dd$ | **Drainage Density ($m/m^2$):** $L_{tide}/D_{tide}$ The ratio of total stream length to drainage area. Only channel segments and drainage area lying within the tidal basin below the elevation of HHWLT were used for this calculation. |

**Hydraulic Geometry:** Describes how at-a-station channel form adjusts to changes in discharge using the equations: $w = aQ^b$, $d = cQ^f$ and $v=kQ^m$, where $Q$ is characteristic discharge, $v$ is characteristic velocity, $w$ is channel width and $d$ is mean depth. By continuity of flow the sum of the exponents (*b, f,* and *m)* as well as the constants (*a,c*, and *k*) is equal to 1 (Leopold and Maddock, 1953). In tidal systems the spring tidal prism (*TP*) can be used as a surrogate for discharge. (Myrick & Leopold, 1963)

$R_h$ **Hydraulic Radius: $A/P_w$. C**hannel cross-sectional area divided by its wetted perimeter. $R_h$ is a measure of channel flow efficiency. Higher values for hydraulic radius indicate a greater cross-sectional area in comparison to the wetted perimeter resulting in decreased friction along the channel bed and higher velocities (Ritter, 2012).

***D*** **Maximum Depth (m):** Depth below bankfull elevation at the deepest point (thalweg) in a channel cross-section.

***d*** **Mean Depth (m):** Average depth below bankfull elevation for a channel cross-section along its bankfull width.

***s*** **Mean Channel Slope (%):** Mean change in bed elevation over a given distance of a channel segment along its thalweg.

**HHWMT** **Higher High Water Mean Tide (5.77 m CGVD28):** The average of all of the higher high water from 19 years of prediction. Geodetic elevation calculated for Hantsport by van Proosdij and Baker (2009) from Canadian hydrographic Service (CHS) Chart 4140, 1982.

**HHWLT** **Higher High Water Large Tide (7.57 m CGVD28):** The average of the highest annual predicted high water from 19 years of prediction. Geodetic elevation calculated for Hantsport by van Proosdij and Baker (2009) from Canadian hydrographic Service (CHS) Chart 4140, 1982.

***O*** **Modified Strahler Stream Order:** A method of numbering streams as part of a drainage basin network. In the traditional framework stream segments are assigned values (ie., 1st order, 2nd order, etc) with the smallest headward segments having the lowest value and order increasing where two segments of the same order meet (Horton, 1945; Strahler, 1952). In the modified method the ordering is reversed, so that the largest seaward channels are assigned lowest order values (see Figure 2-3 in Chapter 2).

| | |
|---|---|
| ***rms*** | **Residual mean square:** a measure of how well a regression line fits the actual data points, where large *rms* values indicate poor fit. |
| ***n*** | **Sample Size** |
| $R_s$ | **Sinuosity ($L_{seg}$/*straight-path distance*):** Channel meander length (length along thalweg) divided by the straight-path distance between segment end points. |
| ***t*** | **Thalweg:** A line drawn joining the lowest points along the entire length of a stream bed and defining its deepest channel. |
| ***TP*** | **Tidal Prism ($m^3$): $tp_b + D_{tide}*(H_t - H_b)$.** Volume of water entering and leaving an estuary or channel during one tidal cycle. To calculate *TP t*he *bankfull tidal prism* (see $tp_b$) is calculated and additional volume added based on tide height. For tide heights ($H_t$) greater than the bankfull elevation the upstream tidal drainage area was used to calculated additional volumes ($D_{tide}*(H_t - H_b)$) and added to $tp_b$. |
| $tp_b$ | **Bankfull Tidal Prism ($m^3$): $\sum A*L_{seg}$.** Volume of water in the channel at bankfull elevation. The sum of the product of cross-sectional area and segment length for all segments upstream of a given cross-section. |
| $H_t$ | **Tide Height (m)** |
| ***v*** | **Velocity (m/s):** Speed at which water is moving in a channel |
| $P_w$ | **Wetted Perimeter (m):** Portion of the channel bed that is "wet" under bankfull conditions. |

## Chapter 1 - Considerations for Restoration Design in a Hypertidal Estuary:

## Introduction

As human populations and activities have increased around the globe tidal wetlands have been significantly impacted (Williams & Orr, 2002; Wolters et al., 2005; van Proosdij et al., 2010). These habitats provide many beneficial ecosystems services including valuable fish habitat, protection against storm surge and sea level rise, and carbon sequestration (Shenker & Dean,1979; Möller et al., 1999**;** Connor et al. 2001). As such, their restoration has become an important issue in many regions (Wolters et al., 2005; Wolanski, 2006). Restoration can occur passively or actively – meaning it can occur with or without human aid or interference. Passive restoration may occur when levees or dykes are no longer maintained and are breached by storm events, as when agricultural lands are abandoned (Crooks et al., 2002; Wolters et al., 2005) . Active restoration, on the other hand, may occur when coastal barriers are removed or replaced with the intent to restore or regulate tidal flooding (van Proosdij et al., 2010). Either scenario may lead to the successful establishment or recovery of tidal wetland functions; however project success is dependent on many factors.

Hydrology, elevation, sediment supply, the availability of a viable seed source, exposure, the presence of bioturbators, and tidal regime are among the most important site characteristics which will contribute to successful habitat recovery in tidal environments (Broome et al, 1988; Haltiner et al., 1997; Wolters et al., 2005). Due to the complex nature of tidal systems, active restoration is the preferred path but requires thorough planning and research to be successful. The presence of an efficient hydraulic network is recognized as a vital component of restoration

success and is often a key first step in project design (Mitsch & Gosselink, 2007; Williams and Orr, 2002; Hammersmark et al., 2005; Konisky et al., 2006). As such it is the primary focus of this research.

This chapter will first examine the development and morphology of salt marshes, with reference to the structures and processes controlling them. Particular attention will be paid to the development and characteristics of tidal creek networks. The purpose of the research conducted was twofold. First, to develop a better understanding of the hydraulic characteristics of salt marshes in a hypertidal environment where there are currently little data available, and secondly to assess the development of a restoration project carried out in 2009 in light of this new information. This analysis will help to improve restoration design approaches in the region and may have significant implications for other hyper or macro-tidal estuaries.

***Salt marsh biogeomorphology***

To effectively restore salt marshes we must understand how they develop, what characterizes them and what factors control their growth and behaviour. Salt marshes occur in the high intertidal zone and in temperate climates which are dominated by halophytic grasses, reeds, and succulents such as *Spartina sp., Juncus gerardii,* and *Salicornia sp.* (Broome et al., 1988; Masselink & Hughes, 2003). J.R.L Allen (2000) delivers a comprehensive review of salt marsh morphodynamics and development, largely in the European context but with examples drawn from North America as well. Based on the work of authors such as Chapman (1960) and Adam (1990) he describes the marsh as consisting of a "vegetated platform high in the tidal frame that is regularly flooded by the tide, and generally unconnected networks of tidal channels

that branch and diminish inland toward the interior of the marsh from its seaward edge." (p 1157).

J.R.L. Allen (2000) identifies the key external factors affecting the growth or decline of a salt marsh as sea-level, tidal regime and sediment supply while vital intrinsic characteristics include vegetation and sediment autocompaction. The interaction of external elements is particularly well articulated in Allen (1997), which details a conceptual model of salt marsh development. He proposes that an increase in hydraulic duty, determined by a change in tidal prism (eg. when sea level rises), leads to changes in channel morphology, increased flooding of the marsh surface and consequently increased deposition of entrained sediment. As the marsh surface elevation rises to meet high astronomical tide (HAT) hydraulic duty should decrease, channels begin to infill and the tidal channel network begins to simplify.

By this mechanism and others, such as vegetation decomposition which provides organic material to the marsh surface, the marsh grows or shrinks over time depending on its ability to keep pace with sea level rise. Allen (2000) states that "platform height relative to the tidal frame defines a cardinal geomorphic threshold in the functioning of an entire marsh" (p 1166). For example, platform elevation relative to tidal frame determines the number of tides resulting in over-marsh flooding and the length of inundation time (i.e. hydroperiod). While young marshes experience over-marsh flooding on roughly half of the tides in a given year, a mature marsh may be flooded on a significantly smaller number of tides (Allen, 2000). This influences characteristics such as pore water salinity, rate of panne recharge, and vegetation composition, survival and distribution.

Vegetation has been shown to play an important role in reducing velocities on the marsh surface thus aiding in sediment flocculation and deposition, particularly at the vegetation edge (Shi et al., 1996; Temmerman et al., 2005). However, additional research has shown that the impact of vegetation on deposition is both scale and species dependent, as stem density and patch size in a developing marsh may encourage re-entrainment of sediment and erosion of tidal channels (Leonard & Luther, 1995; Temmerman et al., 2007). The impact of vegetation may also be dependent on seasons, a conclusion supported by studies of macro-tidal salt marshes in the UK by Möller and Spencer (2002) where observed wave height attenuation was highest in September – November (end of growing season) and lowest in March – July (beginning of growing season). To further complicate matters, the impact of vegetation on flow velocities has been shown to differ under conditions where over-marsh flow water depth exceeds vegetation height (Temmerman et al. 2005; Davidson-Arnott et al., 2002). In short, vegetation will have less impact under spring tide conditions in a macro-tidal setting such as the Bay of Fundy, where water depth on the marsh may exceed two meters (van Proosdij et al., 2010).

***Development and morphometry of tidal channels***

Although the processes of marsh morphogenesis occur over very long time scales, it is generally believed that tidal creeks evolve over much shorter periods. Developing through a process of rapid early incision and progressing by headward growth, this theory is supported by conceptual models, mathematical and physical models, and field observations (Allen, 1997; Allen 2000; Fagherazzi & Sun, 2004; D'Alpaos et al., 2005; D'Alpaos et al., 2006; D'Alpaos et al., 2007; Stefanon et al., 2010). The incision of a creek network on prograding mud flats occurs prior to

vegetative colonization and is driven by water-surface gradients and related bottom shear stresses, with higher order creeks developing from “erosive zones” at meanders in the primary channel. Colonization of the marsh platform occurs once a suitable elevation has been reached, at which time the basic creek structure is “frozen” in place. The vegetatitive canopy may than accelerate vertical growth of the marsh surface as previously discussed. After this, geomorphic processes such as meandering, deepening and widening of channels will occur at a much slower pace and only to a minimal degree, leading to channels that are generally stable in the long term and in dynamic equilibrium with tidal prism in the short term.

The hydraulic network is generally characterized by tidal channels and creeks which are dendritic in plan form and contain both flow-through and dead-end channels (Zeff, 1999). In Britain seven network types have been identified (Figure 1.1) and researchers have noted that a “sequence from linear through linear-dendritic and dendritic to meandering-dendritic is often associated with increasing marsh maturity” (Allen, 2000, p.1170). Many restored marshes in the Bay are likely to develop “superimposed” networks (Figure 1-1) as relict agricultural ditches are incorporated into natural drainage ditches either re-activated by or developing in response to restored tidal flow.

The importance of ebb versus flood dominance as a control on tidal channel morphology should also be noted. Many of the techniques used to analyze tidal channels in the past several decades have been based on research initiated in freshwater systems. For example, creek geometry studies have frequently been based on hydraulic geometry (Leopold & Maddock, 1953) while morphometric studies are often studied based on the work of Horton (1945), who porposed the  laws of drainage composition which can be used to quantify the properties of a

stream network. These studies assume an ebb-dominated system that acts as a drainage network, meaning that morphological features are shaped by flows draining from the system following peak tide. Davidson-Arnott et al. (2002) found that a macro-tidal marsh in the Bay of Fundy was ebb-dominated with high velocity flows occuring on the retreating tide. Lawrence et al. (2004), on the other hand, found channels at a macro-tidal salt marsh in Norfolk, UK, to be flood-dominated as did van Proosdij et al. (2010) in a Bay of Fundy marsh. Because the relative force of ebb and flood flows is linked to tidal prism, channel size and position within the tidal frame and may vary at different locations in the same estuary, we should be cognoscente of the role of bi-directional flow in shaping channel networks.

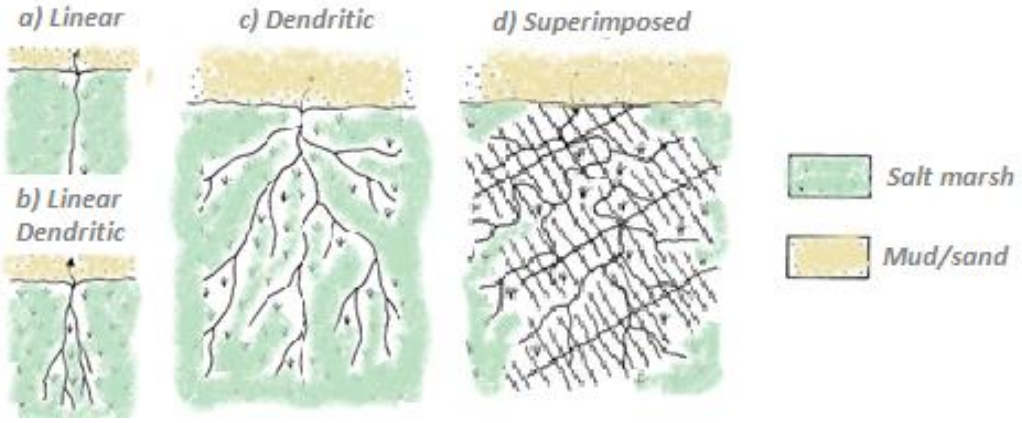


**Figure 1-1: A classification of tidal-creek networks in salt marshes. Modified from (Allen, 2000).**

***Regional Context***

In the Bay of Fundy the loss of salt marsh habitat has been estimated at 80-85% since European settlement, due largely to land reclamation and conversion to agricultural land

through dyking (Gordon, 1989; MacDonald et al., 2010). As an impetus for restoration, this loss alone is substantial and provides ample opportunity. However, we should note the role of wetland protection legislation in prompting restoration activities. At the federal level, wetlands are regulated by the 1996 "*Federal Policy on Wetland Conservation*", which advocates a 'no-net-loss' policy (Lynch-Stewart et al., 1996). Until recently salt marshes were protected as important fish habitat under section 35(1) of the Fisheries Act which states that "no person shall carry out any work or undertaking that results in the harmful alteration, disruption or destruction of fish habitat" (or HADD) (Fisheries Act, 2011). At the provincial level, a Wetland Alteration Approval is required from the Nova Scotia Department of Environment (2011) for any activity that may result in the alteration of a wetland or watercourse. Salt marshes are identified as wetlands of significance and heavily protected, and under these regulations impacted habitat must be compensated for, preferably through restoration activities on a like-for-like basis.

Although salt marsh restoration has been practiced and studied extensively in the Gulf of Maine, it is still in its infancy in Atlantic Canada and is a growing area of interest for multiple organizations (Konisky et al., 2006; Bowron et al., 2011; MacDonald et al., 2010). As land use practices and environmental regulations have evolved in Nova Scotia we have been presented with an opportunity to return tidal flow to some of these habitats. This has been pursued by several proponents, including (but not limited to) Nova Scotia Transportation and Infrastructure Renewal (NSTIR), NS Department of Agriculture, Department of Fisheries and Oceans, Ducks Unlimited, Saint Mary's University and CB Wetlands and Environmental Specialists (CBWES) Inc. (Bowron et al., 2010). CBWES Inc. has provided environmental monitoring services for eight restoration sites to date, with four of these sites occurring in the Bay of Fundy. Recently the scope of restoration services provided has been extended to include a site design phase at

several locations beyond the removal of the tidal barrier. The creation of multiple breaches, excavated channels and open water habitat at these locations has pointed to a need for greater understanding of the morphology and function of salt marshes in the region. The evolution of a restoration project carried out in on the Walton River highlighted the importance of adequate planning particularly well (Bowron et al., 2011). Although the site is developing along an acceptable trajectory rapid erosion of a primary channel initiated during earthworks in 2005 prompted a move towards more active approaches to restoration design. This project will provide critical information about the configuration, structure and dimensions of salt marsh channel networks in the Bay as well as GIS-based tools to improve the efficacy of future restoration efforts.

***Study Objectives and Thesis Structure***

The morphology of salt marsh channels in hypertidal environments is not well understood at present as limited research has been published for estuaries of this type. Tidal ranges frequently exceed 8 meters, resulting in great variability in flow patterns, water velocities, water depth, and tidal prism throughout the tidal cycle. This leads to different hydraulic characteristics than may be found in micro or meso tidal systems. Beyond the recognized need for regional data to be used in planning future restoration projects, the results presented here may be applied to other hypertidal systems across the globe.

The purpose of this research was to improve restoration design in the region and in other hyper or macro-tidal estuaries. To achieve this goal, the following objectives were pursued:

1) Determine morphometric characteristics and relationships for a set of intact salt marshes in the Bay of Fundy. This will initiate the establishment of a reference condition or baseline for the region.
2) Carry out an analysis of the hydraulic geometry of tidal channels by determining morphometric characteristics and relationships for a set of intact salt marshes in the Bay of Fundy.
3) Create custom tools and a restoration design model for use in future work by CBWES Inc. (industrial research partners)
4) Evaluate the development of a restoration project carried out in 2009 by CBWES Inc. on the Cogmagun River using ground surveys, low-altitude photography, and monitoring data.
5) Determine if, given the data collected and analysed for objective (1), the Cogmagun site on an acceptable restoration trajectory or should a different approach have been used.

Chapters 2 and 3 are written as standalone manuscripts formatted for publication. Chapter 2 will address the objectives (1) and (2), while Chapter 3 will address (4) and (5). Objective (3) will be addressed briefly in both chapters, however details of the tools are not published in either paper and can be found in Appendix A.

## *References*


Adam, P. (1990). *Saltmarsh ecology.* Cambridge: Cambridge University Press.

Allen, J. R. L. (1997). Simulation models of salt-marsh morphodynamics: some implications for high-intertidal sediment couplets related to sea-level change. *Sedimentary Geology 113*, 21 l-223.

Allen, J. R. L. (2000). Morphodynamics of Holocene salt marshes: a review sketch from the Atlantic and Southern North Sea coasts of Europe. *Quaternary Science Reviews 19*, 1155-1231.

Bowron, T., Neatt, N., van Proosdij, D., Lundholm, J., & Graham, J. (2011). Macro-tidal Salt Marsh Ecosystem Response to Culvert Expansion. *Restoration Ecology 19:3*, DOI: 10.1111/j.1526-100X.2009.00602.x.

Broome, S. W., Seneca, E. D., & Woodhouse, W. J. (1988). Tidal saltmarsh restoration. *Aquatic Botan y32*, 1-22.

Chapman, V. J. (1960). *Salt Marshes and Salt Deserts of the World.* London: Leonard Hill.

Connor, R. F., Chmura, G. L., & Beecher, B. (2001). Carbon accumulation in Bay of Fundy salt marhes: Implications for restoration of reclaimed marhes. *Global biogeochemical cycles 0*, 1-12.

Crooks, S., Schutten, J., Sheern, G. D., Pye, K., & Davy, A. J. (2002). Drainage and Elevation as Factors in the Restoration of Salt Marsh in Britain. *Restoration Ecology 10:3*, 591–602.

D'Alpaos, A., Lanzoni, S., Marani, M., & Fagherazzi, S. (2005). Tidal network ontogeny: Channel initiation and early development. *Journal of Geophysical Research 110*, doi:10.1029/2004JF000182.

D'alpaos, A., Lanzoni, S., Mudd, S. M., & Fagherazzi, S. (2006). Modeling the influence of hydroperiod and vegetation on the cross-sectional formation of tidal channels. *Estuarine, Coastal and Shelf Science 69*, 311-324.

D'Alpaos, A., Lanzoni, S., Marani, M., Bonometto, A., Cecconi, G., & Rinaldo, A. (2007). Spontaneous tidal network formation within a constructed salt marsh: Observations and morphodynamic modelling. *Geomorphology 91*, 186–197.

Davidson-Arnott, R. G., van Proosdij, D., Ollerhead, J., & Schostak, L. (2002). Hydrodynamics and sedimentation in salt marshes: examples from a macrotidal marsh, Bay of Fundy. *Geomorphology 48*, 209–231.

Fagherazzi, S., & Sun, T. (2004). A stochastic model for the formation of channel networks in tidal marshes. *Geophysical Research Letters 31*, doi:10.1029/2004GL020965.

Fisheries Act. (2011). Canada: Minister of Justice.

Gordon, D. C. (1989). Habitat loss in the Gulf of Maine. *Sustaining our common heritage. Proceedings of the Gulf of Maine Conference.* (pp. 106–119). Portland, Maine: Gulf of Maine Council on the Marine Environment.

Haltiner, J., Zedler, J. B., Boyer, K. E., Williams, G. D., & Callaway, J. C. (1997). Influence of physical processes on the design, functioning and evolution of restored tidal wetlands in California (USA). *Wetlands Ecology and Management 4:2*, 73-91.

Hammersmark, C. T., Fleenor, W. E., & Schladow, S. G. (2005). Simulation of flood impact and habitat extent for a tidal freshwater marsh restoration. *Ecological Engineering 25* , 137–152.

Horton, R. (1945). Erosional development of streams and their drainage basins: hydrophysical approach to quantitative morphology. *Bulletin of the Geological Society of America 56*, 275– 370.

Konisky, R., Burdick, D. M., Dionne, M., & Neckles, H. A. (2006). A regional assessment of salt marsh restoration and monitoring in the Gulf of Maine. *Restoration Ecology 14:4*, 516–525.

Lawrence, D. S., Allen, J. R., & Havelock, G. M. (2004). Salt marsh morphodynamics: an investigation of tidal flows and marsh channel equilibrium. *Journal of Coastal Research 20:1*, 301-316.

Leonard, L. A., & Luther, M. E. (1995). Flow hydrodynamics in tidal marsh canopies. *Limnol. Oceanogr., 40(8)*, 1474-1484.

Leopold, L. B., & Maddock, T. J. (1953). Hydraulic geometry of stream channels and some physiographic implications. *U. S. Geological Survey Professional Paper 252*, 55 p.

Lohani, B., & Mason, D. C. (2001). Application of airborne scanning laser altimetry to the study of tidal channel morphometry. *ISPRS Journal of Photogrammetry & Remote Sensing 56*, 100– 120.

Lynch-Stewart, P., Neice, P., Rubec, C., & Kessel-Taylor, I. (1996). *The federal policy on wetland conservation: Implenetation guide for federal land managers.* Ottawa, Ontario: Wildlife Conservation Branch, Canadian Wildlife Service, Environment Canada.

MacDonald, G. K., Noel, P. E., van Proosdij, D., & Chmura, G. L. (2010). The Legacy of Agricultural Reclamation on Channel and Pool Networks of Bay of Fundy Salt Marshes. *Estuaries and Coasts 33*, 151–160. DOI 10.1007/s12237-009-9222-4.

Masselink, G., & Hughes, M. G. (2003). *Introduction to Coastal Processes and Geomorphology.* London: Hodder Arnold.

Mitsch, W. J., & Gosselink, J. G. (2007). *Wetlands, fourth ed.* New York, NY, USA.: John Wiley& Sons.

Möller, I., & Spencer, T. (2002). Wave dissipation over macro-tidal saltmarshes: Effects of marsh edge typology and vegetation change. *Journal of Coastal Research, Special Issue 36*, 506-521.

Möller, I., Spencer, T., French, J. R., Leggett, D. J., & Dixon, M. D. (1999). Wave Transformation Over Salt Marshes: A Field and Numerical Modelling Study from North Norfolk, England. *Estuarine, Coastal and Shelf Science 49:3*, 411-426.

Nova Scotia Environment. (2011). *Wetland Alteration Approval*. Retrieved 2 15, 2011, from Nova Scotia Environment : http://www.gov.ns.ca/snsmr/paal/nse/paal586.asp

Shenker, J. M., & Dean, J. M. (1979). The Utilization of an Intertidal Salt Marsh Creek by Larval and Juvenile Fishes: Abundance, Diversity and Temporal Variation. *Estuaries 2:3*, 154-163.

Shi, Z., Pethick, J. S., Burd, F., & Murphy, B. (1996). Velocity profiles in a salt marsh canopy. *Geo-Marine Letters 16*, 319-323.

Stefanon, L., Carniello, L., D'Alpaos, A., & Lanzoni, S. (2010). Experimental analysis of tidal network growth and development. *Continental Shelf Research 30*, 950–962.

Temmerman, S., Bouma, T. J., Govers, G., Wang, Z. B., De Vries, M. B., & Herman, P. M. (2005). Impact of vegetation on flow routing and sedimentation patterns: Three-dimensional modeling for a tidal marsh. *Journal of Geophysical Research, 110*, F04019, doi:10.1029/2005JF000301.

Temmerman, S., Bouma, T. J., Van de Koppel, J., Van der Wal, D., De Vries, M. B., & Herman, P. M. (2007). Vegetation causes channel erosion in a tidal landscape. *Geology, 35*, 631-634. doi: 10.1130/G23502A.1.

van Proosdij, D., Lundholm, J., Neatt, N., Bowron, T., & Graham, J. (2010). Ecological re-engineering of a freshwater impoundment for salt marsh restoration in a hypertidal system. *Ecological Engineering 36*, 1314–1332.

Williams, P. B., & Orr, M. K. (2002). Physical evolution of restored levee salt marshes in the San Francisco Bay Estuary. *Restoration Ecology 10:3*, 527–542.

Wolanski, E. (2006). The evolution time scale of macro-tidal estuaries: Examples from the Pacific Rim. *Estuarine, Coastal and Shelf Science 66*, 544 - 549.

Wolters, M., Bakker, J. P., Bertness, M. D., Jeffries, R. L., & Möller, I. (2005). Salt marsh erosion and restoration in south east England: squeezing the evidence requires realignment. *Journal of Applied Ecology 42*, 844–851.

Zeff, M. L. (1999). Salt marsh tidal channel morphometry: Applications for wetland creation and restoration. *Restoration Ecology 7:2*, 205-211.

# Chapter 2 - An analysis of hyper-tidal salt marsh hydraulic characteristics at varying positions in the tidal frame

*To be submitted to: Estuarine and Coastal Shelf Science*

***Introduction***

Tidal wetlands provide many beneficial ecosystems services including valuable fish habitat, protection against storm surge and sea level rise, and carbon sequestration (Shenker & Dean, 1979; Möller et al., 1999**;** Connor et al., 2001). Human activities have led to degradation and loss of these habitats, particularly in macro-tidal (4-8 meter tidal range) and hypertidal (>8 meter tidal range) environments. In these areas the loss of salt marsh has been even more acute, largely due to the practice of land reclamation through dyking (e.g. Weishar et al., 1997; Wolters et al., 2005a; French, 2008; van Proosdij et al., 2010). Rising sea levels and a host of other environmental concerns such as declining fish stocks has led to a widespread interest in the restoration of these important habitats.

Although there are many factors which play an important role in restoration success, hydrology is commonly recognized as a vital component and is often a key first step in project design (Mitsch & Gosselink, 2007; Williams & Orr, 2002; Hammersmark et al., 2005; Konisky et al., 2006). In a survey of passively restored marshes in the UK under a macrotidal regime Crooks et al. (2002) found that vegetation communities did not differ significantly from mature marshes within a century of restoration, provided an effective hydraulic network was able to evolve. Moreover, poorly planned or inefficient networks may lead to degradation of the system through excessive erosion or inefficient drainage (Weisher et al., 2005).

There is a significant body of work regarding the development, morphology and function of hydraulic networks in tidal marshes. Although salt marshes develop over very long time periods, channels normally form rapidly through early incision and expand by headward growth. They are generally stable in the long term and maintain a dynamic equilibrium with the tidal

prism (Allen, 1997; Allen, 2000; Fagherazzi & Sun, 2004; D'Alpaos et al., 2005; D'Alpaos et al., 2006; D'Alpaos et al., 2007; Stefanon et al., 2010). Many studies of tidal hydraulic networks are based on the well-established framework generated by Horton (1945) for freshwater systems. Cross-section geometry (mean channel width, depth, etc), order, sinuosity, drainage density, bifurcation ratio's and hydraulic geometry equations are parameters frequently quantified in this type of analysis. Published values can vary considerably dependent on factors such as tidal regime, sediment supply and exposure (Zeff, 1999; Allen, 2000; Lohani & Mason, 2001; Teal & Weishar, 2005; Weisher et al., 2005; Bowron et al., 2011; Macdonald et al., 2010; van Proosdij et al., 2006). Because these characteristics play an important role in the health and long term sustainibility of a salt marsh, most restoration practitioners recognize the importance of constructed or restored marshes that are comparable to natural marshes (Zeff, 1999).

Currently the morphology of hypertidal creeks is not well understood due to a lack of published studies carried out in these unique systems. With tidal ranges exceeding eight meters the tidal prism for these systems can vary dramatically from neap to spring tides, leading to a greater variability in flow patterns, water velocities, and water depth than are found in meso or micro tidal settings. The purpose of this study was to develop a better understanding of the hydraulic characteristics of hypertidal salt marshes. This will help to improve restoration design in the study region and in other hypertidal systems. Analysis of tidal channel morphology and hydraulic geometry were carried out for four marshes in the Upper Bay of Fundy and the results presented below.

***Study Area***

The Upper Bay of Fundy is a hypertidal estuary with semi-diurnal tides with a range of 6 to 16 m, and during spring tides water depth on the marsh may exceed 2 m (van Proosdij et al., 2010). The Bay has high suspended sediment loads, with variations in sedimentation dictated by seasonal and spatial patterns. Ice coverage during winter months also plays a significant role in vegetation distribution and sedimentation as ice blocks and winter storms may shear off vegetation or protect it (Chmura et al., 2001; Davidson-Arnott et al., 2002; van Proosdij et al., 2006b; van Proosdij & Townsend, 2006). The loss of salt marsh habitat in the Bay has been estimated at 80-85% since European settlement, due largely to land reclamation and conversion to agricultural land through dyking (Gordon 1989; MacDonald et al. 2010). Land use practices and environmental regulations have changed in Nova Scotia and New Brunswick leading to increased opportunities for restoration.

In Nova Scotia several restoration projects have now been completed within the Avon River estuary in the Minas Basin (Figure 2-1), making the Avon an excellent region for further study. Four salt marshes containing fourteen independent channel networks of varying complexity were selected within the Avon and its tributaries as representative sites (Figure 2-1 and Figure 2-2). They were selected based on accessibility, location in the tidal frame (both high and low), historical use, ecological integrity and maturity. Due to the agricultural history of the area and the development of considerable infrastructure there are few salt marshes in pristine condition. Researchers in the region have recognized the prevalence of a hybrid network fitting Allen's (2000) "superimposed" classification (Bowron et al., 2010; MacDonald et al., 2010) whereby relict agricultural ditches are incorporated into natural drainage ditches either re-

activated by or developed in response to restored tidal flow. For restoration purposes the inclusion of some marshes with these relict agricultural features is desirable as they are likely to be present at restored sites, however care was taken to exclude sites with intact functioning dykes.

Ecological integrity was assessed through examination of aerial photography, LiDAR, and site visits. The presence of healthy halophytic vegetation, pannes or pools, birds, fish and efficient hydraulic networks were considered indicators of functioning marsh system. Relative maturity was assessed in a similar manner, based on platform elevation relative to geodetic datum, vegetation community (extent of high marsh and dominant species), and site history. As marshes mature surface elevation rises to meet high astronomical tide, causing a decrease in hydraulic duty and producing simplified tidal channel networks (Allen, 2000). Increased platform elevation also results in reduced hydroperiod, decreased pore water salinity, and changes in vegetation communities. In the Bay of Fundy *Spartina alterniflora* is the dominant low marsh species due to its ability to withstand frequent inundation and high salinity conditions encountered at lower elevations. The dominant high marsh species is *Spartina patens,* with *Juncus gerardii* also becoming a dominant species in very mature marshes (Bertness. 1991). Site history was determined using aerial photography, historical records, and consultation with researchers and professionals familiar with the area. Ranked from youngest to most mature, the following four marshes were felt to best represent the varying conditions encountered in the study region. Marshes A-D are described below and site characteristics summarized in Table 2-1.

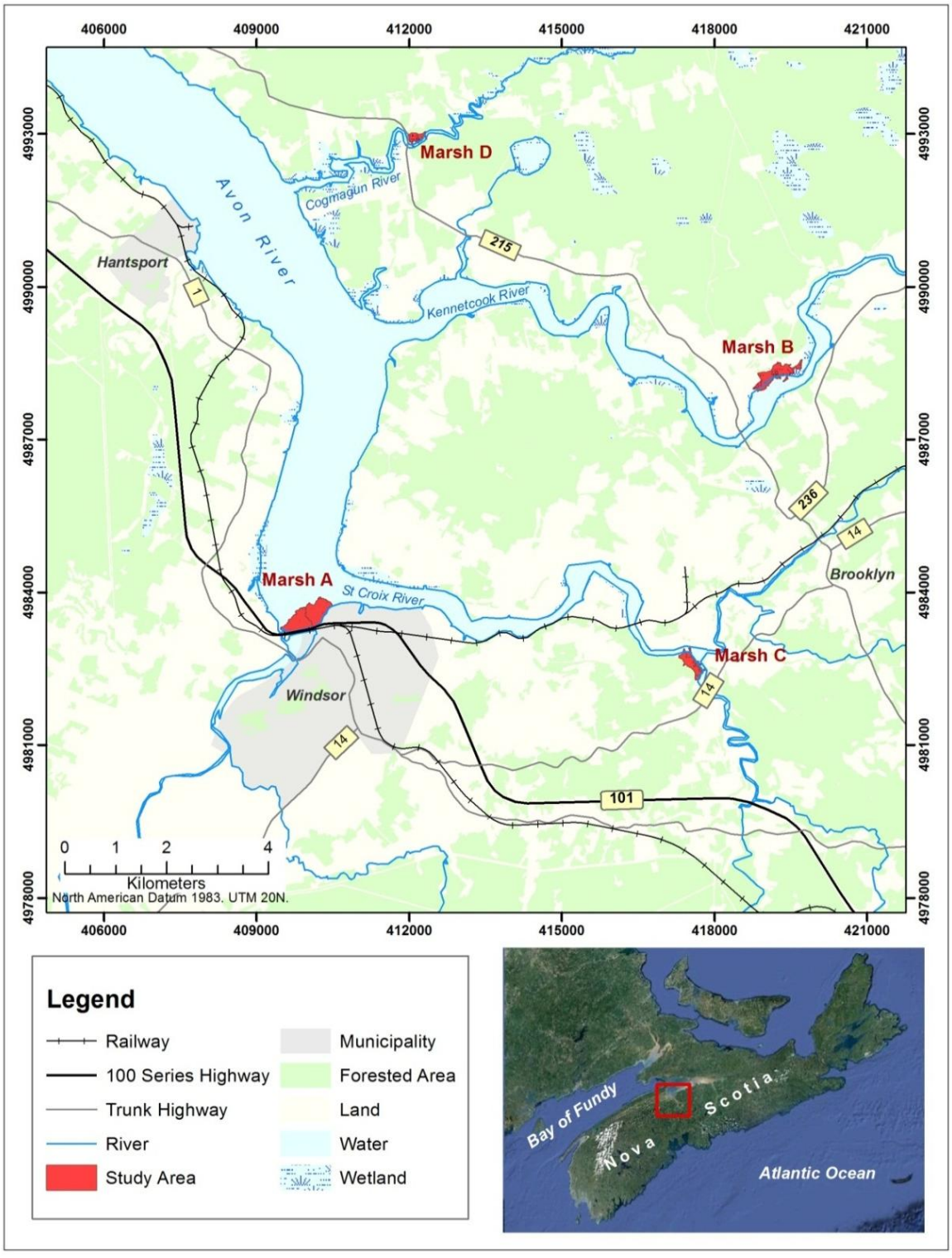


**Figure 2-1: Location of Study sites along the Avon River and tributaries, Nova Scotia**

A) *Marsh A* is located lowest in the tidal frame and has developed adjacent to the Windsor causeway which was completed in 1970. In addition to being the youngest marsh it is also most exposed and the largest. The site is dominated by the low marsh species *Spartina alterniflora*, which was first observed to colonize the mudflat in the early 1980's and had covered nearly the entire mudflat surface by 2005 (van Proosdij et al., 2006). The drainage network here can be classified as dendritic (Allen, 2000) and is the only site with no agricultural history. There is also no significant freshwater input to the tidal channels here. Profiles were taken from two dendritic creek networks at this site.

B) *Marsh B,* located on the Kennetcook River and high in the tidal frame, is a relatively mature marsh with an extensive low marsh zone dominated by *Spartina alterniflora* and a high marsh zone dominated by *Spartina patens*. While the marsh is adjacent to a section of marsh dyked and incorporated by the Nova Scotia Department of Agriculture (NSDA) the networks mapped were not dyked, nor is there any visible evidence of remnant dykes on the site. Three creek networks were surveyed at this site, two of which appeared to receive significant freshwater input from the upland and all of which were classified as superimposed networks (Allen, 2000).

C) *Marsh C,* located on the St. Croix River and high in the tidal frame, has a mostly dendritic drainage network with one relict agricultural ditch on the south-east margin of the site. Dominated by the high marsh species *Spartina patens,* the low marsh zone at the site is not extensive. Although a remnant dyke is present on this

site it pre-dates those constructed by the Nova Scotia Department of Agriculture (NSDA) in the 1940's and the marshbody has never been incorporated. The site is still used as a seasonal pasture, and as such is subject to grazing pressure. Four creek networks were surveyed at this site, one of which appeared to receive significant freshwater input from the upland.

D) *Marsh D* is located on the Cogmagun River high in the tidal frame and is the most mature marsh in the dataset. Although the smallest site it has the highest platform elevation and is dominated by the high marsh species *Juncus gerardii*. Like Marsh B there is some evidence of historical agricultural activities at this site, however the marshbody has never been incorporated and NSDA has not constructed or maintained dykes at this site. The drainage network most resembles the superimposed model, indicating agricultural ditching may have been present in the past. A distinct berm is present at the marsh edge but it is unclear if this is a natural feature, as decreased flooding has led to increased deposition at the margin, or if a dyke was present prior to the 1940's. Of the three networks surveyed here none appeared to receive significant freshwater input.

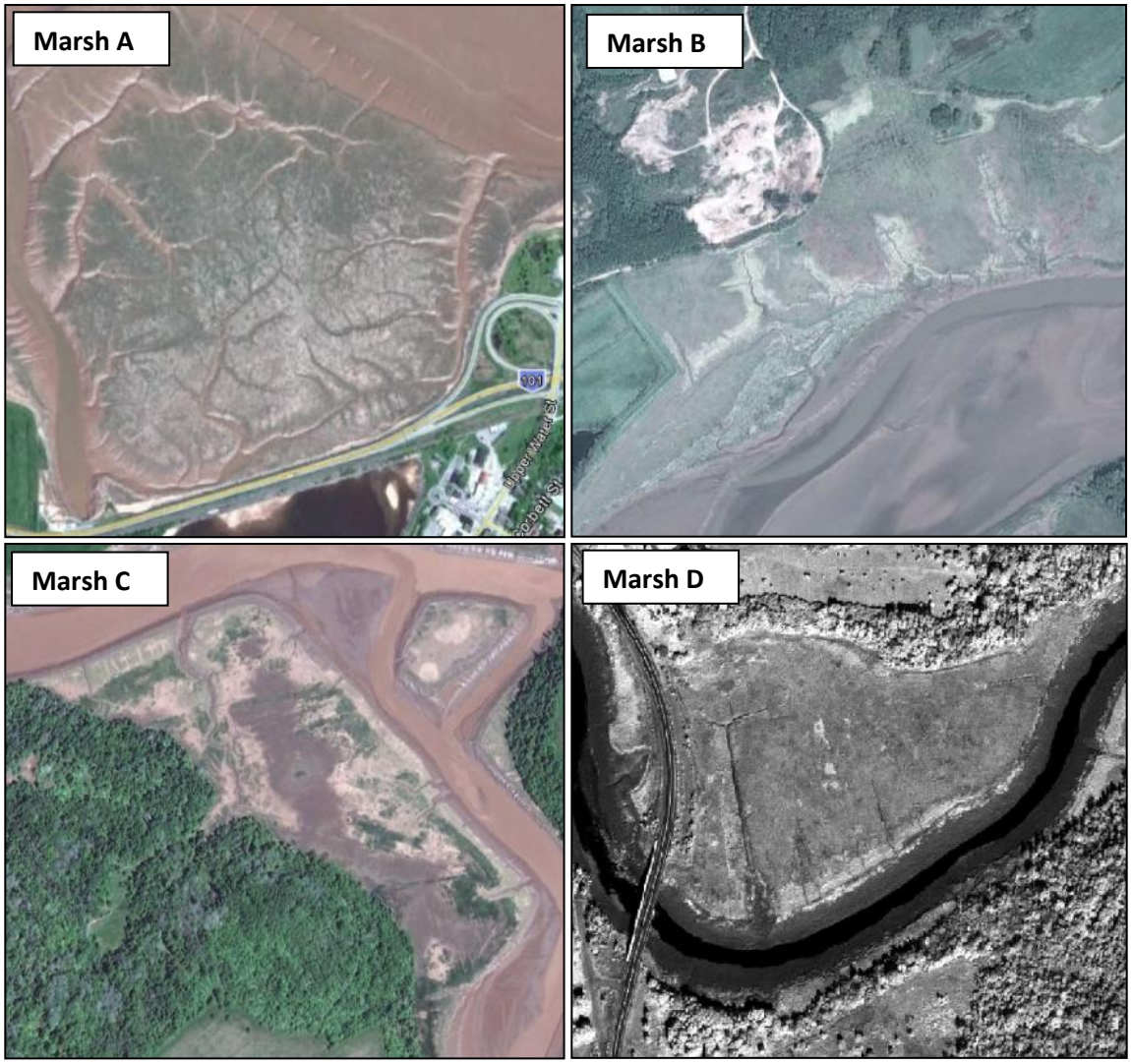


**Figure 2-2: Aerial photography for marshes A-D.**

**Table 2-1: Summary of marsh characteristics.**

| | Marsh A (WIN ) | Marsh B (KEN) | Marsh C (SC) | Marsh D (COG) |
|---|---|---|---|---|
| *River* | Avon | Kennetcook | St. Croix | Cogmagun |
| *Dominant Cover* | *Spartina alterniflora* | *Spartina patens* | *Spartina patens* | *Jucus gerardii* |
| *Mean Platform Elevation (m CGVD28)* | 5.4 | 6.6 | 6.1 | 6.83 |
| *Mean Bankfull Elevation (m CGVD28)* | 5.9 | 6.6 | 7.2 | 6.7 |
| *Min Thalweg Elevation (m CGVD28)* | -1.77 | 2.11 | 2.4 | 2.1 |
| *Max Order (Modified Strahler Order. See **Figure 2-3**)* | 5 | 5 | 5 | 4 |
| *Marsh Area (ha)* | 33.54 | 19.19 | 10.38 | 4.15 |
| *Creek Network Classification* | Dendritic | Superimposed | Dendritic | Superimposed |
| *Distinct Networks* | 2 | 3 | 6 | 3 |
| *Number Of Cross-Sections* | 51 | 24 | 34 | 18 |
| *Percent Tidal Channel Flow Length* | 100 | 37 | 42 | 85 |
| *Development* | Prograding. Marsh vegetation established in 1970's | Undyked 80+ years; NSDA dyke present on western margin of site | Undyked 80+ years; Seasonal pasture | Undyked 80+ years; Roadway & bridge crossing western margin of site |
| *Point of Access* | Adjacent to Hwy 101 | Not adjacent; Accessed from Hwy 215 (~ 1 km away) | Not adjacent; Accessed from Hwy 14 (~1 km away) | Adjacent to Hwy 215 |
| *Relative Maturity (rank)* | *Youngest (1)* | *Moderate (2)* | *Moderate (3)* | *Oldest (4)* |

***Methods***

Morphometric Analysis

To develop a better understanding of the hydraulic characteristics for natural marshes in the region a morphometric analysis was conducted using both survey and digital datasets. Topographic surveys were conducted using a real time kinematic (RTK) GPS for 14 creek networks at Marshes A, B, C and D in the 2011 season during the late spring and early summer. All surveys were conducted in UTM NAD83 and elevations referenced to the Canadian Geodetic Vertical Datum (CGVD28) with a reported survey accuracy of 8 cm horizontal and 15 cm vertically. Cross-section profiles were taken at the beginning, mid, and end of creek segments beginning at the mouth of the network and working towards the upland, resulting in 128 viable profiles for analysis.

These profiles were divided into two groups based on the function of the creeks and observations during restoration projects in the region. Group 1 creeks, referred to from this point forward as tidal creeks, receive little to no freshwater discharge from upland sources and in most cases are dry at low tide. Group 2 creeks, designated as Tidal-Fresh, receive significant freshwater inputs and will have some freshwater flow at low tide, normally no more than a meter or two in depth. However these creeks may experience stronger freshwater flows during rainfall events or the spring freshet.

For each cross-section *Channel Width (w), Cross-sectional area (A), Wetted Perimeter ($P_w$), Maximum depth (D)* and *mean depth (d)* were extracted from GPS survey data using custom tools built in ESRI ArcGIS model builder (see **Appendix A: Python Script for Hydrology Toolbox**). All measurements were calculated relative to *bankfull* elevation, which is the elevation at which

a channel overflows its banks, was identified from cross-section profiles in ESRI ArcGIS 3d analyst and field observations of vegetation growth. Due to variability in terrain both within (on the order of 1 m increase in bankfull elevation from channel mouth to upland edge) and between marshes, bankfull elevation was assessed on a case by case basis rather than applying a study wide threshold. Cross-sectional area was calculated using a modified Trapezoid rule (A = sum of trapezoid areas between *bankfull* elevation and bed elevation between each sample point).

To calculate *upstream channel length ($L_{tot}$, $L_{tide}$)*, *drainage area ($D_{tot}$, $D_{tide}$)* and *tidal prism (TP)* creek network centerlines, referred to as the channel thalweg (*t*) and drainage basins were delineated from a LiDAR Digital Elevation Model (DEM) in ESRI ArcGIS using the hydrology toolset. The Avon River Estuary LiDAR, collected and processed by Applied Geomatics Research Group (AGRG) in April 2007, had 1 m cell resolution and reported vertical accuracy of 15 cm. Drainage networks were extracted using a global accumulation threshold across the estuary based on a visual assessment of creek thalwegs projected on aerial photographs and the LiDAR surface. Custom tools were built to extract channel segments and drainage areas between each cross-section. Total channel length *($L_{tot}$)* was calculated by summing the length of all segments upstream of a given cross-section. Tidal channel length ($L_{tide}$) was calculated using only segments occupying the tidal floodplain. Total Drainage area ($D_{tot}$) was calculated by summing the area of all sub-basins upstream of a given cross-section. Tidal drainage area ($D_{tide}$) was calculated in the same way as tidal channel length. Once Channel lengths and drainage areas were calculated tidal prism could be determined, however this proved to be more complicated than expected.

The extreme tidal range of the Bay of Fundy presented a unique challenge in calculating tidal prism. Tidal prism is the volume of water entering and leaving an estuary or channel during

one tidal cycle between the planes of mean higher high water (MHHW) and mean lower low water (MLLW). Researchers such as Williams et al. (2002) have found MHHW to correspond well with bankfull condition, and there is a widely recognized relationship between spring tidal prism and channel geometry (see Hydraulic Geometry, page 27). For salt marshes in the Avon, low water marks are generally well below the thalweg elevation of tidal creeks in there is nearly a 2 m difference between Higher high water mean tide (HHWMT) and higher high water large tide (HHWLT), which have been calculated at 5.77 and 7.57 m CGVD28 respectively (values for Hantsport obtained from the Canadian Hydrographic Service (CHS) Chart 4140, 1982). Mean bankfull elevation ($H_b$), as calculated for the cross-sections used in this study, was observed to be 6.47 m, ranging from 4.8 m on the large, prograding Marsh A to 7.5 on the smaller, more mature Marsh D. While HHWMT largely under-predicts bankfull conditions, HHWLT over-predicts them.

To address this issue, multiple tidal prisms were calculated at increments of 10 cm and a correlation matrix produced to determine what prism had the strongest relationship with channel geometry. For each cross-section the *bankfull tidal prism ($tp_b$)* was determining by calculating the sum of the volume of water in each channel segment at bankfull elevation (product of cross-sectional area and segment length) for all upstream segments ($tp_b = \sum A*L_{seg}$). For tide heights ($H_t$) greater than the bankfull elevation the upstream drainage area was used to calculated additional volumes and added to the bankfull tidal prism ($TP = D_{tide}*(H_t - H_b) + TP_b$). For tide heights less than bankfull elevation the tidal prism was reduced accordingly.

*Channel order (O), drainage density (Dd), bifurcation ratio ($R_B$), mean channel slope (s)* and *Sinuosity ($R_s$)* were also calculated. Sinuosity, calculated as channel meander length (axial length) divided by the straight-path distance between segment end points, was calculated using

a custom tool in modelbuilder. Mean channel slope was extracted from the LiDAR surface using 3d analyst and was the mean change in bed elevation over a given distance of a channel segment along its thalweg. $R_B$ (number of stream segments in a given order divided by the number of segments in the next highest order) and *Dd* (the ratio of the total stream length to basin area) (Horton, 1945; Lohani & Mason, 2001) were calculated in Microsoft Excel.

Channel order was determined using a modified version of the Strahler method as proposed by Weishar et al. (2005). In the traditional framework stream segments are assigned values (ie., 1$^{st}$ order, 2$^{nd}$ order, etc) with the smallest headward segments having the lowest value and order increasing where two segments of the same order meet (Horton, 1945; Strahler, 1952). In the modified method applied here the ordering is reversed, so that the largest seaward channels are assigned lowest order values (Figure 2-3). This "bottom up" apporach was initially applied in Delaware by Weisher et al. (2005) to address challenges encountered during time-change analysis of a restored salt marsh in California. The rapid development of lower order channels by headward growth caused higher order streams to "disapear" and prohibited comparisons between years. Although this study did not track changes over time, it does attempt to compare channel networks with varying levels of complexity. While several have primary channels that are 5$^{th}$ order in magnitude (using the traditional framework) others are only second or third. Seaward primary channels were observed in the field to be wider and deeper than smaller headward creeks, even in networks that had no higher order segments. Application of the "bottom-up" approach allows comparison of channel segments which are similiar to each other in function and location in the network regardless of network complexity.

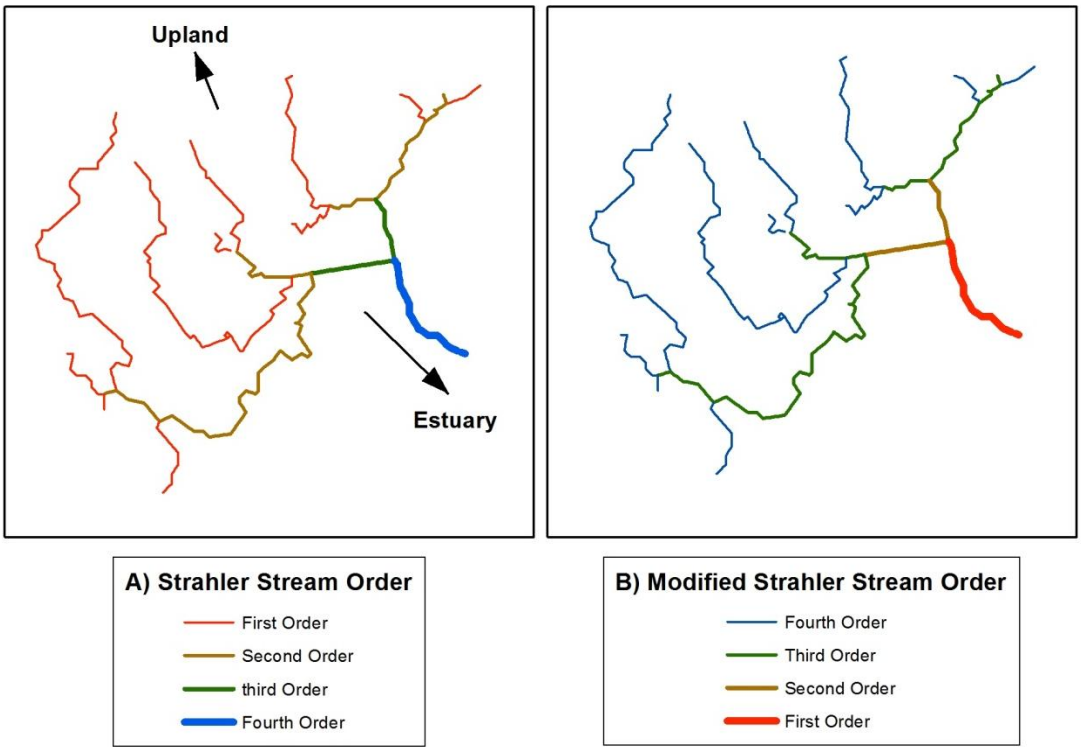


**Figure 2-3: Comparison of "top-down" (A) and "bottom-up" (B) stream order techniques. Adapted from Weisher et al (2005).**

Hydraulic Geometry

Hydraulic geometry describes how at-a-station channel form adjusts to changes in discharge using the equations: $W = aQ^b$, $D = cQ^f$ and $v=kQ^m$, where $W$ is width, $Q$ is characteristic discharge ($m^3$), $D$ is mean depth (m), $v$ is characteristic velocity (m/s), and the sum of the exponents (*b, f,* and *m)* as well as the constants (*a,c*, and *k*) is 1 (Leopold and Maddock, 1953). Furthermore the values of *b, f* and *m* indicate what property will be most sensitive to changes in discharge. For example, an *f* value greater than *b* and *m* should indicate that channel depth will adjust more rapidly than width or velocity to a change in discharge (Zeff, 1999). In tidal systems

the spring tidal prism (volume of water entering the estuary between low and high water marks during spring tidal flows) can be used as a surrogate for discharge. Formulated from empirical observations, the strength of this relationship has been further tested and validated through numeric and hydrodynamic modelling (Myrick & Leopold, 1963; Pestrong, 1965; Leopold et al., 1993; Allen, 2000; D'Alpaos et al., 2007; D'Alpaos et al., 2010). This relationship has been recognized as a powerful tool in restoration design, wherein spring tidal prism is used to determine equilibrium channel geometry and excavations made to the predicted dimensions (Williams & Harvey, 1983; Haltiner & Williams, 1987; Zeff, 1999; Williams et al., 2002; Wallace et al., 2005).

As discussed previously, the extreme tidal range of the Bay causes the volume of water on the marsh surface to vary by orders of magnitude, dependant on tidal stage and presents a unique challenge when calculating tidal prism. When van Proosdij et al. (2010) tested preliminary hydraulic geometry equations at the Walton River Restoration Project in the Bay of Fundy they observed that regression analysis preformed best ($R^2 = 0.76$) when using a prism with the HHWLT upper limit. However the best creek predictions were generated when the upper limit of the tidal prism was calculated using HHWMT. Observations on other Bay of Fundy marshes have found that: 1) over-marsh flooding frequently occurs from creek banks and marsh boundaries simultaneously due to the lack of pronounced levees on creek banks, the short distances involved, and the rapid rise of water levels in the Bay of Fundy and 2) at greater water depths tidal flow frequently follow larger scale river basin current patterns (Davidson-Arnott et al., 2002; van Proosdij et al., 2010). The correlation matrix produced during the morphometric analysis was used to further explore the relationship between channel geometry and tidal prism at different tide heights.

***Results***

Morphometric Analysis

Mean channel dimensions are presented in Table 2-2, classified by channel order and channel type (tidal and tidal-fresh). Also shown in Table 2-2 are three standard measures of channel form: width to mean depth ratio's (*w:d*), maximum to mean depth (*D:d*) ratio, and hydraulic radius($R_h$). High *w:d* ratios indicate wider and shallower channels while low values usually point to a deep and narrow channel. The *D:d* ratio generally indicates channel depth relative to the surrounding bathymetry, where values approaching 1 indicate flatter bottomed channels. $R_h$ is the dividend of cross-sectional area and wetted perimeter and is a measure of channel flow efficiency. Higher values for hydraulic radius indicate a greater cross-sectional area in comparison to the wetted perimeter resulting in decreased friction along the channel bed and higher velocities (Ritter, 2012).

**Table 2-2: Mean Channel geometry with standard error (SE)**

| Type | Order (*O*) | Sample Size (*n*) | XS Area (*A*) $m^2$ | | Max Depth (*d*) *m* | | Mean Depth (*d*) *M* | | Width (*w*) *m* | | Wetted Perimeter ($P_w$) *m* | | *w:d* | *D:d* | *Hydraulic Radius* ($R_h$) |
|---|---|---|---|---|---|---|---|---|---|---|---|---|---|---|---|
| | | | *Mean* | *SE* | *Mean* | *SE* | *Mean* | *SE* | *Mean* | *SE* | *Mean* | *SE* | | | |
| ***Tidal*** | 1 | 21 | 23.42 | 8.26 | 2.23 | 0.36 | 1.27 | 0.18 | 14.87 | 3.29 | 16.03 | 3.37 | 11.7 | 1.75 | 1.46 |
| | 2 | 42 | 6.76 | 1.86 | 1.51 | 0.10 | 0.90 | 0.06 | 8.02 | 1.05 | 8.92 | 1.06 | 8.9 | 1.67 | 0.76 |
| | 3 | 8 | 4.56 | 0.93 | 1.53 | 0.14 | 0.88 | 0.06 | 6.59 | 0.88 | 7.59 | 0.95 | 7.5 | 1.75 | 0.60 |
| | 4 | 17 | 3.59 | 1.70 | 1.16 | 0.16 | 0.70 | 0.09 | 5.10 | 1.06 | 5.92 | 1.11 | 7.3 | 1.65 | 0.61 |
| | 5 | 2 | 2.02 | 0.75 | 1.17 | 0.29 | 0.69 | 0.15 | 3.78 | 0.84 | 4.60 | 0.98 | 5.5 | 1.70 | 0.44 |
| ***Tidal-Fresh*** | 1 | 24 | 14.92 | 3.28 | 2.38 | 0.21 | 1.32 | 0.11 | 10.64 | 1.32 | 12.22 | 1.38 | 8.1 | 1.81 | 1.22 |
| | 2 | 8 | 1.59 | 0.58 | 1.11 | 0.16 | 0.62 | 0.10 | 3.10 | 0.58 | 4.19 | 0.74 | 5.0 | 1.81 | 0.38 |
| | 3 | 5 | 1.15 | 0.40 | 0.85 | 0.16 | 0.54 | 0.07 | 2.86 | 0.73 | 3.50 | 0.76 | 5.3 | 1.58 | 0.33 |
| ***All creeks*** | 1 | 45 | 18.89 | 4.23 | 2.31 | 0.20 | 1.30 | 0.10 | 12.62 | 1.70 | 14.00 | 1.74 | 9.72 | 1.78 | 1.35 |
| | 2 | 50 | 5.93 | 1.58 | 1.45 | 0.09 | 0.86 | 0.05 | 7.24 | 0.92 | 8.17 | 0.93 | 8.43 | 1.69 | 0.73 |
| | 3 | 13 | 3.25 | 0.75 | 1.27 | 0.14 | 0.75 | 0.07 | 5.15 | 0.79 | 6.02 | 0.85 | 6.91 | 1.70 | 0.54 |
| | 4 | 17 | 3.59 | 1.70 | 1.16 | 0.16 | 0.70 | 0.09 | 5.10 | 1.06 | 5.92 | 1.11 | 7.25 | 1.65 | 0.61 |
| | 5 | 2 | 2.02 | 0.75 | 1.17 | 0.29 | 0.69 | 0.15 | 3.78 | 0.84 | 4.60 | 0.98 | 5.49 | 1.70 | 0.44 |

As expected, first order seaward creeks were the largest channels with the highest w:d ratios and hydraulic radius values, indicating efficient channels that are wider and shallower than higher order creeks. Tidal creeks were, on average, wider than tidal-fresh creeks of the same order, however average depths were similar. *D:d* ratios were low with little difference between tidal/tidal-fresh channels or between orders, indicating that channels are narrow relative to floodplain topography regardless of type or order. Plotting width to depth values (Figure 2-4) further supported separation by type for first and second order channels (tidal/tidal-fresh). A trend line plotted for the data illustrates that, for creeks of the same width, tidal-fresh creeks should be deeper – a conclusion also supported by higher w:d ratio's for tidal creeks. For higher order channels (third to fifth order) there was no differentiation between tidal and tidal fresh ratios or between orders (third-fifth).

Mean channel lengths ($L_{tot}$ ; $L_{tide}$), drainage areas ($D_{tot}$ ; $D_{tide}$) and tidal prisms are shown in Table 2-3. Tidal channels generally have less total upstream channel lengths than their tidal-fresh counterparts, which is to be expected given that these networks extend well beyond the tidal platform. Despite lower upstream channel lengths, the tidal prism for tidal creeks is considerably greater for nearly all orders and prisms tested. This can be partly explained by the distribution of channel networks across the tidal platform and is supported by field observations that led to the division of tidal and tidal-fresh creeks. Because primary (first order) seaward creeks are larger, they contain the greatest volume of water, while landward higher order creeks are shallower and narrower.

Where additional upstream channel length for tidal-fresh channels is composed primarily of high order creeks, increasingly less volume is added to the tidal prism by these

creeks. This is also illustrated by the fact that for tidal creeks mean tide prism is greater than bankfull prisms, while the opposite is true for tidal-fresh prisms. Mean bankfull elevation for tidal creeks are lower than tidal-fresh creeks of the same order. Moreover, tidal-fresh channels have a channel length attributed to smaller high order creeks which have higher bankfull elevations and lower depths.

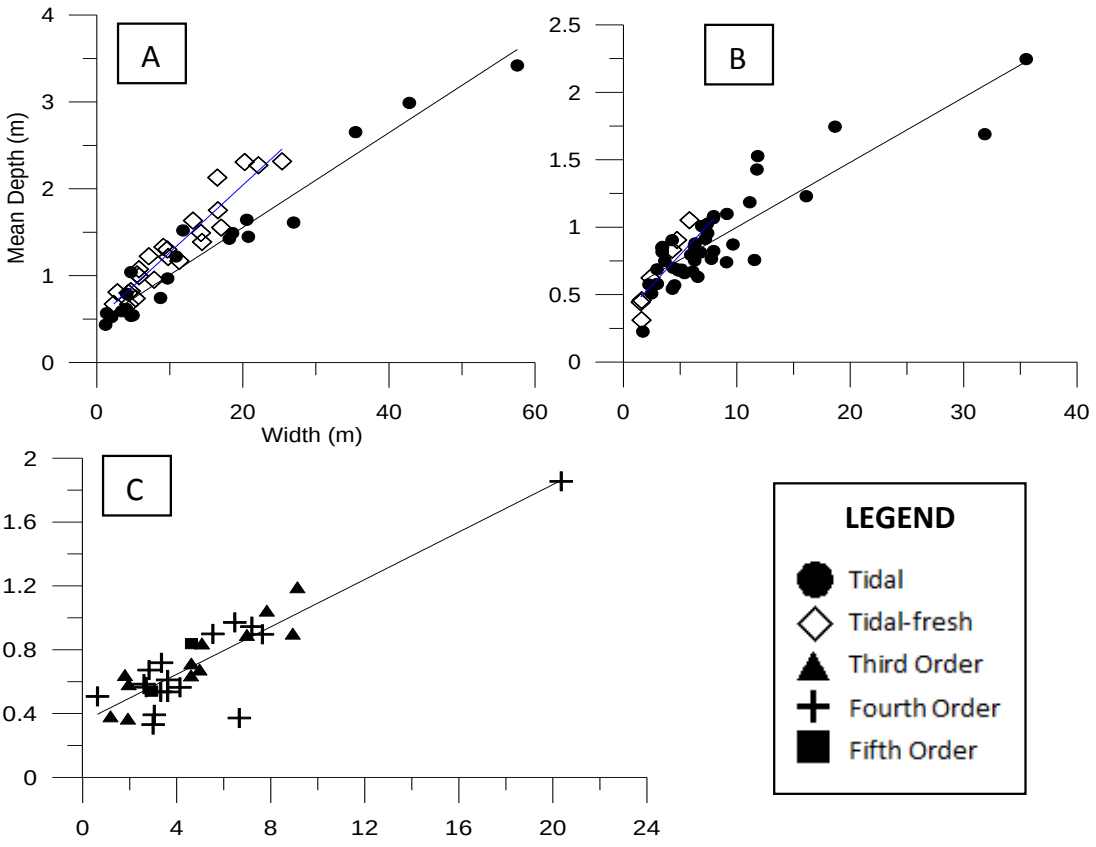


**Figure 2-4: W:d Plots. A) Width vs. depth for first order creeks. B) Width vs. depth for 2nd order creeks. C) Width vs. depth for 3rd-5th order creeks**

**Table 2-3: Mean channel lengths ($L_{tot}$ ; $L_{tide}$), drainage areas ($D_{tot}$ ; $D_{tide}$) and tidal prisms.**

| Type | Order (O) | Sample Size (*n*) | $L_{tot}$ (*m*) | | $L_{tide}$ (*m*) | | $D_{tot}$ ($m^2$) | | $D_{tide}$ ($m^2$) | | *Bankfull TP* ($tp_b$) ($m^3$) | | *HHWMT TP* ($m^3$) | | *HHWLT TP* ($m^3$) | |
|---|---|---|---|---|---|---|---|---|---|---|---|---|---|---|---|---|
| | | | Mean | SE | Mean | SE | Mean | SE | Mean | SE | Mean | SE | Mean | SE | Mean | SE |
| **Tidal** | 1 | 21 | 924 | 311 | 924 | 311 | 31351 | 10621 | 30379 | 10160 | 42672 | 22481 | 58650 | 31293 | 110090 | 49577 |
| | 2 | 42 | 263 | 49 | 262 | 48 | 9196 | 1642 | 9092 | 1585 | 2584 | 1439 | 3362 | 1545 | 17423 | 4388 |
| | 3 | 8 | 261 | 54 | 261 | 54 | 8238 | 1384 | 8070 | 1270 | 687 | 167 | 2293 | 1297 | 14117 | 3209 |
| | 4 | 17 | 58 | 10 | 58 | 10 | 2328 | 333 | 2328 | 333 | 361 | 250 | 707 | 492 | 3869 | 1094 |
| | 5 | 2 | 33 | 26 | 33 | 26 | 1701 | 984 | 1701 | 984 | 52 | 32 | 0 | 0 | 392 | 229 |
| **Tidal-Fresh** | 1 | 24 | 6800 | 1252 | 2044 | 276 | 163470 | 28264 | 45985 | 6210 | 6397 | 1494 | 3944 | 1099 | 99403 | 17431 |
| | 2 | 8 | 897 | 177 | 599 | 179 | 24236 | 5321 | 12674 | 4460 | 421 | 179 | 107 | 73 | 18913 | 5462 |
| | 3 | 5 | 474 | 127 | 317 | 90 | 12103 | 3512 | 6265 | 2334 | 1200 | 1070 | 5 | 5 | 5483 | 1701 |
| **All** | 1 | 45 | 4058 | 808 | 1522 | 221 | 101814 | 18584 | 38702 | 5833 | 23325 | 10737 | 29473 | 14999 | 104390 | 24632 |
| | 2 | 50 | 365 | 59 | 316 | 52 | 11602 | 1778 | 9665 | 1502 | 2238 | 1212 | 2841 | 1306 | 17662 | 3771 |
| | 3 | 13 | 342 | 63 | 282 | 46 | 9725 | 1601 | 7376 | 1158 | 884 | 402 | 1413 | 841 | 10796 | 2353 |
| | 4 | 17 | 58 | 10 | 58 | 10 | 2328 | 333 | 2328 | 333 | 361 | 250 | 707 | 492 | 3869 | 1094 |
| | 5 | 2 | 33 | 26 | 33 | 26 | 1701 | 984 | 1701 | 984 | 52 | 32 | 0 | 0 | 392 | 229 |

Although multiple tidal prisms were calculated, only three were used in this analysis, based on interpretation of the correlation matrix and the importance of the spring tidal prism identified in the literature (Myrick & Leopold, 1963; Pestrong, 1965; Williams & Harvey, 1983; Haltiner & Williams, 1987; Zeff, 1999; Leopold et al., 1993; Allen, 2000; Williams et al., 2002; Wallace et al., 2005; D'Alpaos et al., 2006, 2007, 2010). Pearson's R values were generated from a correlation matrix run on log-transformed data and plotted against tide height (Figure 2-5), which illustrates the relationship between channel geometry parameters and tidal prism. Pearson's R values are highest for tides ranging between bankfull and HHWMT tidal prisms, with Pearson's R declining steadily until HHWLT is reached and there is a sudden increase. This was felt to be significant and the HHLWT prism was incorporated in the analysis.

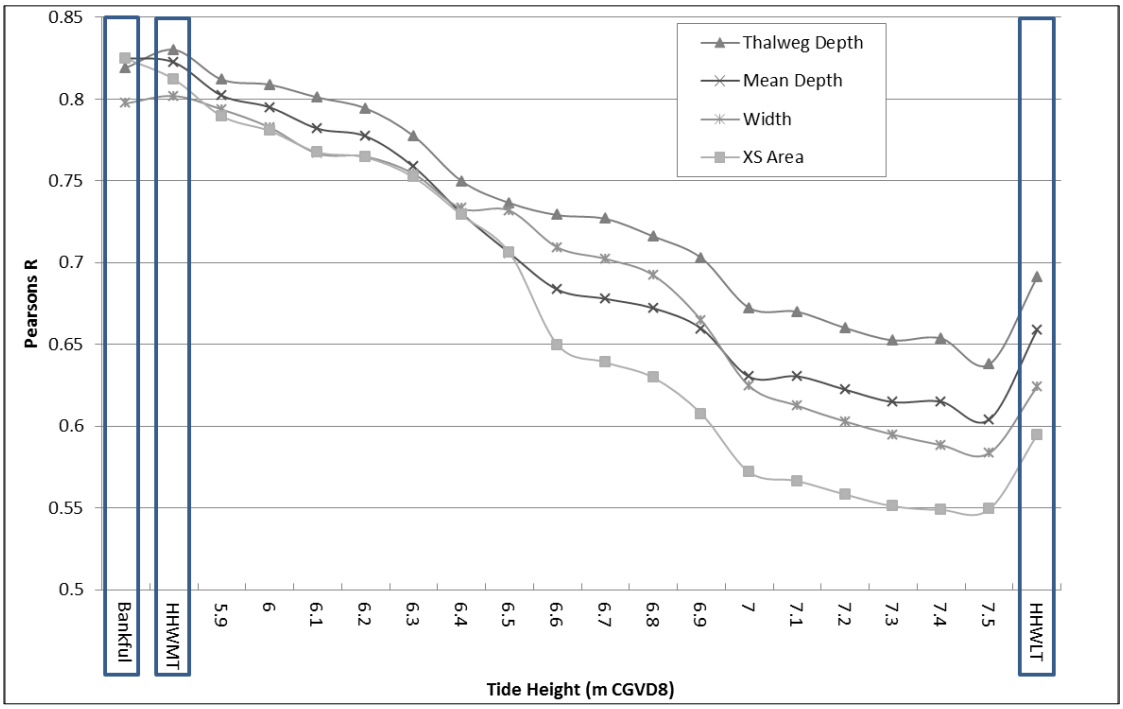


**Figure 2-5: Pearson's R vs. tide height. Pearson's R derived from a correlation matrix for tide height (m CGVD28) vs. corresponding tidal prism for log-linear transformed data.**

Channel length and drainage area were extracted from a high resolution DEM, and used to calculated drainage density, bifurcation ratios and sinuosity (Table 2-4). Regression analysis of total channel length versus drainage area showed a strong power law relationship ($Y = 0.0553x^{0.9808}$) with $r^2 = 0.96$ (**Figure 2-6**). Drainage density was high at all sites examined. Mean bifurcation ratio varied between 1.8 and 2.43 by site, with no clear differentiation between sites and high standard deviations at all sites. Lower bifurcation ratios are indicative of a higher chance of flooding, as water is concentrated in a single channel, an outcome which makes sense given the frequent flooding which occurs on tidal platforms. When networks were grouped by channel type tidal networks had lower density values and higher bifurcation ratios, indicating less dense networks for channels not receiving significant freshwater input. Networks receiving freshwater flows have greater upstream channel lengths, leading to higher channel density.

**Table 2-4: Drainage density, bifurcation ratios, and sinuosity**

| | | Marsh A | Marsh B | Marsh C | Marsh D | Tidal | Tidal-fresh | All |
|---|---|---|---|---|---|---|---|---|
| ***Drainage Density*** | | 0.032 | 0.044 | 0.052 | 0.074 | 0.044 | 0.053 | 0.047 |
| *Standard Deviation* | | 0.000 | 0.004 | 0.009 | 0.023 | 0.017 | 0.017 | 0.017 |
| ***Bifurcation Ratio*** | | 2.00 | 2.43 | 1.80 | 2.14 | 2.29 | 1.58 | 2.04 |
| *Standard Deviation* | | 0.38 | 1.24 | 0.71 | 1.18 | 0.93 | 0.44 | 0.85 |
| ***Sinuosity*** | *1st order* | 1.06 | 1.06 | 1.25 | 1.04 | 1.17 | 1.09 | 1.14 |
| | *2nd order* | 1.08 | 1.13 | 1.24 | 1.16 | 1.15 | 1.22 | 1.18 |
| | *3rd order* | 1.09 | 1.10 | 1.16 | 1.11 | 1.13 | 1.10 | 1.11 |
| | *4th order* | 1.10 | 1.11 | 1.18 | 1.24 | 1.19 | 1.13 | 1.16 |
| | *5th order* | 1.11 | 1.09 | 1.24 | -- | 1.11 | 1.17 | 1.15 |
| | *All* | 1.09 | 1.10 | 1.21 | 1.14 | 1.15 | 1.14 | 1.15 |
| *Standard Deviation* | | 0.02 | 0.05 | 0.20 | 0.14 | 0.18 | 0.10 | 0.14 |

Sinuosity was low throughout the study region, with many segments approaching 1 (ie. perfectly straight channel segments). Generally, higher order segments had greater sinuosity values, with channels at Marsh C appearing to more sinuous than other marshes and no consistent difference between tidal and tidal-fresh marshes. As with bifurcation ratios standard deviations indicate virtually no difference between sites. The spatial pattern of sinuosity scores across the marsh surface is shown in Figure 2-7. Higher order channel and those occurring closer to the upland were generally more sinuous than first order seaward creeks. Channel slope ranged from 0 to 39%, with primary and headwater creeks having steeper slopes than mid-order segments and upland channel segments being steeper than tidal segments. There is also an apparent increase in primary channel slope with marsh maturity, however higher order creeks did not show the same patterns.

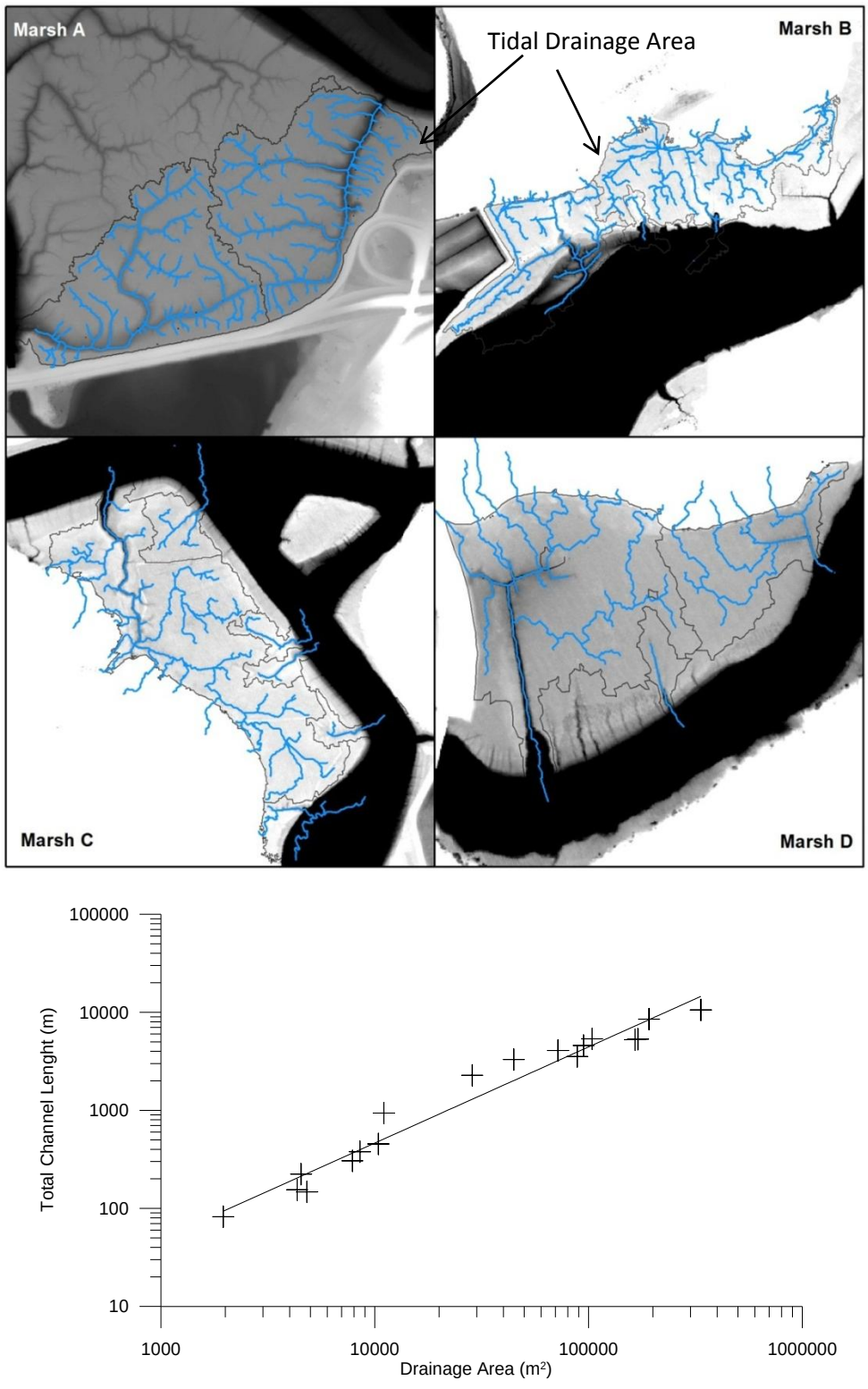


**Figure 2-6: Channel Networks and drainage basins extracted from LiDAR Surface and regression plot for total channel length (m) versus drainage area ($m^2$). Tidal Drainage Area ($D_{tide}$) delineated by gray line**

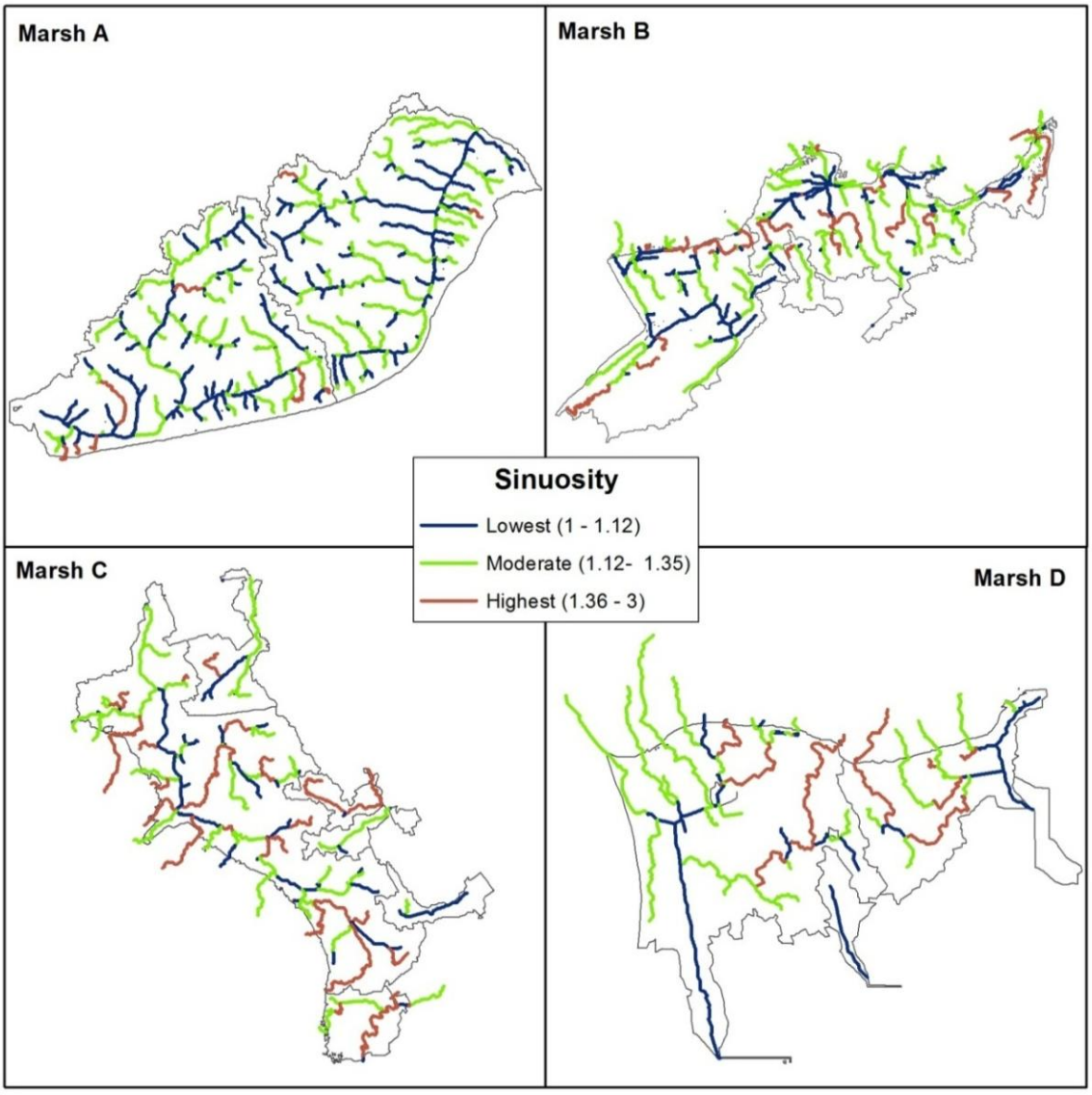


**Figure 2-7: Sinuosity scores for channel segments at Marshes A-D. Higher order channels and those occurring closer to the upland were generally more sinuous than 1st order seaward channels.**

Hydraulic Geometry

The three tidal prisms identified previously (Bankfull, HHWMT, and HHWLT) were tested to determine the strength of hydraulic geometry equations for Tidal and Tidal-Fresh channels by order. Data were log-transformed and regression analysis carried out. In most cases the best regression was achieved for tidal creek geometry and *bankfull tidal prism* in first order creeks (Table 2-5). Although regressions for tidal-fresh creeks were poor, as indicated by lower values for coefficient of determination ($r^2$) and higher values for residual mean squared (*rms)* error, some interesting patterns emerged for HHWMT and HHWLT plots (Figure 2-8). For HHWMT and bankfull prisms first order tidal-fresh creeks had poor correlation to tidal prism but did fall in clusters overlapping tidal creeks. So although the fit was poor, the volume of water contained in tidal-fresh channels was on the same order as tidal channels and the slope of the regression very similar. For HHWLT prisms, on the other hand, there was a visible shift in the location of the tidal-fresh creeks as they no longer overlapped tidal creeks. The slope of the regression line for these plots was very different, indicating a different relationship between tidal prism and channel geometry when the storage capacity of the marsh surface was brought into play. As creek order increased, $r^2$ for all prisms and parameters decreased and any distinction between tidal and non-tidal creeks becomes less evident.

**Table 2-5: Hydraulic geometry coefficents**

| Tidal Prism | Type | Order (O) | Sample Size (n) | Width ($w = aQ^b$) | | | | Mean Depth ($d = cQ^f$) | | | | Velocity ($v = kQ^m$) | | XS Area ($A = eQ^g$) | | | |
|---|---|---|---|---|---|---|---|---|---|---|---|---|---|---|---|---|---|
| | | | | *a* | *B* | $r^2$ | *Rms* | *c* | *f* | $r^2$ | *rms* | *m** | *k** | *e* | *g* | $r^2$ | *rms* |
| **Bankfull** | *Tidal* | 1 | 21 | 0.96 | 0.33 | 0.88 | 0.15 | 0.31 | 0.18 | 0.88 | 0.05 | 0.49 | .27 | 0.53 | 0.20 | 0.91 | 0.44 |
| | *Tidal* | 2 | 42 | 1.41 | 0.26 | 0.60 | 0.17 | 0.32 | 0.17 | 0.66 | 0.05 | 0.58 | 0.73 | 0.45 | 0.25 | 0.71 | 0.33 |
| | *Tidal-Fresh* | 1 | 24 | 1.41 | 0.23 | 0.27 | 0.33 | 0.44 | 0.13 | 0.24 | 0.12 | 0.64 | 0.86 | 0.45 | 0.23 | 0.33 | 0.97 |
| | *All* | 3-5 | 27 | 1.20 | 0.28 | 0.55 | 0.26 | 0.34 | 0.15 | 0.52 | 0.09 | 0.57 | 0.54 | 0.45 | 0.25 | 0.62 | 0.63 |
| **HHWMT** | *Tidal* | 1 | 13 | 2.57 | 0.23 | 0.88 | 0.08 | 0.56 | 0.12 | 0.86 | 0.03 | 0.65 | 2.08 | 0.37 | 0.94 | 0.89 | 0.20 |
| | *Tidal* | 2 | 36 | 2.37 | 0.19 | 0.50 | 0.17 | 0.46 | 0.11 | 0.54 | 0.05 | 0.70 | 1.83 | 0.34 | 0.55 | 0.62 | 0.36 |
| | *Tidal-Fresh* | 1 | 23 | 2.01 | 0.21 | 0.38 | 0.25 | 0.51 | 0.13 | 0.42 | 0.09 | 0.66 | 1.52 | 0.42 | 0.43 | 0.48 | 0.76 |
| | *All* | 3-5 | 20 | 2.99 | 0.13 | 0.51 | 0.20 | 0.47 | 0.10 | 0.53 | 0.09 | 0.78 | 2.46 | 0.24 | 0.89 | 0.59 | 0.48 |
| **HHWLT** | *Tidal* | 1 | 21 | 0.40 | 0.35 | 0.75 | 0.32 | 0.17 | 0.21 | 0.87 | 0.05 | 0.44 | 0.44 | 0.57 | 0.043 | 0.81 | 0.63 |
| | *Tidal* | 2 | 42 | 0.52 | 0.29 | 0.53 | 0.20 | 0.19 | 0.17 | 0.50 | 0.08 | 0.54 | 0.30 | 0.50 | 0.05 | 0.60 | 0.44 |
| | *Tidal-Fresh* | 1 | 24 | 0.08 | 0.42 | 0.25 | 0.34 | 0.08 | 0.25 | 0.25 | 0.12 | 0.34 | 0.84 | 0.85 | 0.001 | 0.33 | 0.97 |
| | *All* | 3-5 | 27 | 0.65 | 0.24 | 0.24 | 0.32 | 0.24 | 0.13 | 0.22 | 0.12 | 0.63 | 0.11 | 0.38 | 0.10 | 0.25 | 0.83 |

*Velocity coefficient's calculated from width and depth, as $a+c+k = 1$ and $b+f+k = 1$

**Figure 2-8: Hydraulic geometry plots for Mean Depth vs. Tidal Prism. Black squares are tidal creeks and white diamonds are tidal-fresh creeks**

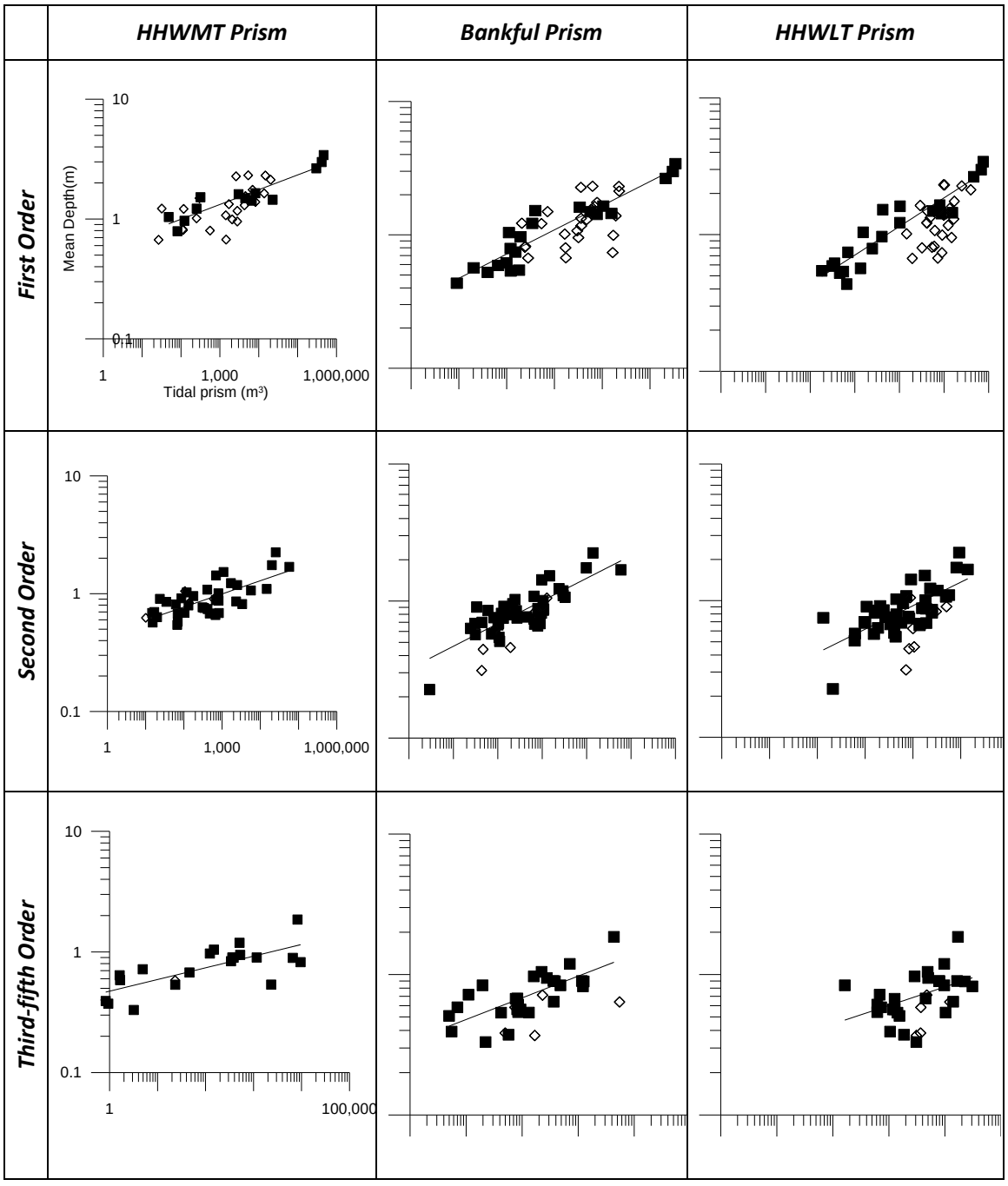

***Discussion***

The results presented above provide a great deal of information about the morphology of tidal creeks in the Bay of Fundy and have potential application in other hypertidal settings. Channel geometry was strongly related to channel order and type, while site maturity and history were more important in network structure (ie., drainage density, bifurcation ratio and sinuosity). The following discussion will focus on a comparison to the findings of other researchers and applications for restoration design.

Although tidal channels can have many configurations, such as V-shaped, U-shaped, rectangular-trapezoidal, the channels observed in this study were largely V-shaped (Figure 2-9) with w:d ratios ranging from 1.2 to 18.9 and in line with the observations of other authors (Allen, 2000; Teal & Weisher, 2005). Allen (2000) suggests that channels of low w:d ratio should be more common in muddier systems such as the Bay of Fundy. Primary channels often have higher w:d ratios for in the range 5 to 30 (Myrick and Leopold, 1963; Pestrong, 1965; Bayliss-Smith et al., 1979) while headwater creeks have w:d ratios of 1 to 2 (Pestrong, 1965; Pethick, 1980; French and Stoddart, 1992; Leopold et al., 1993). In a study of back-barrier marshes in New Jersey Zeff (1999) found w:d ratios ranging from 5 to 34, with an outlying value at one channel of 129. She found that larger flow-through channels which conducted water from one source to another had higher w:d ratios than narrower dead-end creeks. Consistent with the results of other researchers in both freshwater and tidal systems w:d ratio's decrease moving upstream (Myric & Leopold, 1963; Zeff, 1999).

In this analysis first order channels also have higher w:d ratios and could be considered similar to flow-through channels, channeling water from the river to higher order creeks. When

carrying out restoration projects the under sizing of channels can lead to excessive erosion, advection of sediments into the river system and loss of marsh habitat. Over-sizing channels, on the other hand, can increase project costs associated with excavation of channels and transportation/disposal of excavated material and alter hydrology. Although researches such as Teal and Weisher (2005) found constructed channels reached design specifications within 1-2 years regardless of the initial channel form excavated, it is still preferable to construct channels which are as near to their equilibrium dimensions as possible.

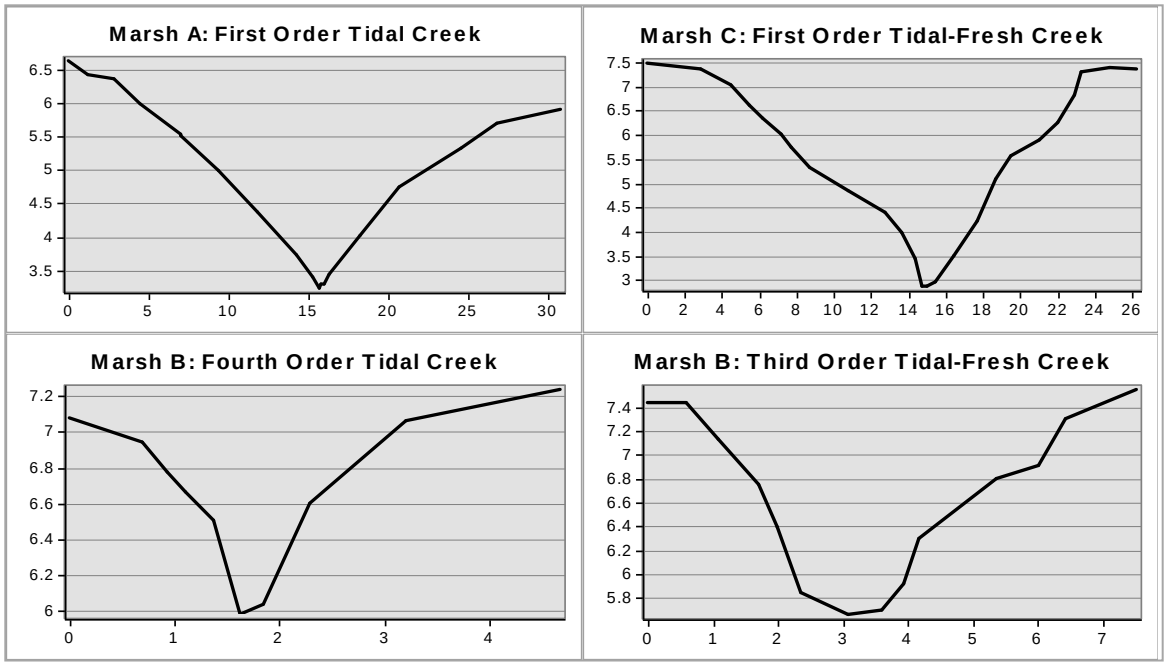


**Figure 2-9: Cross- Section profiles showing variations in form. Elevations in meters CGVD28**

During a five year experiment in the Tijuana estuary, California, Wallace et al. (2005) found that sites without excavated hydraulic networks did not reach drainage densities

comparable to reference sites, while excavated cells did. They also demonstrated that headwater creeks, termed “volunteer creeks”, developed independently without the aid of excavation. The ecological engineering philosophy dictates that natural processes will complete the restoration more efficiently than man-made excavations. To date this has been the preferred approach in the Bay of Fundy. The above characteristics should be used to determine dimensions for excavated primary creeks, while higher order channels can be allowed to develop through natural processes as the drainage network adapts to the re-introduction of tidal flow.

Drainage density can vary considerably depending on site characteristics such as sediment type, vegetation cover and tidal regime (Zeff, 1999; Wallace et al., 2005). While studying drainage density for salt marshes in South California Novakowski et al. (2004) suggested the salt marsh island (where major through-flowing channels define its boundaries) as an appropriate scale for geomorphic analysis as processes operating at this scale are spatially uniform due to depth of inundation. In the Bay of Fundy the four marshes examined (each of which contain multiple networks) are well defined by steep upland edges and large deep rivers and function in a similar way. Using the marsh platform, as opposed to individual networks, as the unit of analysis provided interesting results and is more easily applied to restoration projects.

Densities, calculated at the marsh level, were comparable to that of other researchers in the region. MacDonald et al. (2010) found drainage densities in upper Bay of Fundy ranging from 0.009 to 0.056 $m/m^2$ and attributed the high densities primarily to the fact that channel density increases with increasing tidal prism and water depth (Friedrichs and Perry, 2001; Novakowski et

al., 2004). Steel and Pye (1997) also reported similar values at macro-tidal salt marshes in the UK, ranging from 0.015 to 0.128 $m/m^3$.

The results of the regression analysis of total channel length and drainage area agree with those of Marani et al. (2003) who, found total channel length to be strongly related to salt marsh area. They suggest that the relationship further supports the concept of inheritance whereby the network structure undergoes very little change once vegetation colonizes a mudflat surface (Allen, 2000; Fagherazzi & Sun, 2004; D'Alpaos et al., 2005; D'Alpaos et al., 2006; D'Alpaos et al., 2007; Stefanon et al., 2010).

Drainage density, however, was somewhat contradictory to models such as that proposed by Allen (1997) whereby channels should in-fill and networks simplify over time. The lowest drainage density in this study occurred at the least mature site and increased with maturity for marshes B, C, and D. This increase in drainage density does fit the model proposed by Steel and Pye (1997), whereby a simple network incised on a mudflat grows through headward extension once the platform becomes vegetated. Once a critical threshold is reached, reducing the number of overmarsh tides and hydraulic duty at the site, drainage density decreases and the network simplifies. No threshold was observed in this study, however `the amount of disturbance in the region and lack of very mature marshes makes it likely that none of the marshes studied were mature enough to reach it.

When total channel planform area was used to calculate drainage density results are considerably different. Density at marsh A was calculated at 0.62 $m/m^2$ while marshes B-D range from 0.036 to 0.068 $m/m^2$. This is in line with what would be expected given Allen's (2000) proposed model. It also agrees with the findings of Novakowski et al. (2004), who hypothesized

that tidal channel networks will adjust to changes in tidal prism though changes in total channel planform area as well as channel length. Both Novakowski et al.(2004) and Marani et al. (2003) observed an upper limit on total channel length based on drainage basin area and presumably on regional constraints (ie, sediment and vegetation). Thus greater tidal prism may be accommodated by increased channel area where channel length is unable to increase.

MacDonald et al. (2010) used a similar method when analysing recovering marshes in the Bay of Fundy with particular attention being paid to the incorporation of agricultural ditches. They found that when primary channel area was included in density calculations there was no difference between natural and recovering marshes. Taken together this suggests that channels in a hypertidal marsh, as in other regions, may accommodate the tidal prism through changes in total channel area, and furthermore that relict agricultural ditches can be successfully incorporated into these networks through reductions in planform area as opposed to reductions in channel length.

Sinuosity at the marshes examined was variable but seemed be closely related to order and site history. Zeff (1999) found that sinuosity was highest in mid-order channels and lower for high and low order channels in a New Jersey back-barrier marsh. In MacDonald's (2010) study the incorporation of relict agricultural ditches was shown to decrease sinuosity for headwater channels. This study shows some agreement with both of Zeff and MacDonald, but contradicts them as well. Marshes A and B have superimposed networks, and at these sites mid and high order creeks are more sinuous than first order creeks. At marsh C, on the other hand, mid-order creeks are the least sinuous and first and fifth order creeks are the most sinuous in the data set. Although incorporation of relict agricultural ditches may have reduced sinuosity for primary

creeks at Marshes B-D, the least sinuous channels were measured at Marsh A which has no agricultural history at all. These patterns may be attributed in part to the short channel segments in the study areas, particularly at Marsh A (high bifurcation ratio and complex dendritic network).

Mean channel length ranged from 18 m to 23 m for first to fifth order creeks respectively. These patterns are also related to the spatial distribution of agricultural creeks and network complexity. At Marsh C the reversal of patterns may be a result of the presence of multiple first order tidal creeks in simple small networks which skewed the resulting data (increasing sinuosity of first order and decreasing sinuosity of mid order creeks) as well as seasonal grazing. Although agricultural ditches are clearly visible in the superimposed networks at marshes B and D, they are not limited to a particular order.

Patterns in both drainage density and sinuosity may also be partly attributed to methods used in this paper. Figure 2-6 shows channel centerlines overlaying the LiDAR surface used to generate the drainage network. Because networks were generated using the hydrology toolset in ArcGIS small channels may have been excluded as too few cells drained to these locations. Data resolution and the choice of flow accumulation thresholds may result in different network densities, as well as different drainage divides. None the less the decision was made not to manually edit the network to include these small channels (which in some cases can be easily identified in the LiDAR or in the field) to maintain consistency in the overall network. Manual delineation would also have introduced further uncertainty due to difficulty in delineating drainage area for these very small channels

Hydraulic geometry also provided some useful insights for restoration design in the Avon estuary and other hypertidal estuaries. Tidal creeks exponents were in the range of other published values (Table 2-6). First order creeks tidal creeks have high *f* values, indicating that depth will adjust before width. Tidal creeks in the region typically have un-vegetated banks and thalwegs, with fine sediments that are easily mobilized during tidal flows and weather events. Bankfull conditions generally correspond with or are above the low marsh margin, where vegetation reduces velocities, increases sedimentation and decreases erosion (Temmerman et al., 2005). Higher order creeks have exponents indicating width is marginally more responsive to changes in tidal prism, however in all case velocity is predicted to adjust before channel morphology.

Hydraulic geometry regressions were strongest for bankfull elevation. Various studies have shown that bankfull channelized tidal flows tend to be spatially uniform with undermarsh flows being weaker than overmarsh flows and velocity surges common on the ebb/ flood tide (Friedrichs and Perry, 2001; French and Stoddart, 1992; Rinaldo et al. 1999; Allen, 2000). Fagherazzi et al. (2008), studying marshes in the UK using a numerical model called TIGER, was able to accurately model velocity surges occurring on the flood and ebb tides near and slightly above the marsh surface elevation. In this study the HHWMT prism is representative of weak undermarsh tidal flows, while at HHWLT depth of inundation alters the flow dynamics within the marsh to follow basin-wide patterns (van Proosdij et al., 2010; Davidson-Arnott et al., 2002). The strong correlation to bankfull elevation found in this study was interpreted to reflect the prevalence of ebb and flood velocity surges in shaping channel structure.

**Table 2-6: Hydraulic geometry exponents for this and other studies**

| Study | Location | Channel Type | *b (width)* | *f (depth)* | *m (velocity)* |
|---|---|---|---|---|---|
| **This Study**[1] | Nova Scotia | 1st order | 0.23 | 0.56 | 0.65 |
| | | 2nd order | 0.19 | 0.11 | 0.7 |
| | | 3rd order | 0.13 | 0.1 | 0.78 |
| **van Proosdij et al (2010)** | Nova Scotia | | 0.54 | 0.17 | 0.29 |
| **Williams et al. (2002)** | California | | 0.46 | 0.18 | 0.36 |
| **Zeff (1999)**[2] | New Jersey | TF | -0.01 | -0.51 | 1.50 |
| | | TF | -0.01 | -0.03 | 1.02 |
| | | DE | 0.09 | -0.07 | 0.61 |
| | | DE | 0.14 | 0.26 | 0.33 |
| | | DE | 0.17 | 0.49 | 0.17 |
| | | DE | 0.22 | 0.62 | 0.78 |
| **Leopold et al. (1993)** | California | Mouth | 0.11 | 0.35 | 0.55 |
| | | Mid | 0.11 | 0.35 | 0.55 |
| | | Head | 0.17 | 0.40 | 0.25 |
| **Woldenberg (1972)** | Theoretical | | 0.727 | 0.227 | 0.045 |
| **Geyl (in Woldenberg 1972)** | Netherlands | | 0.72 | 0.23 | 0.05 |
| **Myrick & Leopold (1963)** | Virginia | | 0.04 | 0.18 | 1.05 |
| | | | -0.01 | -0.04 | 0.78 |
| | Delaware | | 0.08 | 0.14 | 0.78 |
| **Pestrong (1965)** | California | | 0.10 | 0.27 | 0.68 |
| **Redfield (1965)** | California | | 0.74 | 0.17 | 0.09 |
| **Langbein (1963)** | American | | 0.72 | 0.23 | 0.05 |
| | East Coast | | 0.72 | 0.22 | 0.06 |

1. Coefficients for bankfull condition only
2. TF = Through Flow channel; DE = Dead End channel

Also apparent in the hydraulic geometry scatter plots (Figure 2-8) was the differentiation of tidal and tidal-fresh channels. While regressions analysis showed a strong relationship between tidal channel geometry and bankfull prism, the regression for tidal-fresh channels was weak. As tidal prism increases, the differentiation of these two channel types becomes more apparent, with the slope of the regression line changing dramatically for the HHWLT prism (although $r^2$ values for tidal-fresh regressions remain low). This was believed to be an indication

that the morphology of tidal-fresh creeks responds primarily to changes in fresh-water discharges rather than tidal prism. So, while hydraulic geometry of the bankfull tidal prism may be used to determine dimensions for tidal channels, tidal-fresh channels should be treated differently. This implies that a good understanding of upland hydrology is required when planning restoration projects, and consideration given to freshwater discharge where relevant.

***Conclusion***

For marshes in the Avon estuary channel type and order should be primary considerations in determining channel dimensions. Where there is a significant input of freshwater, channel geometry was shown to be different, particularly for large creeks. High drainage density and low sinuosity seem to be typical for the region, and should be determined by site specific conditions such as marsh maturity, site history, and platform elevation in future restoration efforts. In the long term, incorporation of agricultural ditches and dykes has not appeared to reduce drainage density or sinuosity of creeks studied due to short channel segments and high drainage densities. Therefore agricultural ditches can and should be incorporated at restoration sites where it is appropriate to do so.

Hydraulic geometry equations (Bankfull prism) were shown to be valid for primary tidal channels in the study region, and can potentially be used to size tidal channels of primary creeks ($1^{st}$ and $2^{nd}$ order). However the relationships did not perform well for headwater creeks or freshwater channels. Based on observations of other authors headwater creeks should be allowed to develop through natural processes and through the incorporation of relict features (agricultural ditches, historic channels) whenever possible (Steel and Pye, 1997; Zeff 1999;

Williams et al., 2002; Wallace et al. 2005). Hydraulic geometry equations (all prisms) were not validated for tidal-fresh creeks, where it is believed freshwater discharges are the primary driver of channel morphology. Further investigation of this phenomenon could provide interesting results but is beyond the scope of this paper.

The importance of restoration practices that mimic local conditions has been acknowledged by restoration practitioners in many locations (Zeff, 1999; Wallace et al., 2005). The morphometric analysis conducted here allowed the determination of baseline conditions such as w:d ratio's, planform geometry, and drainage density which can greatly improve our ability to do this. Furthermore, the integration of custom GIS tools developed for this study provides tools which could be used again to further improve the data set. Finally the validation of hydraulic geometry equations for primary channels, which can be used in planning a restoration project, may be applicable in other macro and hyper-tidal estuaries.

## *References*


Allen, J. R. (1997). Simulation models of salt-marsh morphodynamics: some implications for high-intertidal sediment couplets related to sea-level change. *Sedimentary Geology 113*, 21 l-223.

Allen, J. R. (2000). Morphodynamics of Holocene salt marshes: a review sketch from the Atlantic and Southern North Sea coasts of Europe. *Quaternary Science Reviews 19*, 1155-1231.

Bayliss-Smith, T., Heakey, R., Lailey, R., Spencer, T., & Stoddart, D.R. (1979). Tidal flow in salt marsh creeks. *Estuarine, Coastal and Marine Scienct 9*, 235-255.

Bowron, T., Neatt, N., van Proosdij, D., Lundholm, J., & Graham, J. (2010). Macro-tidal Salt Marsh Ecosystem Response to Culvert Expansion. *Restoration Ecology 19:3*, DOI: 10.1111/j.1526-100X.2009.00602.x.

Chmura, G. L., Coffey, A., & Crago, R. (2001). Variation in Surface Sediment Deposition on Salt Marshes in the Bay of Fundy. *Journal of Coastal Research 17:1*, 221-227.

Connor, R. F., Chmura, G. L., & Beecher, B. (2001). Carbon accumulation in Bay of Fundy salt marhes: Implications for restoration of reclaimed marhes. *Global biogeochemical cycles 0*, 1-12.

Crooks, S., Schutten, J., Sheern, G. D., Pye, K., & Davy, A. J. (2002). Drainage and Elevation as Factors in the Restoration of Salt Marsh in Britain. *Restoration Ecology 10:3*, 591–602.

D'Alpaos, A., Lanzoni, S., & Marani, M. (2010). On the tidal prism–channel area relations. *Journal Of Geophysical Research 115, F01003*, doi:10.1029/2008JF001243, 2010.

D'Alpaos, A., Lanzoni, S., Marani, M., & Fagherazzi, S. (2005). Tidal network ontogeny: Channel initiation and early development. *Journal of Geophysical Research 110*, doi:10.1029/2004JF000182.

D'Alpaos, A., Lanzoni, S., Marani, M., Bonometto, A., Cecconi, G., & Rinaldo, A. (2007). Spontaneous tidal network formation within a constructed salt marsh: Observations and morphodynamic modelling. *Geomorphology 91*, 186–197.

Davidson-Arnott, R. G., van Proosdij, D., Ollerhead, J., & Schostak, L. (2002). Hydrodynamics and sedimentation in salt marshes: examples from a macrotidal marsh, Bay of Fundy. *Geomorphology 48*, 209–231.

Fagherazzi, S., & Sun, T. (2004). A stochastic model for the formation of channel networks in tidal marshes. *Geophysical Research Letters 31*, doi:10.1029/2004GL020965.

Fagherazzi, S., Hannion, M., & D'Odorico, P. (2008). Geomorphic structure of tidal hydrodynamics in salt marsh creeks. *Water Resources Research 44 (W02419)*, doi:10.1029/2007WR006289.

French, J. (2008). Hydrodynamic modeling of estuarine flood defense realignment as an adaptive management response to sea level rise. *JCR 24 (2B)*, 1-12.

French, J., & Stoddart, D. (1992). Hydrodynamics of salt marsh creek systems: Implications for marsh morphological development and material exchanges. *Earth Surface Processes and Landforms 17*, 235-252.

Friedrichs, C. T. & Perry, P.E., (2001). Tidal Saltmarsh Morphodynamics: A Synthesis. Journal of Coastal Research (SI 27), 7–37.Gordon, D. C. (1989). Habitat loss in the Gulf of Maine. *Sustaining our common heritage. Proceedings of the Gulf of Maine Conference.* (pp. 106–119). Portland, Maine: Gulf of Maine Council on the Marine Environment.

Gordon, D. C. (1989). Habitat loss in the Gulf of Maine. *Sustaining our common heritage. Proceedings of the Gulf of Maine Conference.* (pp. 106–119). Portland, Maine: Gulf of Maine Council on the Marine Environment.

Haltiner, J. H., & Williams, P. B. (1987). Slough channel design for salt marsh restoration. *Proceedings of the Eighth Annual Meeting of the Society of Wetland Scientists, May 6, 1987.* Seattle, Washington.

Hammersmark, C. T., Fleenor, W. E., & Schladow, S. G. (2005). Simulation of flood impact and habitat extent for a tidal freshwater marsh restoration. *Ecological Engineering 25* , 137–152.

Horton, R. (1945). Erosional development of streams and their drainage basins: hydrophysical approach to quantitative morphology. *Bulletin of the Geological Society of America 56*, 275– 370.

Konisky, R., Burdick, D. M., Dionne, M., & Neckles, H. A. (2006). A regional assessment of salt marsh restoration and monitoring in the Gulf of Maine. *Restoration Ecology 14:4*, 516–525.

Leopold, L. B., & Maddock, T. J. (1953). Hydraulic geometry of stream channels and some physiographic implications. *U. S. Geological Survey Professional Paper 252*, 55 p.

Leopold, L. B., Collins, J. N., & Collins, L. M. (1993). Hydrology of some tidal channels in esuarine marshland near San Francisco. *Catena 20*, 469-493.

Lohani, B., & Mason, D. C. (2001). Application of airborne scanning laser altimetry to the study of tidal channel morphometry. *ISPRS Journal of Photogrammetry & Remote Sensing 56*, 100– 120.

MacDonald, G. K., Noel, P. E., van Proosdij, D., & Chmura, G. L. (2010). The Legacy of Agricultural Reclamation on Channel and Pool Networks of Bay of Fundy Salt Marshes. *Estuaries and Coasts 33*, 151–160. DOI 10.1007/s12237-009-9222-4.

Marani, M., Belluco, E., D'Alpaos, A., Defina, A., Lanzoni, S., & Rinaldo, A. (2003). On the drainage density of tidal networks. *Water Resour. Res 39(2)*, 1040. doi:10.1029/2001WR001051.

Mitsch, W. J., & Gosselink, J. G. (2007). *Wetlands, fourth ed.* New York, NY, USA.: John Wiley& Sons.

Möller, I., Spencer, T., French, J. R., Leggett, D. J., & Dixon, M. D. (1999). Wave Transformation Over Salt Marshes: A Field and Numerical Modelling Study from North Norfolk, England. *Estuarine, Coastal and Shelf Science 49:3*, 411-426.

Myrick, R. M., & Leopold, L. B. (1963). Hydraulic geometry of a small tidal estuary. *USGS Professional Paper 411-B*. U.S. Printing Office, Washington, DC.

Novakowski, K. I., Torres, R., Gardner, L., & Voulgaris, G. (2004). Geomorphic Analysis of Tidal Creek Networks. *Water Resources Research, Vol. 40*, W05401, doi:10.1029/2003WR002722.

Pestrong, R. (1965). The development of drainage patterns on tidal marshes. *Stanford University Publications in the Geological Sciences. Volume X, Number 2. School of Earth Sciences. Stanford University, Stanford, California*.

Pethick, J. (1980). Velocity surges and asymmetry in tidal channels. *Estuarine, Coastal and Marine Science 11*, 331-345.

Redfield, A. (1965). Ontogeny of a salt marsh estuary. *Science 147*, 50-55.

Rinaldo, A., Fagherazzi, S., Lanzoni, A., Marani, M., & Dietrich, W. (1999). Tidal networks: 3. Landscape forming discharges and studies in empirical geomorphic relationships. *Water Resour. Res., 35(12)*, 3919-3929.

Shenker, J. M., & Dean, J. M. (1979). The Utilization of an Intertidal Salt Marsh Creek by Larval and Juvenile Fishes: Abundance, Diversity and Temporal Variation. *Estuaries 2:3*, 154-163.

Steel, T., & Pye, K. (1997). The development of salt marsh tidal creek networks: evidence from the UK. *Proceedings of the Canadian Coastal Conference, 22-25 May* (pp. 267 - 280). University of Guelph.

Stefanon, L., Carniello, L., D'Alpaos, A., & Lanzoni, S. (2010). Experimental analysis of tidal network growth and development. *Continental Shelf Research 30*, 950–962.

Teal, J. M., & Weishar, L. L. (2005). Ecological engineering, adaptive management, and restoration management in Delaware Bay salt marsh restoration. *Ecological Engineering 25*, 304–314.

van Proodsij, D., Babrick, J., & Baker, G. (2006b) . *Spatial and Temporal Variations in the Intertidal Geomorphology of the Avon River Estuary.* Halifax: Final report submitted to the Nova Scotia Department of Transportation and Public Works (NSTPW), 74.

van Proosdij, D., & Townsend, S. M. (2006). Spatial and Temporal Patterns of Salt Marsh Colonization Following Causeway Construction in the Bay of Fundy. *Journal of Coastal Research, SI 39 (Proceedings of the 8th International Coastal Symposium)* (pp. 1859 - 1863). Itajaí,SC Brazil: ISSN 0749-0208.

van Proosdij, D., Lundholm, J., Neatt, N., Bowron, T., & Graham, J. (2010). Ecological re-engineering of a freshwater impoundment for salt marsh restoration in a hypertidal system. *Ecological Engineering 36*, 1314–1332.

van Proosdij, D., Ollerhead, J., & Davidson-Arnott, R. G. (2006). Seasonal and annual variations in the volumetric sediment balance of a macro-tidal salt marsh. *Marine Geology 225*, 103– 127.

Wallace, K. J., Callaway, J. C., & Zedler, J. B. (2005). Evolution of Tidal Creek Networks in a High Sedimentation Environment: A 5-year Experiment at Tijuana Estuary, California. *Estuaries 28:6*, 795-811.

Weishar, L. L., Teal, J. M., & Hinkle, R. (2005). Stream order analysis in marsh restoration on Delaware Bay. *Ecological Engineering 25*, 252–259.

Weisher, L., Balleto, J., Teal, J., & Ludwig, D. (1997). Success criteria and adaptive management for a large-scale wetland restoration project. *Speacil Issue: Hydrologic Restoration of Coastal Wetlands. Wetlands Ecol. Manage. 4 (2)*, 111-127.

Williams, P. B., & Harvey, H. T. (1983). California coastal salt marsh restoration design. *Proceedings: Coastal Zone '83 Conference, American Society of Civil Engineers.* New York, June: O. T. Magoon and H. Converse, eds.

Williams, P. B., & Orr, M. K. (2002). Physical evolution of restored levee salt marshes in the San Francisco Bay Estuary. *Restoration Ecology 10:3*, 527–542.

Williams, P. B., Orr, M. K., & Garrity, N. J. (2002). Hydraulic Geometry: A geomorphic design tool for tidal marsh channel evolution in wetland restoration projects. *Restoration Ecology 10:3*, 577–590.

Woldenberg, M. (1972). Relations between Horton's Laws and hydraulic. *Harvard Papers in Theoretical Geography 45*, 1-39.

Wolters, M., Bakker, J. P., Bertness, M. D., Jeffries, R. L., & Möller, I. (2005). Salt marsh erosion and restoration in south east England: squeezing the evidence requires realignment. *Journal of Applied Ecology 42*, 844–851.

Zeff, M. L. (1999). Salt marsh tidal channel morphometry: Applications for wetland creation and restoration. *Restoration Ecology 7:2*, 205-211.

# Chapter 3 - Development of a superimposed hydraulic network at a hyper-tidal restoration site

To be submitted to: Ecological Engineering

***Introduction***

Tidal wetlands around the world have been significantly impacted by human activities leading to degradation and loss of habitat (Williams & Orr, 2002; Wolters et al., 2005; van Proosdij et al., 2010). In macrotidal (4-8 m) and hypertidal (> 8 m) environments where land reclamation through dyking has been prevalent, the loss of saltmarsh has been more acute (e.g. Weishar et al., 1997; Wolters et al., 2005; French, 2008; van Proosdij et al., 2010). In the Bay of Fundy, a hypertidal estuary, the loss of salt marsh has been estimated at 80-85% since European settlement (Gordon 1989; MacDonald et al. 2010). This has made the preservation and restoration of these habitats a priority in the region.

When restoration involves the breaching of dykes careful planning is important, as poorly executed projects can result in high velocity sheet flows leading to erosion, loss of vegetation, and braided stream channel systems unfavorable to sedimentation (Weisher et al, 2005). Although there are many factors to consider in this kind of restoration design (e.g. platform elevation, proximity of seed sources), appropriate hydrology is generally recognized as a vital component of project success and a driving factor in salt marsh morphology (Mitsch & Gosselink, 2007; Williams and Orr, 2002; Hammersmark et al., 2005; Konisky et al., 2006). The establishment of an efficient tidal channel network allows the movement of water through the system which provides sediment and nutrients to reach the marsh surface, as well as allowing flow paths for fish movement and panne habitat for waterfowl, particularly on tides which do not result in over-marsh flows (eg., neap tides) (Allen, 2000).

Another widely recognized feature of successful restoration projects is the recreation of marshes which resemble natural marshes in the region (Zeff, 1999; Wallace et al., 2005). In

chapter 2 we quantified important characteristics of tidal channel networks for salt marshes in the Bay of Fundy. They found important differences in the morphometric properties of channel networks, depending on the channel type and the maturity of the marsh being examined. This paper will first evaluate the progress of a salt marsh restoration project carried out in the region in the summer of 2009 in light of lessons learned at a site breached in 2005 with a similar history. Secondly it will assess the efficacy of the design methods used for these projects and suggest alternative approaches given new knowledge gained in the region since these projects were carried out. The lessons learned here will inform future projects in the region and may have applications elsewhere and provide valuable insight into the behaviour of restored hypertidal salt marshes.

***Project Design and Study Areas***

In 2009 CBWES Inc. developed the project design and undertook the restoration of a former tidal wetland in the Avon Estuary (Figure 3-1). The *Cogmagun Restoration Site (COG)*, an 8 ha site on the Cogmagun River, was dyked in 1991 by Ducks Unlimited Canada (DUC) to create a freshwater impoundment for waterfowl. Salt water intrusion led to poor water quality and high maintenance costs, ultimately leading to the decision to restore full tidal exchange. Prior to restoration the site was dominated by *Typha latifolia/Typha angustifolia*, and detrital material still covered part of the site by 2011.

Experience at a similar restoration project on the Walton River had raised the question of how to re-create drainage networks in the Bay of Fundy – a task not previously addressed in the region. The Walton River restoration, also a former DUC impoundment, was restored in 2005

and a 7 year monitoring program implemented. At this site a small channel was initiated in one of five excavated breaches and allowed to self-design. Between dyke breaching in August 2005 and the 2009 field season approximately 730 $m^3$ of material was eroded from the primary channel (van Proosdij et al., 2010). Seven years post-restoration the channel banks are fully vegetated and appear to be stable and a functioning hybrid drainage network has developed within the site (van Proosdij et al., 2010).

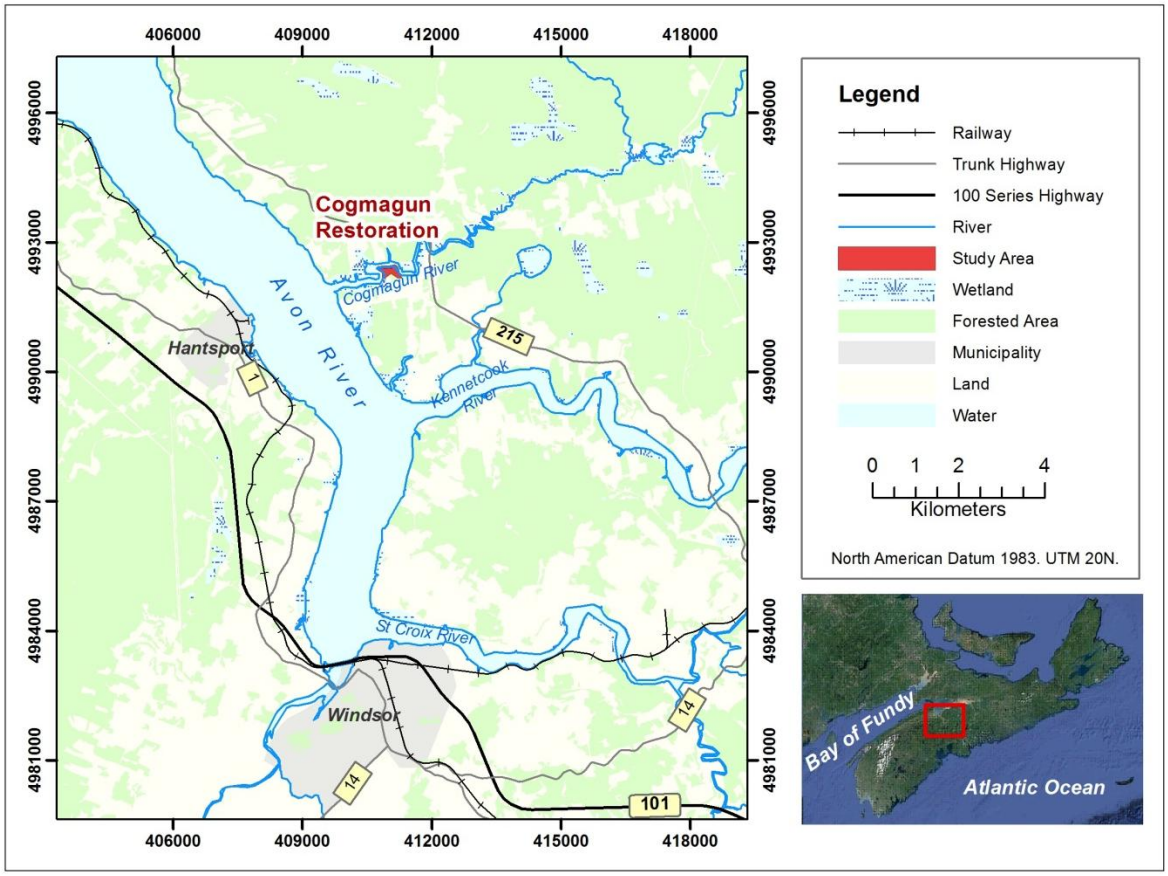


**Figure 3-1: Location of the Cogmagun Restoration in the Bay of Fundy**

Although the Walton River restoration site has progressed along acceptable trajectory, research has shown that is not always the case (Crooks et al., 2002; Weisher et al., 2005) and prompted a more active approach at the Cogmagun site. To that end, a preliminary data set collected from digital sources and observations in the Bay of Fundy were used to guide the restoration design (Graham et al., 2009). Beyond the creation of primary channels, the project was intended to follow the principles of ecological engineering, whereby the system is allowed to self-design or self-organize with as little human intervention as possible (e.g. Mitsch and Jørgensen, 2004; Weishar et al., 2005).

Historic aerial photographs and a LiDAR DEM were used to identify locations for dyke breaches and the excavation of channels, to better exploit existing drainage pathways. Due to the complex history of the restoration site, several pre-existing features needed to be incorporated into the design. A borrow pit of unknown depth, (formerly used to create and maintain the dyke structure) circumnavigated the inner edge of the dyke. A fairly extensive foreshore marsh dominated by the halophytic grass *Distichlis spicata* was present beyond the dyke and will be referred to from this point on as the fringe marsh. In addition to the impoundment dyke, the low-lying remnants of an agricultural dyke was located on the fringe marsh and dominated by the marsh elder. Aerial photographs show that by 1964 the dyke had been abandoned and breached in multiple locations, presumably by storm activity and not human intervention (Figure 3-2). During the period the site was actively farmed it was also extensively ditched, however the same imagery shows the incorporation of ditches into a developing hybrid or superimposed drainage network. It was anticipated the hybrid network would be re-activated and the borrow pit incorporated following the re-introduction of tidal flow.

Several designs were developed by CBWES Inc., however consultation with the landowners and other constraints resulted in the decision to excavate a single breach (60 m in length) and channel at the location of the water control structure, connecting the borrow pit with the river (Figure 3-2) rather than multiple breaches as at Walton (van Proosdij et al., 2010).

The existing channel at the site of the water control structure was used so that only a small portion of the channel needed to be excavated (ie, where the dyke and water control structure were located). The channel mouth was not disturbed and was allowed to adjust through natural processes to accommodate the new flow regime. Based on observations in the Bay it was decided that widening the channel and removing the vegetative cover that was in place would be more detrimental than helpful, potentially destabilizing the banks and leading to excessive erosion. Widening of the channel was anticipated to occur through natural processes of erosion and deposition.

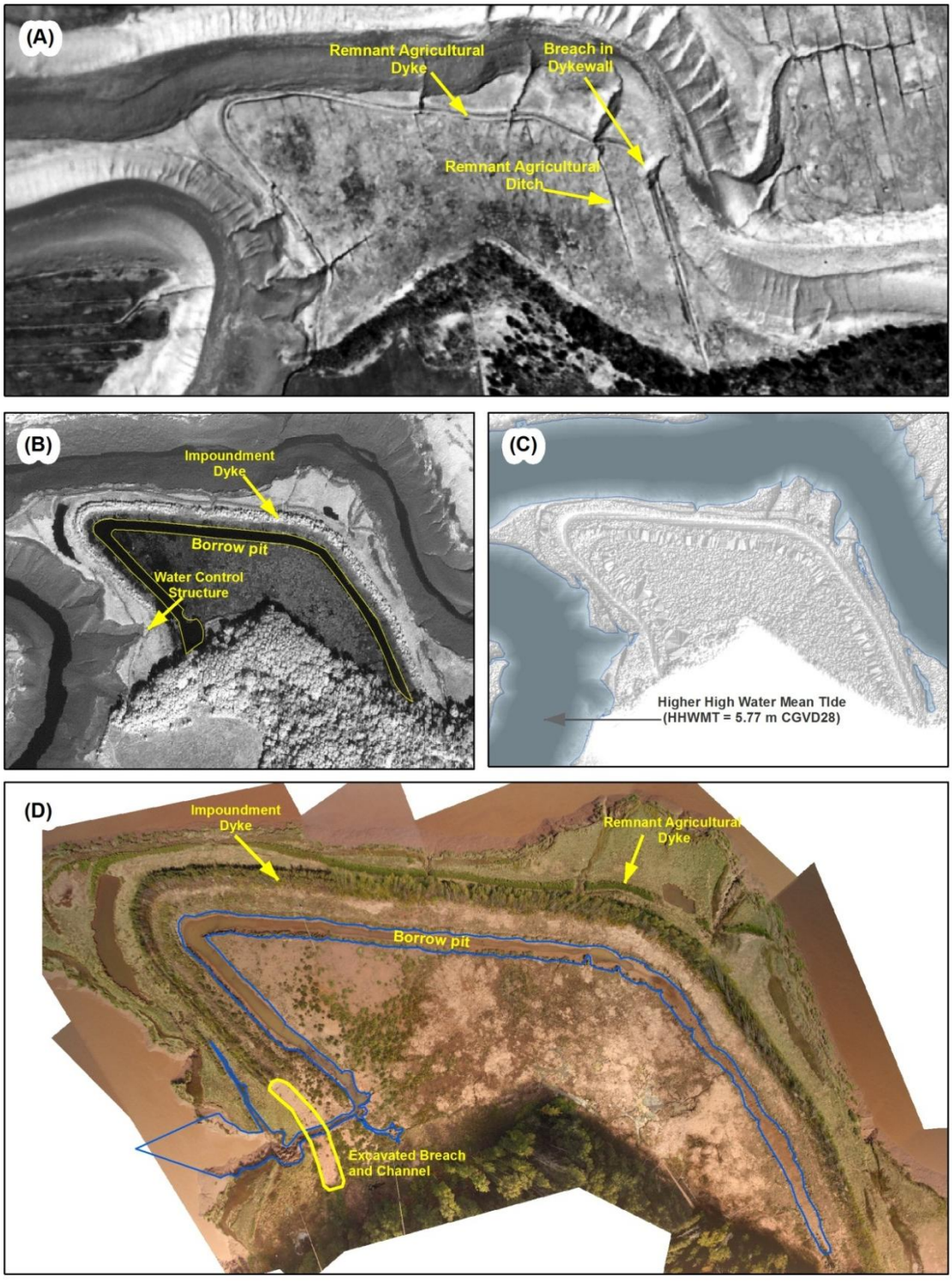


**Figure 3-2: A) 1964 air photo with relict agricultural features. B) 2007 IKONOS Satellite imagery with impoundment features. C) 2007 LiDAR DEM used in flood modeling analysis. D) 2011 low-altitude aerial photography of restored marsh**

***Methods***

To assess the development the hydraulic network at the restoration site several methods were employed. Development of the excavated channel was measured using cross-section profiles taken periodically along four established transects between August 18, 2010 and August 19, 2011. Two surveys were performed (November 1, 2010 and May 1, 2011) using a real time kinematic (RTK) GPS with a reported survey accuracy of 8 cm horizontal and 15 cm vertically. All surveys were conducted in UTM NAD83 and elevations referenced to the Canadian Geodetic Vertical Datum (CGVD28). These were used to create cross-sectional profiles and high resolution digital elevation models (DEM).

Channel dimensions and the volume of sediments removed the excavated channel in a GIS environment were calculated in ESRI ArcGIS using 3d analyst toolbox. Several triangulated irregular network (TIN) surfaces were created using the survey data and points extracted from a LiDAR surface to provide additional structure where necessary. A TIN is a vector based surface model constructed by triangulating a set of vertices (points) (ESRI ArcGIS, Desktop Help, 2012). Custom tools, constructed for and described in chapter 2 were used to delineate upstream area, contributing marsh area and tidal prism based on the last GPS survey.

In addition four low-tech surveys throughout the summer seasons of 2010 and 2011 were conducted using a cross-section method recommend by the US Geological Survey (2011). In this method, surveyed permanent benchmarks (in this case wooden stakes) were used to run a rope across the creek. Benchmarks were established 5, 10 and 15 meters from the creek bank at time of set-up (August 2010). Measurements were initiated from the south bank and the rope tide to the 5 m stake unless erosion or other field conditions prevented use of this stake, in

which case the 10 m stake was used and so on. A stadia rod was used to determine depth below the rope at given points from the known benchmarks at a 1 meter interval. Special note was made of the thalweg position and for well-defined banks (ie, cliff face) if it did not fall at the prescribed 1 m interval. Processing of the rope-and-stadia data was done in MS Excel and cross-sections plotted for comparison. The location of transects and an illustration of the survey methods used are shown in Figure 3-3.

Low-altitude aerial photography taken in September 2010 and l 2011 were used to assess the development of the drainage network and dewatering of the site. Plover I (Figure 3-4) is a remotely operated, tethered balloon and suspended camera system (SLR with wide-angle lens). When deployed at 100 m altitude, the system has the potential to give image ground footprints of 240 m by 140 m with 10 cm resolution. Further details of image processing techniques (eg. mosaic, ortho-rectification) can be found in Lemieux (2012).

Ancillary data, specifically for surface elevation and vegetation, were drawn from data provided by CBWES Inc. to better understand the development of the overall marsh morphology for Cogmagun restoration in comparison to the Walton restoration. At both Walton and Cogmagun restorations CBWES Inc. are conducting a 5-7 year monitoring program (Bowron and Chaison, 2006; van Proosdij et al, 2010). Based on a modified version of the GPAC protocol (Neckles et al., 2002; Konisky et al., 2006) the program incorporates methods from other studies as well as lessons learned by the company over the past decade. Further details of the monitoring program can be viewed in reports found at www.cbwes.com.

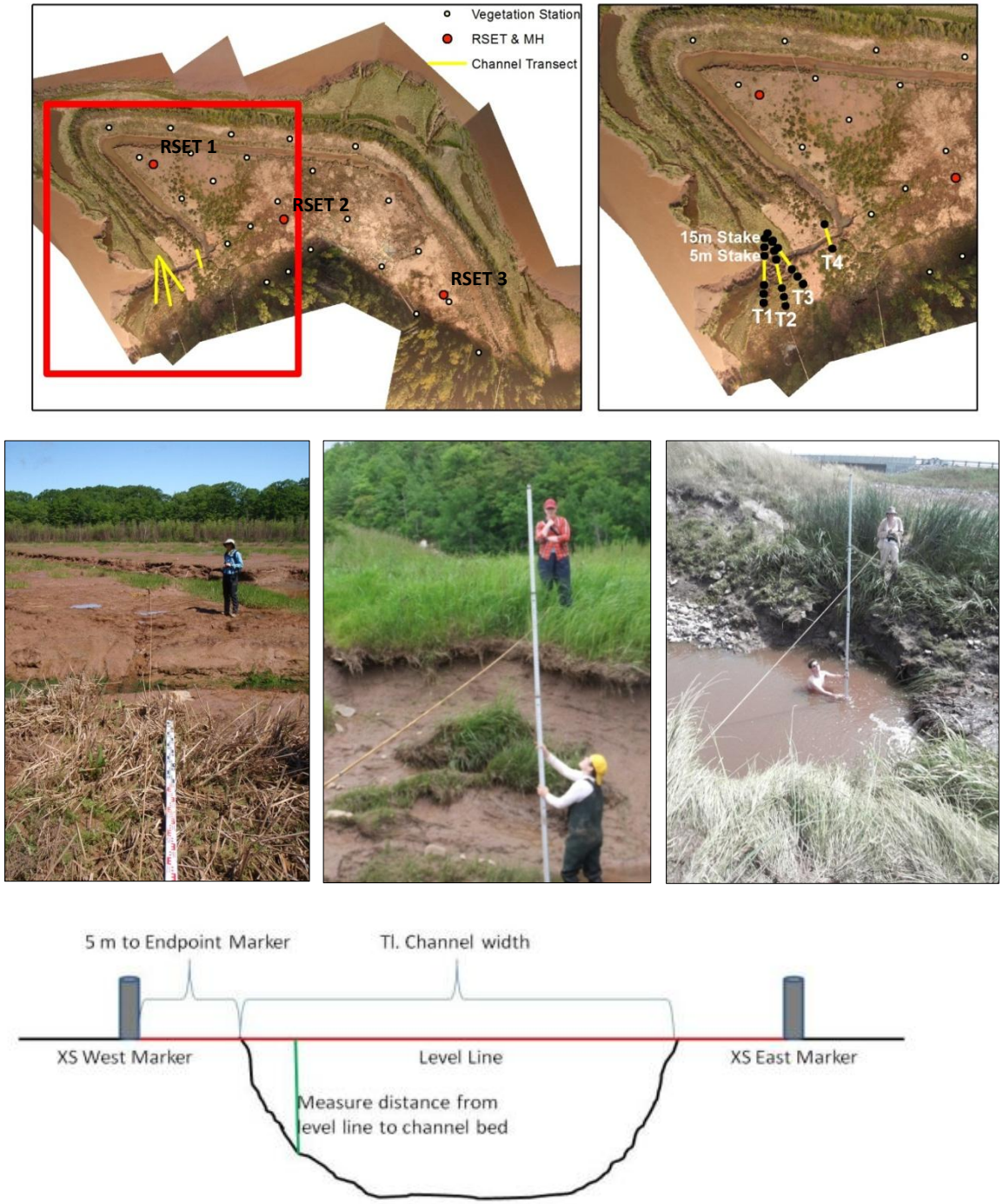


**Figure 3-3: Location of transects at excavated channel and illustration of the low-tech rope-and-stadia method used to obtain cross-section profiles (figure adapted from USGS (2011))**

**Figure 3-4: Plover 1 during site survey and example of low altitude oblique imagery for Cogmagun Restoration site**

Marsh surface elevation change (±0.001m) was measured once per year using a rod sediment elevation table (RSET; Cahoon et al., 2002). All measurements were taken at low tide and at the same time in the growing season (September) to minimize the influence of evapotranspiration (Paquette et al., 2004). Vertical accretion at all sites was measured using feldspar marker horizons as described by Cahoon et al. (1996), with three horizons matched to each SET. Vegetation surveys were conducted using a point intercept method (Roman et al., 2001; Bowron et al., 2009) at these stations and used to determine species composition and abundance.

During the feasibility study for Cogmagun restoration equilibrium channel dimensions were calculated using modified hydraulic geometry equations, a method developed by the consulting firm Phillip Williams and Associates (PWA) for restoration projects in the San

Francisco Bay beginning in the 1980's. Hydraulic geometry "connotes the relationships between the mean stream channel form and discharge both at-a-station and downstream along a stream network in a hydrologically homogeneous basin" (Singh, 2003, p. 196). Williams et al. (2002) developed empirical relationships using potential mean tidal prism (volume of water entering and leaving the estuary during a tidal cycle between the planes of MHHW water and mean low low water (MLLW) and contributing marsh area as a surrogate for discharge. Channel dimensions were based on geomorphic criteria (ie., elevation of Mean higher high water, MHHW). Because Williams et al. (2002) recommend the use of regional data when applying this approach equations were generated for the Bay of Fundy using a preliminary set of marshes and a high resolution LiDAR DEM. Due to the extreme tidal range of the Bay of Fundy tidal prism was felt to be a more appropriate metric than contribution marsh area (Graham et al. 2009).

The extreme tidal range of the Bay and its potential effect on tidal flows prompted testing of different tidal prisms. Because the relationships generated in this preliminary work were based entirely on digital data there were errors inherent in the data, regressions were weak ($r^2$<0.8) and more work needed to be done. Van Proosdij et al. (2010) tested the preliminary equations at Walton and found that, depending on the tidal prism used, equilibrium conditions were either under-predicted or over-predicted. In chapter two new hydraulic geometry equations were developed from ground surveyed data. These were tested at the Cogmagun site.

***Results***

Annual GPS surveys augmented with stadia rod measurements at the mouth of the primary channel showed an overall widening and deepening of the channel along 3 of the 4 transects. Little change was observed at T4, located farthest from the creek mouth. There appeared to be seasonal trends of deposition and erosion (Figure 3-5). When cross-sectional area and depth were examined the same trends were apparent, however width is steadily increasing with no apparent decrease (Table 3-1).

The RTK survey data was used to calculate the volume of material removed from the creek in each year. In the first season following restoration (August 2009 to November 2010) an estimated 480 $m^3$ of material was eroded from the channel. Over the winter season (November 2010 – May 2011) an additional 160 $m^3$ was eroded, considerably less than in the initial year. Although a fall survey was not completed, rope and stadia rod data imply that channel area did not further increase in the 2011 summer season, and that some deposition or redistribution of sediments occurred.

Delineation of the drainage network and open-water habitat from high resolution low-altitude photography was accomplished manually and revealed some interesting patterns on the marsh (Figure 3-6). Open water (borrow pit and panne habitat) accounted for roughly 16.8 % of the site in 2010 and 15.2% in 2011 as several pannes reformed in shape or disappeared all-together as the surface consolidated and low lying areas filled in. The reactivation of drainage ditches observed in the 1964 air-photos was apparent in both images. Some drainage ditches were visible only in 2010, while other ditches were visible in 2011 but not clearly connected to

the borrow pit or panne network. Pannes also are frequently oriented along ditches and connected by them, although this can be more difficult to detect.

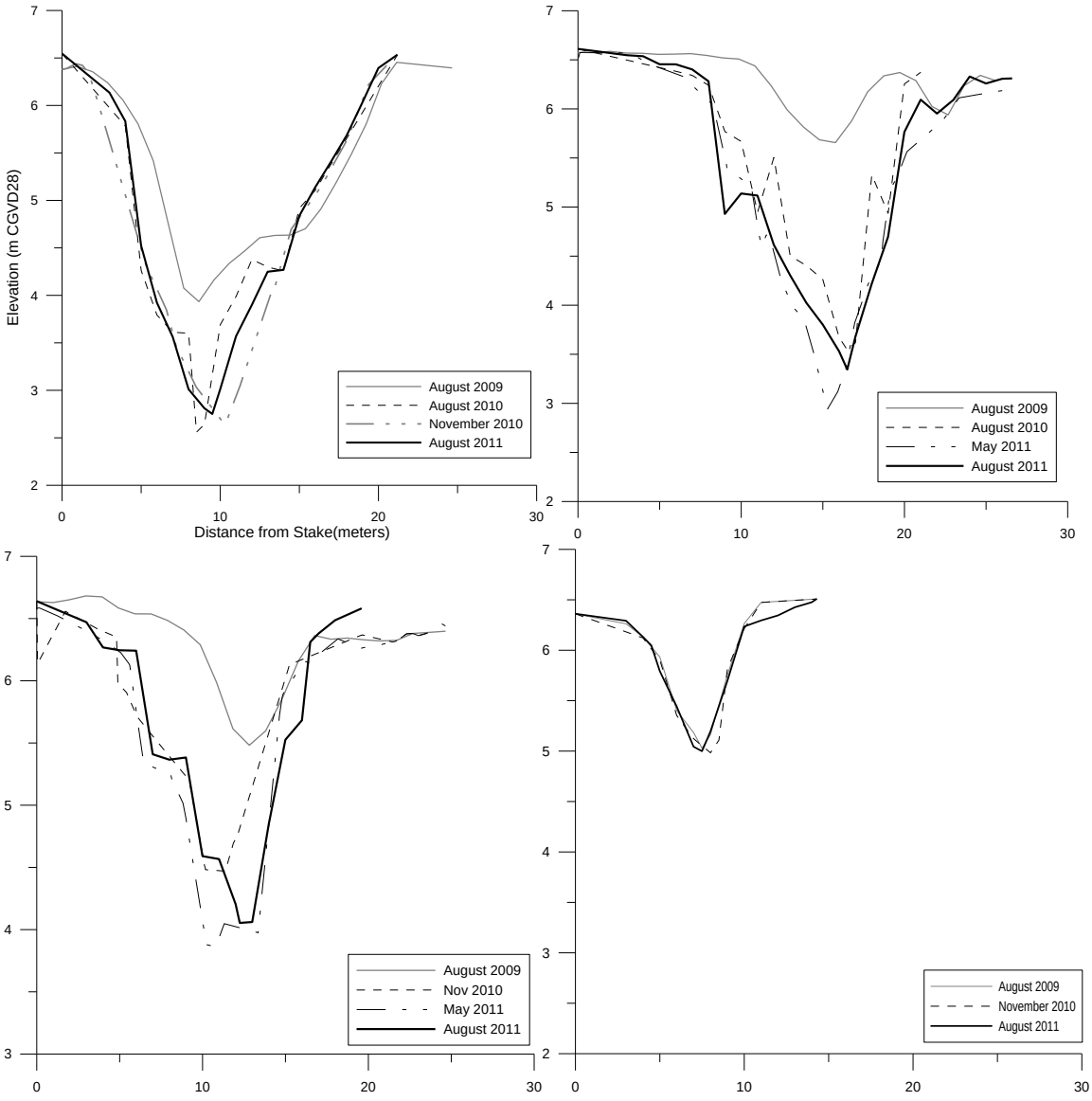


**Figure 3-5: Cross-sectional profiles for Cogmagun Restoration T1-T4. Deepening and widening of the channel at T1-T3 is evident. Change over time shows seasonal infilling of the channel as well as erosion. T4 appears stable.**

**Table 3-1: A) Cross-sectional area ($m^2$); B) Thalweg elevation and mean elevation (m CGVD28) and C) Width (m) from field observations at bankfull condition for rope and stadia rod cross-sections.**

| A) | *Date* | *Survey method* | *T1* | *T2* | *T3* | *T4* | *Total* |
|---|---|---|---|---|---|---|---|
| | *August 1, 2009* | Modified LiDAR | 28.16 | 4.68 | 7.28 | | 40.12 |
| | *August 19, 2010* | Rope and Stadia | 35.11 | 19.58 | 14.16 | 5.53 | 74.38 |
| | *October 1, 2010* | Rope and Stadia | 37.76 | 20.42 | 17.63 | 6.09 | 81.89 |
| | *November 1, 2010* | RTK GPS | 38.73 | 21.23 | 17.19 | 3.63 | 80.79 |
| | *May 1, 2011* | RTK GPS | 39.30 | 27.77 | 21.75 | 5.13 | 93.94 |
| | *June 20, 2011* | Rope and Stadia | 37.20 | 28.08 | 15.28 | 5.99 | 86.55 |
| | *August 18, 2011* | Rope and Stadia | 35.92 | 25.37 | 17.12 | 6.13 | 84.54 |

| B) | *Date* | *Thalweg elevation* | | | | *Mean elevation* | | | |
|---|---|---|---|---|---|---|---|---|---|
| | | **T1** | **T2** | **T3** | **T4** | **T1** | **T2** | **T3** | **T4** |
| | *Aug, 2009* | 3.93 | 5.66 | 5.48 | 5.57 | 5.26 | 6.29 | 6.31 | 6.56 |
| | *Aug 19, 2010* | 2.56 | 3.54 | 4.15 | 5.03 | 4.37 | 5.24 | 5.35 | 5.81 |
| | *Oct 1, 2010* | 2.68 | 3.56 | 3.81 | 4.98 | 4.59 | 5.16 | 5.15 | 5.75 |
| | *Nov 1, 2010* | 2.64 | 3.43 | 4.47 | 5.08 | 4.74 | 5.61 | 5.88 | 6.36 |
| | *May 1, 2011* | 2.83 | 2.94 | 3.86 | 5.04 | 4.78 | 5.18 | 5.94 | 6.04 |
| | *June 20, 2011* | 2.69 | 2.99 | 3.98 | 5.06 | 4.85 | 5.33 | 5.49 | 5.89 |
| | *Aug 18, 2011* | 2.75 | 3.34 | 4.05 | 5.00 | 4.67 | 5.40 | 5.62 | 5.95 |

| D) | *Date* | *T1* | *T2* | *T3* | *T4* |
|---|---|---|---|---|---|
| | *August 19, 2010* | 16.50 | 20.90 | 14.15 | 4.30 |
| | *October 1, 2010* | 16.70 | 21.10 | 14.45 | 4.30 |
| | *June 20, 2011* | 17.22 | 21.84 | 15.64 | 4.60 |
| | *August 18, 2011* | 17.22 | 23.58 | 15.75 | 5.01 |

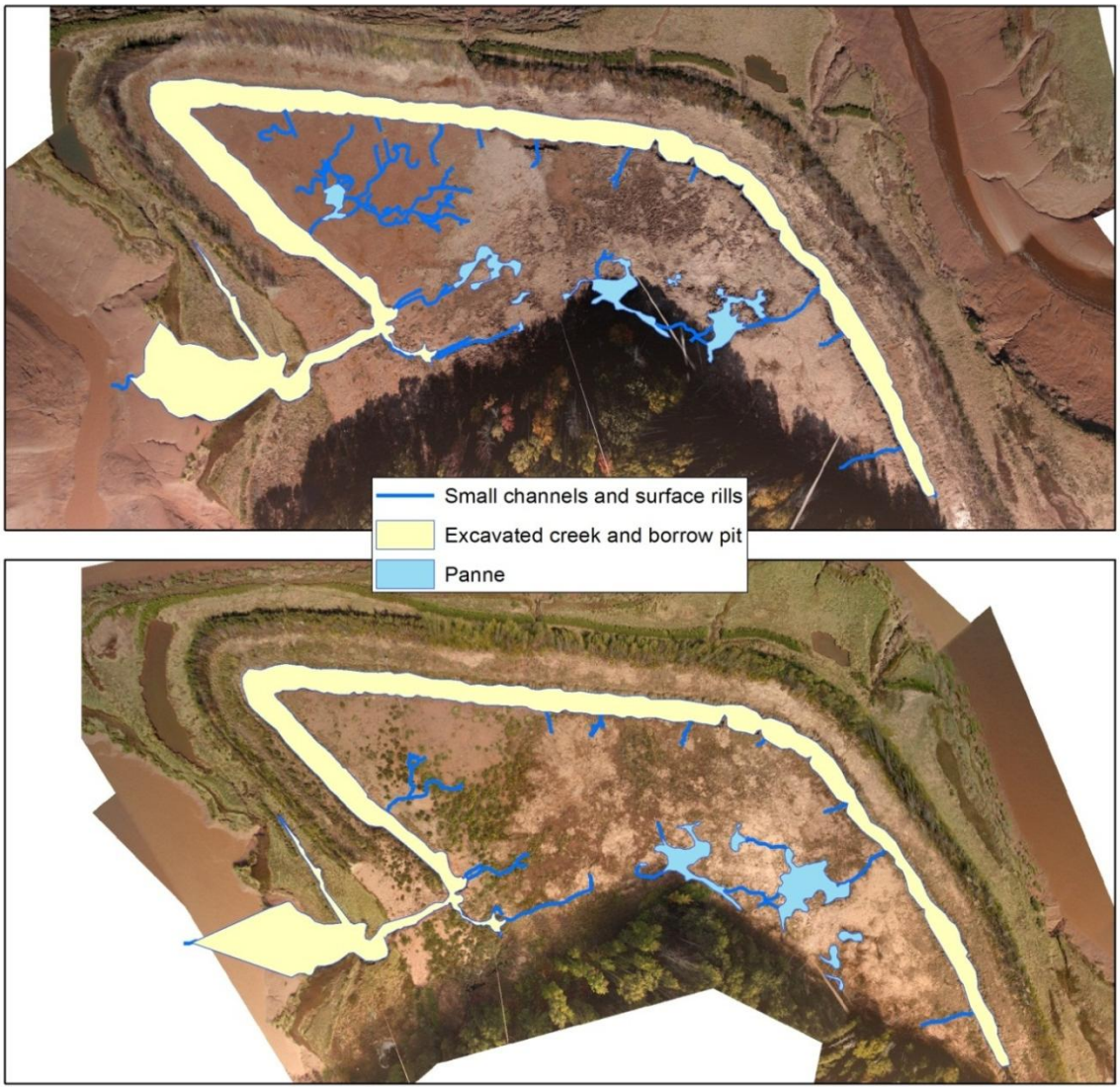


**Figure 3-6: Network delineation for the September 2010 and September 2011.**

Drainage density in the initial year was 0.032 $m/m^2$ and decreased to 0.027 $m/m^2$ in fall 2011. The formation of small surficial rills and channels which were absent in 2011 accounted for the differences in drainage density, particularly in the North-west corner of the site. Shown in detail in Figure 3-7, this area was very unconsolidated and waterlogged with low elevations immediately post-restoration.

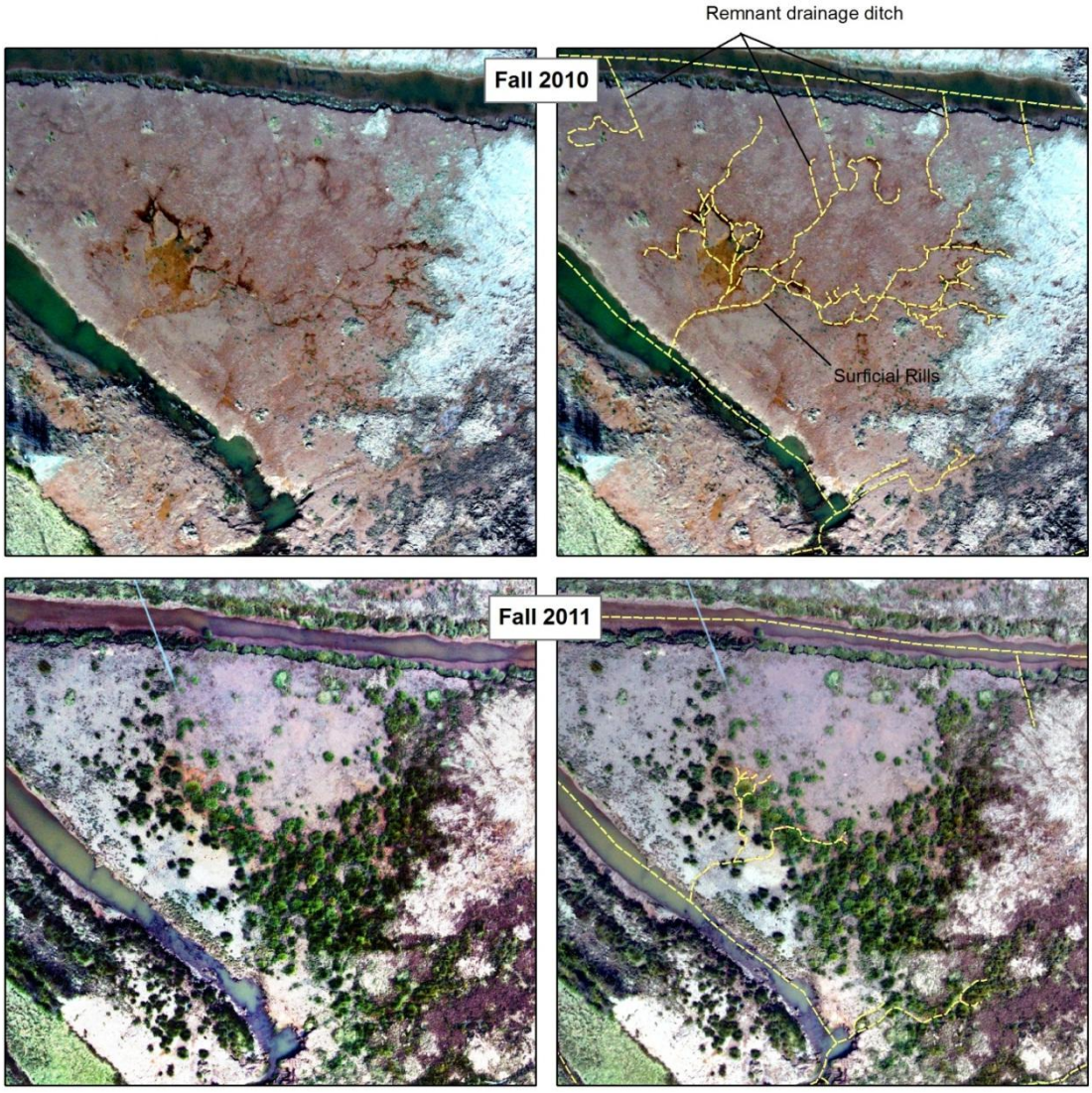


**Figure 3-7: Close up of North-western corner of site, where a complex network of surficial rills formed in 2010 but has largely disappeared or been obscured by the expansion of Spartina alterniflora.**

RSET data showed a decrease of 2.1 cm in the first year for that portion of the site, and with very little accretion at the associated marker horizons it was attributed to de-watering and consolidation. In 2011 the same RSET recorded an increase of 1.32 cm, the highest accretion rates recorded at the site and in line with accretion rates observed at an upstream reference site (Bowron et al., 2012). The presence of vegetation (*Spartina alterniflora*) in 2011 which had been

absent the previous season was another sign of sediment consolidation as seedlings were able to take root.

Planimetric changes in the excavated creek can be seen in the 2010 and 2011 imagery, particularly slumping of the southern bank and the development of riffles (white water), pools (calm water), and slump blocks in the channel (**Figure 3-8**). Straightening of the creek thalweg also occurred as the channel erodes. A longitudinal profile of the creek thalweg showed a gradual "smoothing" of the channel bottom over time, leading to a more uniform slope. Photos taken of the creek evolution further illustrate the migration backwards of a "waterfall" and plunge-pool created by a very shallow channel pre-restoration (Figure 3-9).

Accretion rates recorded by the marker horizons and RSETS (Figure 3-10 and Table 3-2) showed a lowering of the marsh surface over the first year of monitoring despite accretion at marker horizons. This was associated with dewatering of the site and potentially with decomposition of below-ground root mass. In the second year of monitoring surface elevations increased and additional deposition was recorded by the marker horizons.

Hydraulic geometry equations, developed Chapter 2 were tested to determine how well the predicted equilibrium conditions would correspond with channel dimensions observed at the Cogmagun site in the final survey of this study (Table 3-3). In the 2009 feasibility study only the dimensions for the mouth (T1) were predicted, so testing was limited to this transect. The 2009 feasibility study (which used the spring tidal prism as a surrogate for discharge and a preliminary digital dataset) overestimated the dimensions of the channel considerably. However when the bankfull tidal prism and refined equations presented in Chapter 2 were used they were underestimated.

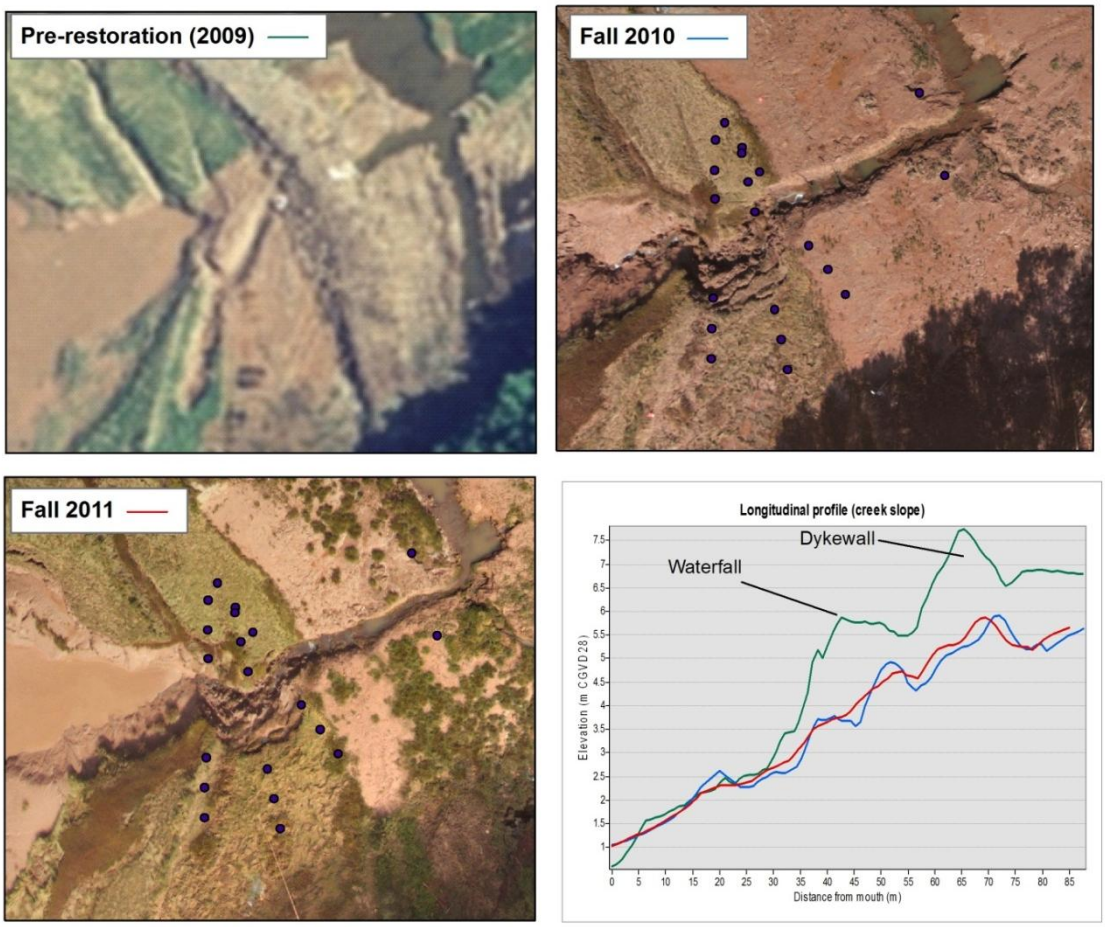


**Figure 3-8: Development of excavated creek. Pre-restoration imagery from 1992 aerial photograph, while 2010 and 2011 from low-altitude photography. Longitudinal profiles (extracted from 2007 Lidar surface 2010, and 2011 elevation surveys) show illustrates the gradual elimination of waterfall and plunge pool and the "smoothing" of the channel thalweg, with some riffle and pool sections still remaining.**


**Figure 3-9: Development of the excavated channel at Cogmagun. (A) Excavated channel during earthworks (August 2009). (B) May 2010 - waterfall migration backwards to T3 and slumping throughout. (C) September 2011 - Complete elimination of restriction and development of a series of pools and riffles.**

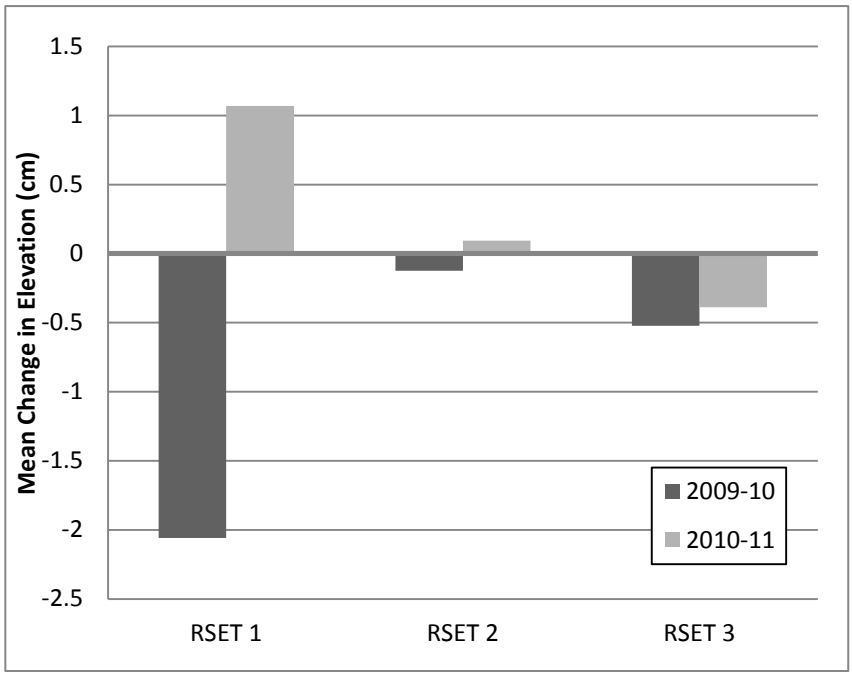


**Figure 3-10: RSET measurements from 2009-2010 and 2010-2011**

**Table 3-2: Marker horizon measurements from 2009-2010 and 2010-2011**

| Cogmagun - MH measurements 2010-11 | | | | net accretion (cm/yr) | |
|---|---|---|---|---|---|
| **RSET-01 HM** | **mean (cm)** | **# cores** | **quality** | **2009-10** | **2010-11** |
| core 1a | 0.95 | 1 | great | 0.00 | |
| core 1b | 1.34 | 1 | great | 0.00 | |
| core 1c | 1.10 | 1 | ok | 0.00 | |
| **mean** | **1.13** | | | **0.00** | **1.13** |
| **RSET-02 - MM** | **mean (cm)** | **# cores** | **quality** | **2009-10** | **2010-11** |
| core 2a | 2.53 | 1 | ok | 1.19 | |
| core 2b | 1.70 | 1 | great | 1.28 | |
| core 2c | 3.99 | 1 | ok | 1.81 | |
| **mean** | **2.74** | | | **1.43** | **1.32** |
| **RSET -03 LM** | **mean (cm)** | **# cores** | **quality** | **2009-10** | **2010-11** |
| core 3a | 2.28 | 1 | good | 0.61 | |
| core 3b | 2.40 | 1 | good | 0.86 | |
| core 3c | 2.95 | 3 | great | 0.89 | |
| **mean** | **2.54** | | | **0.79** | **1.76** |

**Table 3-3: Observed and predicted equilibrium conditions for Cogmagun restoration T1**

| | | |
|---|---|---|
| **Observed Geometry (2011)** | *Width (w)* | 23.3 |
| | *Mean Depth (d)* | 1.6 |
| | *Thalweg Depth (D)* | 3.2 |
| | *XS Area (A)* | 36.6 |
| **Feasibility Report (2009) Predicted Geometry** | *Width (w)* | 33.6 -37.9 |
| | *Mean Depth (d)* | |
| | *Thalweg Depth (D)* | 3.42 |
| | *XS Area (A)* | |
| **Graham et al. (2012) Predicted Geometry** | *Width (w)* | 20.4 |
| | *Mean Depth (d)* | 1.7 |
| | *Thalweg Depth (D)* | 5.0 |
| | *XS Area (A)* | 25.6 |

***Discussion***

The development of an effective hydraulic network has been rapid and thus far has met anticipated outcomes for the site. Since tidal flow was restored the site has significantly dewatered and relict creeks have been activated (Allen, 200; MacDonald et al. 2010; van Proosdij et al., 2010). Although a more active approach was taken in the creation of an excavated channel than at the Walton site, a considerable volume of sediment has been eroded from the creek none the less. Some of this sediment may have been transported to the site interior, interpretation of the data suggests the majority of the material was exported from the site. Accretion rates recorded by the RSETS and marker horizons at the restoration sites ranged from 1.13-1.76 cm and are in line with a reference site used for monitoring work by CBWES Inc., where rates ranged from 0.78 – 1.42 (Bowron et al,. 2012). Furthermore, the RSET closest to the excavated creek recorded the lowest accretion rates.

Migration backwards of the “waterfall” initially located at the mouth of the creek also has implications for the movement of sediment in the system. The erosion of this feature was observed to occur predominantly when water was leaving the site, both during the removal of the dyke and during ebb tide. Several studies have observed pulses in velocity throughout the ebb tide, particularly during spring tidal flows, which would be capable of eroding or re-suspending sediments in the tidal channel and initiating headward channel extension (French and Stoddart, 1992; Steel and Pye 1997; Allen 2000). At Allen Creek, located in the upper Bay of Fundy, Davidson-Arnott et al. (2002) found the strongest velocity pulses were restricted to the very end of the ebb tide. Because much of the outgoing tide in this macrotidal marsh drained directly from the marsh margin the flow/volume was distributed over a large cross-sectional area and high velocity flows were limited.

The impoundment dyke at the Cogmagun site prevents drainage via the marsh margin as would be observed at a natural marsh or even at Walton where multiple breaches were created. Therefor the excavation of a single breach would be expected to prolong high velocity flows and potentially intensify them by preventing the flow of the outgoing tide over the marsh margin except at the breach location. Although infilling and consolidation has occurred in the part of the borrow pit farthest from the dyke breach the pit remains deep and shows little evidence of sedimentation near the main channel. Erosion occurring on the outgoing tide would cause sediment to be lost from the site, rather than returned to it. In an environment such as the Bay of Fundy, where suspended sediment loads are exceptionally high, this does not present a large concern for accretion within the restored area. However, in a sediment-limited environment this scenario could be detrimental to the overall-recovery of the site.

The development of the primary channel has been characterised by periods of erosion and deposition – with cross-sectional area increasing throughout the initial year and a half but decreasing throughout the summer of 2011. While investigating seasonal variability at Allen Creek van Proosdij et al. (2006) found increased deposition in the low marsh throughout the summer season. This also agrees with field observations in the Bay, where sediment in the creeks is scoured out during the winter and deposited over the summer season. Variability in creek cross-section may also be associated with a redistribution of the sediment in the creek, as observed at Walton. Much of the erosion occurring in this channel has been through slumping of the banks, leaving large chunks of intact vegetation along the banks and in the channel bottom. As vegetation has been shown to increased deposition, these vegetated slump blocks may be trapping sediments and decreasing cross-sectional area (Shi et al., 1996; Temmerman et al., 2005).

At the Walton River Restoration van Proosdij et al. (2010) noted a rate of headward growth for the primary creek of 12 m/year, which was within the range reported by D'Alpaos et al. (2007) in Venice Lagoon but much greater than those reported by Wallace et al (2005) in California. Taken from the location of the waterfall at the time of restoration to the excavated portion of the channel which has not experienced significant erosion since restoration a rate of headward growth of roughly 13.5 m/year was calculated. While the Walton channel maintained a slope of 1% the Cogmagun channel has a slope of 7% for the segment of channel that was actively eroding. It is plausible that the channel may not have reached its equilibrium dimensions yet, as vegetation has not colonized the dyke footprint or the banks of that portion of the channel. It is also possible that equilibrium channel slope for a site at this location in the tidal frame is higher. Mean channel slopes for the region, based on data collected for four reference

marshes in the Avon, ranged from 0.3 to 29 % for primary creeks (See Chapter 2). Wallace et al. (2005) found that channels reached equilibrium dimensions with four to five years, while van Proosdij et al. (2010) found that Walton appeared to be reaching equilibrium conditions within five years.

Beyond the evolution of the primary channel, the hydraulic network at Cogmagun appeared to be developing effectively. Drainage densities are comparable to those observed at other sites in the region and in other estuaries (Wallace et al., 2005; MacDonald et al. 2010) and in chapter 2. The development of surficial rills and reactivation of agricultural ditches has allowed for a more effective dewatering of the site, particularly in the North-western quadrant. Unexpectedly, many of these small channels and ditches are not detectable in the 2011 imagery, and site visits confirm that the channels have either become substantially less extensive or disappeared altogether. It is believed that these formed temporarily in response to site de-watering but filled in as the marsh elevation began to build and discharge decreased.

Low-altitude photography was exceptionally useful in this project, facilitating channel delineation over a relatively short period of time and without the need for intense field surveys. The resolution of these images (10 cm), when compared to traditional air-photos or satellite imagery, allowed the delineation of very small channels that would have been otherwise undetectable. However there were also limitations of the technology. Where vegetation was dense channels were obscured and difficult to identify. Shadows along the upland edge also made channel identification difficult. Finally there were challenges yet to be addressed in the processing and orthorectification of the imagery due to inherent errors in the lenses of off-the-

shelf cameras and flying the helium balloon (ie, field conditions, GCP construction, photo distribution) (Lemieux, 2012).

Despite similar site histories the recovery of the Cogmagun site appears to be on a different trajectory than that of the Walton site. Accretion rates and changes in surface elevation have been similar at both sites (Bowron et al., 2012), however the creation of only one breach in the dyke at Cogmagun (as opposed to five at Walton) resulted in substantial differences in the movement of tidal waters through the site. A major component of sediment transportation in the Bay is associated with ice which can move large chunks of sediment and vegetation around during the winter months (van Proosdij et al., 2006). These ice block deposits have not been observed at Cogmagun as they were at Walton, however this may be attributed to mild winters and further monitoring will be required. Furthermore, remains of the Typha community which dominated the site pre-restoration formed a thick matt of detrital material on the eastern portion of the site. This could not be effectively removed from the system. While the currents at the Walton site follow basin wide patterns at spring tides, as observed at other macro-tidal sites (Davidson-Arnott et al., 2002), the lack of a breach on the eastern dyke prevents this flow. Although not observed at the site to date, the decay of the detrital matt could create anoxic soils which suppress new growth (Portnoy, 1999) and limit the recovery of vegetation.

On the other hand the developing plant community at Cogmagun, two years in, is more diverse than that of Walton. In its third-year post restoration the Walton site continued to be dominated by *Spartina alterniflora*, the low marsh cord-grass characteristic of the region, and was lacking a high marsh community (van Proosdij et al., 2010). By its second-year post-

restoration halophytic richness at the Cogmagun site was equivalent to that at the reference site (Bowron et al., 2012). This may be in attributed in part to the condition of each site at the time or restoration. Walton was a bare mudflat to, while some halophytes were already present at Cogmagun prior to restoration. On the other hand, examination of 2011 habitat map shows *S. alterniflora* colonizing areas that in 2010 were bare mudflat. Where the detrital material is present other halophytes such as *Spartina patens, Suaeda maritima, Sciprus maritimum,* and *Juncus gerardi* have taken hold (Bowron et al., 2012). So although the decaying cattails could lead to anoxia in the soil, they may also be providing mirco-habitats for seedlings and limiting the growth of *S.alterniflora*, thus increasing species diversity within the site.

Although the excavated channel at Cogmagun appears to be developing at an acceptable rate additional planned restoration in the region led to a re-examination of design methods. The feasibility study, using preliminary LiDAR-generated data, predicted a creek mouth (T1) measuring between 33.6 and 37.9 meters depending on the tidal prism used. When the equations developed in Chapter 2 for bankfull prism (best regression) were tested the equilibrium conditions were underestimated (ie., current conditions already exceed those predicted). This may be partly attributed to difficulties in correctly quantifying the tidal prism. Accurate dimensions for the borrow pit were unattainable due to water depths and unsafe conditions, therefor the prism is probably under-estimated. It also may be partly attributed to the impacts of a single dyke breach discussed earlier. All relationships developed in chapter 2 are based on marshes with open marsh margins, as opposed to the constrained flow encountered at Cogmagun due to the impoundment dyke.

In a restoration context this is a problem we are likely to encounter again (ie., difficulty in correctly quantifying the tidal prism). Another metric recommended by Williams et al. (2002) is contributing marsh area – a value more easily determined. Contributing marsh are, also called the tidal drainage area ($D_{tide}$), is the area lying within the tidal floodplain below the elevation of HHWLT that drains all tidal waters, precipitation received as a runoff or base flow (groundwater sources) into a particular channel. Work by Rinaldo et al. (1999) also illustrated strong relationships between cross-sectional area, channel width and contributing marsh area. Furthermore, Marani et al. (2003) found drainage area to be well related to total channelized length which is relevant when determining drainage density. Because tidal prism is inextricably linked to channel dimensions, particularly where bankfull prism proved to be the strongest regression, there is some confusion as to which is the dependent variable (Steel and Pye, 1997). That is to say that as creek dimensions change, so does the tidal prism.

Contributing marsh area, on the other hand, is more easily defined when elevations are well known and an upland edge is easily identifiable as is the case in many Fundy marshes (ie, steep topographic jump at marsh edge which constrains marsh extent). When contributing marsh area was used equilibrium conditions exceed those currently observed but are still more conservative than initial predictions (Table 3-4). Whether this is because the channel has not yet reached equilibrium or inaccuracy in the relationship is yet to be determined. None the less, contributing marsh area appears to be the more appropriate metric based on current conditions as well as on-site observations and hand-on applications.

**Table 3-4: Observed and predicted equilibrium conditions for Cogmagun restoration T1 where tidal prism is replaced with contributing marsh area.**

| | | |
|---|---|---|
| **Observed Geometry (2011)** | *Width (w)* | 23.3 |
| | *Mean Depth (d)* | 1.6 |
| | *Thalweg Depth (D)* | 3.2 |
| | *XS Area (A)* | 36.6 |
| **Feasibility Report (2009) Predicted Geometry** | *Width (w)* | 33.6 - 37.9 |
| | *Mean Depth (d)* | |
| | *Thalweg Depth (D)* | 3.42 |
| | *XS Area (A)* | |
| **Contributing Marsh Area Predicted Geometry** | *Width (w)* | 30.6 |
| | *Mean Depth (d)* | 2.1 |
| | *Thalweg Depth (D)* | 3.7 |
| | *XS Area (A)* | 48.83 |

***Conclusions***

Development of the hydraulic network at Cogmagun is occurring at a rate comparable to other studies and is well under way to becoming an efficient system (Allen, 2000; Wallace et al., 2005; Weisher et al., 2005; MacDonald et al. 2010; van Proosdij et al., 2010). The incorporation of drainage ditches, relict creeks, and surficial rills throughout the site into a hybrid/superimposed network allowed rapid dewatering and efficient movement of water through the site in the initial year of restoration. However, many of these channels were no longer detectable through aerial photography or site visits by the second year of the restoration. It is anticipated that channels will continue to be activated or in-filled as needed as the site elevation increases and discharge decreases.

Although the channel mouth eroded rapidly in the short term excavated portions of the channel remain relatively stable. The decision to excavate only the minimum area needed and

leave the vegetated banks of the channel mouth intact has led to slumping of large vegetation blocks which are capable or trapping sediment, helping to stabilise the channel in the long term. The creation of a single breach at the Cogmagun site has had significant impacts on how the system functions with regards to tidal inundation and circulation, creek erosion, and species diversity. A lack of sedimentation in the borrow pit near the main channel and the high probability of prolonged velocity pulses in the channel indicate that more breaches are preferable. The long term impact of this decision may not be apparent for many years yet, making continued monitoring of the site very important.

Testing hydraulic geometry relationship yielded mixed results. Application of the regression equations developed in chapter 2 underestimated channel dimensions. This was attributed primarily to errors in correctly calculating the tidal prism as the borrow pit could not be surveyed as well as constrained drainage via the marsh margin. This presents a significant limitation for the application of hydraulic geometry in restorations were accurate bathymetry are not available or where substantial excavation is anticipated. Contributing marsh area, however, is a more easily measured and has been shown to work in other locations (Williams et al., 2002). Although this method over-estimated channel dimensions the channel has not yet reached equilibrium conditions the magnitude of error will be determined only with continued monitoring of the restoration site.

### *References*


Allen, J. R. (1997). Simulation models of salt-marsh morphodynamics: some implications for high-intertidal sediment couplets related to sea-level change. *Sedimentary Geology 113*, 21 l-223.

Allen, J. R. (2000). Morphodynamics of Holocene salt marshes: a review sketch from the Atlantic and Southern North Sea coasts of Europe. *Quaternary Science Reviews 19*, 1155-1231.

ArcGIS, E. (n.d.). *ArcGIS Desktop Help*. Retrieved 10 15, 2012, from http://webhelp.esri.com/arcgisdesktop/9.2

Bowron, T. C. (2006). *Pre- and Immediate Post-Construction Monitoring of the Walton River Salt Marsh Restoration Project.* Halifax NS: CBWES Inc., Publication No 2.

Bowron, T., Neatt, N., van Proosdij, D., Lundholm, J., & Graham, J. (2009). Macro-tidal Salt Marsh Ecosystem Response to Culvert Expansion. *Restoration Ecology*, DOI: 10.1111/j.1526-100X.2009.00602.x.

Bowron, T. N. (2012). *Post-Restoration Monitoring (Year 2) for the Cogmagun River Salt Marsh Restoration Project.* Halifax, NS: CBWES Inc., Publication No 31.

Cahoon, D., Lynch, J., Perez, C., Segura, B., Holland, R., Stelly, C., et al. (2002). A device for high precision measurement of wetland sediment elevation. II. The rod surface elevation table. *Journal of Sediment. Res. 72 (5)*, 734-739.

Crooks, S., Schutten, J., Sheern, G. D., Pye, K., & Davy, A. J. (2002). Drainage and Elevation as Factors in the Restoration of Salt Marsh in Britain. *Restoration Ecology 10:3*, 591–602.

D'Alpaos, A., Lanzoni, S., Marani, M., Bonometto, A., Cecconi, G., & Rinaldo, A. (2007). Spontaneous tidal network formation within a constructed salt marsh: Observations and morphodynamic modelling. *Geomorphology 91*, 186–197.

Davidson-Arnott, R. G., van Proosdij, D., Ollerhead, J., & Schostak, L. (2002). Hydrodynamics and sedimentation in salt marshes: examples from a macrotidal marsh, Bay of Fundy. *Geomorphology 48*, 209–231.

French, J. (2008). Hydrodynamic modeling of estuarine flood defense realignment as an adaptive management response to sea level rise. *JCR 24 (2B)*, 1-12.

French, J., & Stoddart, D. (1992). Hydrodynamics of salt marsh creek systems: Implications for marsh morphological development and material exchanges. *Earth Surface Processes and Landforms 17*, 235-252.

Graham, J. T. (2009). *Compensation Proposal for the Cogmagun River Salt Marsh Restoration Project.* Halifax, NS: CBWES Inc., Report No 5.

Hammersmark, C. T., Fleenor, W. E., & Schladow, S. G. (2005). Simulation of flood impact and habitat extent for a tidal freshwater marsh restoration. *Ecological Engineering 25* , 137–152.

Konisky, R., Burdick, D. M., Dionne, M., & Neckles, H. A. (2006). A regional assessment of salt marsh restoration and monitoring in the Gulf of Maine. *Restoration Ecology 14:4*, 516–525.

MacDonald, G. K., Noel, P. E., van Proosdij, D., & Chmura, G. L. (2010). The Legacy of Agricultural Reclamation on Channel and Pool Networks of Bay of Fundy Salt Marshes. *Estuaries and Coasts 33*, 151–160. DOI 10.1007/s12237-009-9222-4.

Marani, M., Belluco, E., D'Alpaos, A., Defina, A., Lanzoni, S., & Rinaldo, A. (2003). On the drainage density of tidal networks. *Water Resour. Res 39(2)*, 1040. doi:10.1029/2001WR001051.

Mitsch, W. J., & Gosselink, J. G. (2007). *Wetlands, fourth ed.* New York, NY, USA.: John Wiley& Sons.

Mitsh, W., & Jørgensen, S. (2004). *Ecological Engineering and Ecosystem Restoration.* John Wiley an Sons, 500 p.

Neckles, H. A., Dionne, M., Burdick, D. M., Roman, C. T., Buchsbaum, R., & Hutchins, E. (2002). A monitoring protocol to assess tidal restoration of salt marshes on local and regional scales. *Restoration Ecology 10*, 556–563.

Paquette, C., Sundberg, K., Bouman, R., & Chmyra, G. (2004). Changes in saltmarsh surface elevation due to variability in evapotranspiration and tidal flooding. *Estuaries 27*, 82-89.

Portnoy, J. (1999). Salt marsh diking and restoration: biogeochemical implications of altered wetland hydrology. *Environ. Manage. 24 (1)*, 111-120.

Rinaldo, A., Fagherazzi, S., Lanzoni, A., Marani, M., & Dietrich, W. (1999). Tidal networks: 3. Landscape forming discharges and studies in empirical geomorphic relationships. *Water Resour. Res., 35(12)*, 3919-3929.

Roman, C., James-Pirri, M., & Heltshe, J. (n.d.). *Monitoring salt marsh vegetation: a protocol for the long-term coastal ecosystem monitoring program at Cape Cod National Seashore.* Retrieved from www.nature.nps.gov/im/monitor/protocolcdb.cfm

Shi, Z., Pethick, J. S., Burd, F., & Murphy, B. (1996). Velocity profiles in a salt marsh canopy. *Geo-Marine Letters 16*, 319-323.

Singh, V. P. (2003). On the theories of hydraulic geometry. *International Journal of Sediment Research, 18:3*, 196-218.

Steel, T., & Pye, K. (1997). The development of salt marsh tidal creek networks: evidence from the UK. *Proceedings of the Canadian Coastal Conference, 22-25 May* (pp. 267 - 280). University of Guelph.

Survey, U. G. (2011). *Channel cross-section standard operating procedure*. Retrieved October 15, 2012, from Unpublished protocols. USGS, Western Ecological Research Center, San Francisco Bay

Estuary Field Station, Vallejo, CA. : http://www.tidalmarshmonitoring.org/pdf/USGS_WERC_Channe

Temmerman, S., Bouma, T. J., Govers, G., Wang, Z. B., De Vries, M. B., & Herman, P. M. (2005). Impact of vegetation on flow routing and sedimentation patterns: Three-dimensional modeling for a tidal marsh. *Journal of Geophysical Research, 110*, F04019, doi:10.1029/2005JF000301.

van Proodsij, D., Babrick, J., & Baker, G. (2006). *(206b) . Spatial and Temporal Variations in the Intertidal Geomorphology of the Avon River Estuary.* Halifax: Final report submitted to the Nova Scotia Department of Transportation and Public Works (NSTPW), 74.

van Proosdij, D., Lundholm, J., Neatt, N., Bowron, T., & Graham, J. (2010). Ecological re-engineering of a freshwater impoundment for salt marsh restoration in a hypertidal system. *Ecological Engineering 36*, 1314–1332.

Wallace, K. J., Callaway, J. C., & Zedler, J. B. (2005). Evolution of Tidal Creek Networks in a High Sedimentation Environment: A 5-year Experiment at Tijuana Estuary, California. *Estuaries 28:6*, 795-811.

Weishar, L. L., Teal, J. M., & Hinkle, R. (2005). Stream order analysis in marsh restoration on Delaware Bay. *Ecological Engineering 25*, 252–259.

Weisher, L., Balleto, J., Teal, J., & Ludwig, D. (1997). Success criteria and adaptive management for a large-scale wetland restoration project. *Speacil Issue: Hydrologic Restoration of Coastal Wetlands. Wetlands Ecol. Manage. 4 (2)*, 111-127.

Williams, P. B., & Orr, M. K. (2002). Physical evolution of restored levee salt marshes in the San Francisco Bay Estuary. *Restoration Ecology 10:3*, 527–542.

Williams, P. B., Orr, M. K., & Garrity, N. J. (2002). Hydraulic Geometry: A geomorphic design tool for tidal marsh channel evolution in wetland restoration projects. *Restoration Ecology 10:3*, 577–590.

Wolters, M., Bakker, J. P., Bertness, M. D., Jeffries, R. L., & Möller, I. (2005). Salt marsh erosion and restoration in south east England: squeezing the evidence requires realignment. *Journal of Applied Ecology 42*, 844–851.

Zeff, M. L. (1999). Salt marsh tidal channel morphometry: Applications for wetland creation and restoration. *Restoration Ecology 7:2*, 205-211.

## Chapter 4 - Considerations for Salt Marsh Restoration Design in a Hypertidal Estuary: Synthesis

The primary objective of this study was to improve restoration design in the Bay of Fundy and in other hyper or macro-tidal estuaries. This was done by establishing morphometric parameters for marshes in the region and assessing the development of a salt marsh restoration project in the region. The restoration of functional marshes requires knowledge of morphometric characteristics which are currently lacking for hypertidal marshes. Furthermore it is expected that the relationships investigated in this work will be applicable and useful in other hypertidal estuaries. This study required the use of multiple technologies, including several survey methods ("low" and "high" tech), analysis of aerial photography is several formats, and monitoring data collected by CBWES Inc. The integration of these data, particularly in a GIS environment using custom tools, was challenging but proved to have substantial advantages.

In chapter 2 an analysis of reference marshes showed a clear distinction between channels that were purely tidal and those that had a large portion of their channel length in the upland and received freshwater input (tidal-fresh). This was evident in both channel dimensions and hydraulic geometry relationships. While hydraulic geometry equations were shown to be valid for primary tidal channels in the study region, they did not perform well for freshwater channels. Furthermore, both channel dimensions and hydraulic geometry relationships differed with channel order when a modified Strahler method was used (Horton, 1945; Weisher et al., 2005). Primary tidal channels ($1^{st}$ and $2^{nd}$ order) were the largest channels with higher w:d ratios than tidal-fresh creeks. They performed best in regression analysis when the bankfull tidal prism

was used, establishing exponents for hydraulic geometry. Headwater creeks, however, had very poor regressions with no differentiation between 3rd, 4th, and 5th order. Drainage density and sinuosity seem to be dictated by marsh maturity and site history rather than the amount of freshwater influence at the site, with high drainage densities and low sinuosity scores at all sites. Relict agricultural features did not decrease sinuosity scores or density and were incorporated into hybrid networks.

In chapter three the development of the hydraulic network at the Cogmagun restoration site was analyzed, and found to be occurring at a rate comparable to other studies and is well under way to becoming an efficient system (Allen, 2000; Wallace et al., 2005; Weisher et al., 2005; MacDonald et al., 2010; van Proosdij et al., 2010). The incorporation of drainage ditches, relict creeks, and surficial rills throughout the site into a hybrid/superimposed network allowed rapid dewatering and efficient movement of water through the site in the initial year following restoration. Despite erosion at the channel mouth, excavated portions of the channel are stable and the site is developing on an acceptable trajectory. The creation of a single breach at the Cogmagun site has had significant impacts on how the system functions with regards to tidal inundation, circulation, creek erosion, and species diversity. The results of this study seem to indicate that more breaches are preferable, as additional breaches restore a more natural hydrology by allowing drainage of the ebb tide across the marsh margin thus improving the circulation of tidal water and reducing the magnitude and duration of velocity pulses. The long term impact of this decision may not be apparent for many years yet, making continued monitoring of the site very important.

Testing the hydraulic geometry relationships established in chapter two yielded mixed results. While the best regression (bankfull tidal prism) underestimated channel dimensions, this was attributed primarily to errors in correctly calculating the tidal prism and alteration of marsh hydrology due to dykes which constrained ebb flow drainage. Using contributing marsh area instead of tidal prism over-estimated channel dimensions, however the magnitude of error is unknown as the channel has not yet reached equilibrium condition (ie., still actively eroding, banks not yet fully vegetated). Taken together, the results of chapter's one and two tell us several important things. First, that hydraulic geometry can be a useful tool for predicting tidal (but not tidal-fresh) equilibrium channel geometry in a hyper-tidal environment using the bankfull prism as opposed to the spring tidal prism. Secondly, that it is also necessary to have accurate bathymetry for channel networks. If not available, or if extensive excavation is anticipated which will alter the tidal prism, than contributing marsh area is a more useful and accurate metric.

The importance of restoration practices that mimic local conditions has been acknowledged by restoration practitioners in many locations (Zeff, 1999; Wallace et al., 2005). The morhpometric analysis conducted here allowed the determination of baseline conditions such as w:d ratio's, planform geometry, and drainage density which can greatly improve our ability to do this. Observations of the development of a hybrid network at the Cogamaun site can further improve our ability to understand how these networks form and develop, and how the number/placement of beaches might impact the site. Furthermore, the integration of custom GIS tools developed for this study provides tools which could be used again to further improve the data set. Finally the validitation of hydraulic geometry equations for primary

channels, which can be used in planning a restoration project, may be applicable in other macro and hyper-tidal estuaries.

### *References*


Allen, J. R. (2000). Morphodynamics of Holocene salt marshes: a review sketch from the Atlantic and Southern North Sea coasts of Europe. *Quaternary Science Reviews 19*, 1155-1231.

Horton, R. (1945). Erosional development of streams and their drainage basins: hydrophysical approach to quantitative morphology. *Bulletin of the Geological Society of America 56*, 275– 370.

MacDonald, G. K., Noel, P. E., van Proosdij, D., & Chmura, G. L. (2010). The Legacy of Agricultural Reclamation on Channel and Pool Networks of Bay of Fundy Salt Marshes. *Estuaries and Coasts 33*, 151–160. DOI 10.1007/s12237-009-9222-4.

van Proosdij, D., Lundholm, J., Neatt, N., Bowron, T., & Graham, J. (2010). Ecological re-engineering of a freshwater impoundment for salt marsh restoration in a hypertidal system. *Ecological Engineering 36*, 1314–1332.

Wallace, K. J., Callaway, J. C., & Zedler, J. B. (2005). Evolution of Tidal Creek Networks in a High Sedimentation Environment: A 5-year Experiment at Tijuana Estuary, California. *Estuaries 28:6*, 795-811.

Weishar, L. L., Teal, J. M., & Hinkle, R. (2005). Stream order analysis in marsh restoration on Delaware Bay. *Ecological Engineering 25*, 252–259.

Zeff, M. L. (1999). Salt marsh tidal channel morphometry: Applications for wetland creation and restoration. *Restoration Ecology 7:2*, 205-211.

## Appendix A: Python Script for Hydrology Toolbox

***Created Adjusted Survey Profile***

```
# ---------------------------------------------------------------------------
# AdjustProfile.py
# Created on: 2012-10-30 04:53:53.00000
#   (generated by ArcGIS/ModelBuilder)
# Usage: AdjustProfile <Adjusted_survey_polyline> <SC_APpts> <Line_Field> <Sort_Field>
# Description:
# Creates z-aware creek profile polyline from survey points.
#
#
# This tool separates surveys points into shapefiles by transect, identifies the linear directional mean of each transect, snaps points to this line and creates an adjusted z-aware polyine.
#
#
# Input survey points should be z-aware and each transect identified by a unique number (ie, Profile ID). Default snap tolerence is 5 m.
#
# Once the tool has been successfully run add Bankfull elevation field (BnkT) to be used in flood surface creation
# ---------------------------------------------------------------------------

# Set the necessary product code
import arceditor


# Import arcpy module
import arcpy

# Script arguments
Adjusted_survey_polyline = arcpy.GetParameterAsText(0)
if Adjusted_survey_polyline == '#' or not Adjusted_survey_polyline:
   Adjusted_survey_polyline = "C:\\Users\\Jennie Graham\\Documents\\SMU\\RDT V3\\AdjustedProfiles\\AP_SC.shp" # provide a default value if unspecified

SC_APpts = arcpy.GetParameterAsText(1)
if SC_APpts == '#' or not SC_APpts:
   SC_APpts = "SC_APpts" # provide a default value if unspecified

Line_Field = arcpy.GetParameterAsText(2)
if Line_Field == '#' or not Line_Field:
```

```
   Line_Field = "PnID" # provide a default value if unspecified

Sort_Field = arcpy.GetParameterAsText(3)

# Local variables:
Uncorrected_tranect_line = SC_APpts
Linear_directional_Mean_line___3_ = Uncorrected_tranect_line
Adjusted_survey_points = Linear_directional_Mean_line___3_

# Process: Points To Line (3)
arcpy.PointsToLine_management(SC_APpts, Uncorrected_tranect_line, Line_Field, Sort_Field, "NO_CLOSE")

# Process: Linear Directional Mean (3)
arcpy.DirectionalMean_stats(Uncorrected_tranect_line, Linear_directional_Mean_line___3_, "DIRECTION", "PnID")

# Process: Snap
arcpy.Snap_edit(SC_APpts, "'C:\\Users\\Jennie Graham\\Documents\\ArcGIS\\Default.gdb\\Win1_APpts2_PointsToLine_Dir' EDGE '5 Unknown'")

# Process: Points To Line (2)
arcpy.PointsToLine_management(Adjusted_survey_points, Adjusted_survey_polyline, Line_Field, "", "NO_CLOSE")
```

***Create Flood Surface***

```
# ---------------------------------------------------------------------------
# ChannelWidth.py
# Created on: 2012-10-30 04:55:56.00000
#   (generated by ArcGIS/ModelBuilder)
#       Usage: ChannelWidth <Input__DEM_Thalweg> <Input__Adjusted_profiles> <Input__Flood_surface_multipatch> <Output__Bankfull_Intersection_Points> <Output__Bankfull_segmented_cross-section> <BANKFULL_WIDTH> <Width_segDEM_shp>
# Description:
# This tool creates a flood surface multipatch from the bankfull height field contained in the adjusted profile polyline
# ---------------------------------------------------------------------------

# Set the necessary product code
# import arcinfo


# Import arcpy module
```

```
import arcpy

# Check out any necessary licenses
arcpy.CheckOutExtension("3D")

# Script arguments
Input__DEM_Thalweg = arcpy.GetParameterAsText(0)
if Input__DEM_Thalweg == '#' or not Input__DEM_Thalweg:
   Input__DEM_Thalweg = "C:\\Users\\Jennie Graham\\Documents\\SMU\\RDT
V3\\Thalwegs\\Thals_DEM.shp" # provide a default value if unspecified

Input__Adjusted_profiles = arcpy.GetParameterAsText(1)
if Input__Adjusted_profiles == '#' or not Input__Adjusted_profiles:
   Input__Adjusted_profiles = "COG_CreekTrans2011" # provide a default value if unspecified

Input__Flood_surface_multipatch = arcpy.GetParameterAsText(2)
if Input__Flood_surface_multipatch == '#' or not Input__Flood_surface_multipatch:
   Input__Flood_surface_multipatch = "C:\\Users\\Jennie Graham\\Documents\\SMU\\RDT
V3\\Flood\\COG_floodsurface.shp" # provide a default value if unspecified

Output__Bankfull_Intersection_Points = arcpy.GetParameterAsText(3)
if Output__Bankfull_Intersection_Points == '#' or not Output__Bankfull_Intersection_Points:
   Output__Bankfull_Intersection_Points = "C:\\Users\\Jennie Graham\\Documents\\SMU\\RDT
V3\\Geometry\\Win1DEM_pts.shp" # provide a default value if unspecified

Output__Bankfull_segmented_cross-section = arcpy.GetParameterAsText(4)
if Output__Bankfull_segmented_cross-section == '#' or not Output__Bankfull_segmented_cross-
section:
   Output__Bankfull_segmented_cross-section = "C:\\Users\\Jennie
Graham\\Documents\\SMU\\RDT V3\\Geometry\\Intermediate\\FullLine.shp" # provide a
default value if unspecified

BANKFULL_WIDTH = arcpy.GetParameterAsText(5)
if BANKFULL_WIDTH == '#' or not BANKFULL_WIDTH:
   BANKFULL_WIDTH = "C:\\Users\\Jennie Graham\\Documents\\SMU\\RDT
V3\\Geometry\\Win1\\WidthDEM.shp" # provide a default value if unspecified

Width_segDEM_shp = arcpy.GetParameterAsText(6)
if Width_segDEM_shp == '#' or not Width_segDEM_shp:
   Width_segDEM_shp = "C:\\Users\\Jennie Graham\\Documents\\SMU\\RDT
V3\\Geometry\\Win1\\Width_segDEM.shp" # provide a default value if unspecified

# Local variables:
Output_Layer = Output__Bankfull_segmented_cross-section
v_name__tot_Layer = Output_Layer
Intersection_Count = Input__Flood_surface_multipatch
```

```
# Process: Intersect 3D Line With Multipatch
arcpy.Intersect3DLineWithMultiPatch_3d(Input__Adjusted_profiles,
Input__Flood_surface_multipatch, "ALL", Output__Bankfull_Intersection_Points,
Output__Bankfull_segmented_cross-section)

# Process: Make Feature Layer
arcpy.MakeFeatureLayer_management(Output__Bankfull_segmented_cross-section,
Output_Layer, "", "", "FID FID VISIBLE NONE;Shape Shape VISIBLE NONE;Bnk_T Bnk_T VISIBLE
NONE;ID ID VISIBLE NONE;Shape Shape VISIBLE NONE;Bnk_T Bnk_T VISIBLE NONE;ID ID VISIBLE
NONE;LINE_OID LINE_OID VISIBLE NONE;FROM_MP_ID FROM_MP_ID VISIBLE NONE;TO_MP_ID
TO_MP_ID VISIBLE NONE;DIST_3D DIST_3D VISIBLE NONE;LENGTH_3D LENGTH_3D VISIBLE
NONE")

# Process: Select Layer By Location (2)
arcpy.SelectLayerByLocation_management(Output_Layer, "INTERSECT", Input__DEM_Thalweg,
"", "NEW_SELECTION")

# Process: Feature To Line
arcpy.FeatureToLine_management("FullLine_Layer", BANKFULL_WIDTH, "", "ATTRIBUTES")

# Process: Split Line At Vertices
arcpy.SplitLine_management(BANKFULL_WIDTH, Width_segDEM_shp)
```

***Generate Selection Shapefiles***

```
# ---------------------------------------------------------------------------
# GenerateSelectionShapefiles.py
# Created on: 2012-10-30 04:55:04.00000
#   (generated by ArcGIS/ModelBuilder)
# Usage: GenerateSelectionShapefiles <Sub-Basin_Polygons> <Stream_Network>
<Adjusted_Profiles> <BASIN_SPLITTER> <CROSS_SECTION_THALWEG>
<SEGMENTED_STREAM_NETWORK> <BASIN_INTERSECTION_POINT>
<BUFFERED_STREAM_NETWORK> <CROSS_SECTION_SPLITTER> <SBI_CS_ONLY>
<StrmBas_bufseg_s_shp> <AV_StrmBas_bufseg_clipped_shp> <AVON_Marsh>
<AV_StrmBas_bufseg_clipped_shp__2_>
# Description:
# Creates shapefiles (poins, polygons) through a series of buffers, intersecitons and symmetrical
differences. These files are used to delineate cross-section and upstream channel lengths,
drainage areas and tidal prisms
#
# Inputs: Drainage basins, a drainage network, and Cross-section profiles are required  to run
this tool. If a cross-section does not fall at the mouth of a drainage basin than the basin should
be divided just downstream (5-10 cm) of the cross-section.
# ---------------------------------------------------------------------------
```

```
# Set the necessary product code
# import arcinfo


# Import arcpy module
import arcpy

# Script arguments
Sub-Basin_Polygons = arcpy.GetParameterAsText(0)
if Sub-Basin_Polygons == '#' or not Sub-Basin_Polygons:
   Sub-Basin_Polygons = "basins" # provide a default value if unspecified

Stream_Network = arcpy.GetParameterAsText(1)
if Stream_Network == '#' or not Stream_Network:
   Stream_Network = "Creek Thalweg" # provide a default value if unspecified

Adjusted_Profiles = arcpy.GetParameterAsText(2)
if Adjusted_Profiles == '#' or not Adjusted_Profiles:
   Adjusted_Profiles = "COG_CreekTrans2011" # provide a default value if unspecified

BASIN_SPLITTER = arcpy.GetParameterAsText(3)
if BASIN_SPLITTER == '#' or not BASIN_SPLITTER:
   BASIN_SPLITTER = "C:\\Users\\Jennie Graham\\Documents\\SMU\\RDT
V3\\strmnt_wrk\\Intersects\\StrmBasin_splitter_s.shp" # provide a default value if unspecified

CROSS_SECTION_THALWEG = arcpy.GetParameterAsText(4)
if CROSS_SECTION_THALWEG == '#' or not CROSS_SECTION_THALWEG:
   CROSS_SECTION_THALWEG = "C:\\Users\\Jennie Graham\\Documents\\SMU\\RDT
V3\\Thalwegs\\Thals_DEM.shp" # provide a default value if unspecified

SEGMENTED_STREAM_NETWORK = arcpy.GetParameterAsText(5)
if SEGMENTED_STREAM_NETWORK == '#' or not SEGMENTED_STREAM_NETWORK:
   SEGMENTED_STREAM_NETWORK = "C:\\Users\\Jennie Graham\\Documents\\SMU\\RDT
V3\\Thalwegs\\Win1_strmnt_seg.shp" # provide a default value if unspecified

BASIN_INTERSECTION_POINT = arcpy.GetParameterAsText(6)
if BASIN_INTERSECTION_POINT == '#' or not BASIN_INTERSECTION_POINT:
   BASIN_INTERSECTION_POINT = "C:\\Users\\Jennie Graham\\Documents\\SMU\\RDT
V3\\strmnt_wrk\\Intersects\\stmnt_basin_intersect.shp" # provide a default value if unspecified

BUFFERED_STREAM_NETWORK = arcpy.GetParameterAsText(7)
if BUFFERED_STREAM_NETWORK == '#' or not BUFFERED_STREAM_NETWORK:
   BUFFERED_STREAM_NETWORK = "C:\\Users\\Jennie Graham\\Documents\\SMU\\RDT
V3\\strmnt_wrk\\buf\\strmnt_buf.shp" # provide a default value if unspecified

CROSS_SECTION_SPLITTER = arcpy.GetParameterAsText(8)
```

```
if CROSS_SECTION_SPLITTER == '#' or not CROSS_SECTION_SPLITTER:
    CROSS_SECTION_SPLITTER = "C:\\Users\\Jennie Graham\\Documents\\SMU\\RDT V3\\strmnt_wrk\\Intersects\\StrmXS_splitter_s.shp" # provide a default value if unspecified

SBI_CS_ONLY = arcpy.GetParameterAsText(9)
if SBI_CS_ONLY == '#' or not SBI_CS_ONLY:
    SBI_CS_ONLY = "C:\\Users\\Jennie Graham\\Documents\\SMU\\RDT V3\\strmnt_wrk\\Intersects\\SBint_XSonly.shp" # provide a default value if unspecified

StrmBas_bufseg_s_shp = arcpy.GetParameterAsText(10)
if StrmBas_bufseg_s_shp == '#' or not StrmBas_bufseg_s_shp:
    StrmBas_bufseg_s_shp = "C:\\Users\\Jennie Graham\\Documents\\SMU\\RDT V3\\strmnt_wrk\\buf\\StrmBas_bufseg_s.shp" # provide a default value if unspecified

AV_StrmBas_bufseg_clipped_shp = arcpy.GetParameterAsText(11)
if AV_StrmBas_bufseg_clipped_shp == '#' or not AV_StrmBas_bufseg_clipped_shp:
    AV_StrmBas_bufseg_clipped_shp = "C:\\Users\\Jennie Graham\\Documents\\SMU\\RDT V3\\strmnt_wrk\\buf\\AV_StrmBas_bufseg_clipped.shp" # provide a default value if unspecified

AVON_Marsh = arcpy.GetParameterAsText(12)
if AVON_Marsh == '#' or not AVON_Marsh:
    AVON_Marsh = "AVON_Marsh" # provide a default value if unspecified

AV_StrmBas_bufseg_clipped_shp__2_ = arcpy.GetParameterAsText(13)
if AV_StrmBas_bufseg_clipped_shp__2_ == '#' or not AV_StrmBas_bufseg_clipped_shp__2_:
    AV_StrmBas_bufseg_clipped_shp__2_ = "C:\\Users\\Jennie Graham\\Documents\\SMU\\RDT V3\\strmnt_wrk\\buf\\AV_strmnt_buf_marsh.shp" # provide a default value if unspecified

# Local variables:
Strmnet_split1_shp = Stream_Network
Strmnt_split2_shp = Strmnet_split1_shp
strm_basinsplitter_shp = BUFFERED_STREAM_NETWORK
Strm_CS_splitter = BUFFERED_STREAM_NETWORK
Strmnt_Bas_buf3_shp = BUFFERED_STREAM_NETWORK
Win1_strmnt_ordr_seg_shp = SEGMENTED_STREAM_NETWORK
Win1_strmnt_ordr_seg_shp__3_ = Win1_strmnt_ordr_seg_shp
Output_Feature_Class = CROSS_SECTION_THALWEG
Thals_DEM_shp = Output_Feature_Class
stmnt_basin_intersect_Layer = Thals_DEM_shp
Output_Layer = BASIN_INTERSECTION_POINT
Basins_line_shp = Sub-Basin_Polygons
honeycomb_shp = Basins_line_shp
Strmnt_basinsplitter_s_Layer = BASIN_SPLITTER
Output_Layer_Name = Strmnt_basinsplitter_s_Layer
XS_buf = Adjusted_Profiles
```

```
# Process: Split Line At Vertices
arcpy.SplitLine_management(Stream_Network, Strmnet_split1_shp)

# Process: Polygon To Line
arcpy.PolygonToLine_management(Sub-Basin_Polygons, Basins_line_shp, "IDENTIFY_NEIGHBORS")

# Process: Intersect (2)
arcpy.Intersect_analysis("'Creek Thalweg' #;'C:\\Users\\Jennie Graham\\Documents\\SMU\\RDT V3\\strmnt_wrk\\Intermediate\\Basins_line.shp' #", BASIN_INTERSECTION_POINT, "ALL", "", "POINT")

# Process: Split Line at Point (2)
arcpy.SplitLineAtPoint_management(Strmnet_split1_shp, BASIN_INTERSECTION_POINT, Strmnt_split2_shp, "")

# Process: Intersect
arcpy.Intersect_analysis("'Creek Thalweg' #;COG_CreekTrans2011 #", CROSS_SECTION_THALWEG, "ALL", "", "POINT")

# Process: Split Line at Point
arcpy.SplitLineAtPoint_management(Strmnt_split2_shp, CROSS_SECTION_THALWEG, SEGMENTED_STREAM_NETWORK, "")

# Process: Add Field
arcpy.AddField_management(SEGMENTED_STREAM_NETWORK, "LENGTH", "FLOAT", "", "", "", "", "NON_NULLABLE", "NON_REQUIRED", "")

# Process: Calculate Field
arcpy.CalculateField_management(Win1_strmnt_ordr_seg_shp, "LENGTH", "!shape.length@meters!", "PYTHON_9.3", "")

# Process: Buffer (3)
arcpy.Buffer_analysis(Adjusted_Profiles, XS_buf, "0.04 Meters", "FULL", "ROUND", "ALL", "")

# Process: Buffer
arcpy.Buffer_analysis(Stream_Network, BUFFERED_STREAM_NETWORK, "0.25 Meters", "FULL", "ROUND", "ALL", "")

# Process: Intersect (3)
arcpy.Intersect_analysis("'C:\\Users\\Jennie Graham\\Documents\\SMU\\RDT V3\\strmnt_wrk\\buf\\XS_buf.shp' #;'C:\\Users\\Jennie Graham\\Documents\\SMU\\RDT V3\\strmnt_wrk\\buf\\strmnt_buf.shp' #", Strm_CS_splitter, "ALL", "", "INPUT")

# Process: Multipart To Singlepart (2)
arcpy.MultipartToSinglepart_management(Strm_CS_splitter, CROSS_SECTION_SPLITTER)
```

```
# Process: Buffer (2)
arcpy.Buffer_analysis(Basins_line_shp, honeycomb_shp, "0.04 Meters", "FULL", "FLAT", "NONE", "")

# Process: Intersect (4)
arcpy.Intersect_analysis("'C:\\Users\\Jennie Graham\\Documents\\SMU\\RDT V3\\strmnt_wrk\\buf\\honeycomb.shp' #;'C:\\Users\\Jennie Graham\\Documents\\SMU\\RDT V3\\strmnt_wrk\\buf\\strmnt_buf.shp' #", strm_basinsplitter_shp, "ALL", "", "INPUT")

# Process: Multipart To Singlepart
arcpy.MultipartToSinglepart_management(strm_basinsplitter_shp, BASIN_SPLITTER)

# Process: Make Feature Layer (2)
arcpy.MakeFeatureLayer_management(BASIN_SPLITTER, Strmnt_basinsplitter_s_Layer, "", "", "LEFT_FID LEFT_FID VISIBLE NONE;RIGHT_FID RIGHT_FID VISIBLE NONE;BUFF_DIST BUFF_DIST VISIBLE NONE;FID_strmnt FID_strmnt VISIBLE NONE;Id Id VISIBLE NONE;ORIG_FID ORIG_FID VISIBLE NONE")

# Process: Make Feature Layer
arcpy.MakeFeatureLayer_management(BASIN_INTERSECTION_POINT, Output_Layer, "", "", "FID FID VISIBLE NONE;Shape Shape VISIBLE NONE;FID_Win1_s FID_Win1_s VISIBLE NONE;ARCID ARCID VISIBLE NONE;GRID_CODE GRID_CODE VISIBLE NONE;FROM_NODE FROM_NODE VISIBLE NONE;TO_NODE TO_NODE VISIBLE NONE;FID_Basins FID_Basins VISIBLE NONE;LEFT_FID LEFT_FID VISIBLE NONE;RIGHT_FID RIGHT_FID VISIBLE NONE")

# Process: Near
arcpy.Near_analysis(CROSS_SECTION_THALWEG, "'C:\\Users\\Jennie Graham\\Documents\\SMU\\RDT V3\\strmnt_wrk\\Intersects\\stmnt_basin_intersect.shp'", "", "NO_LOCATION", "NO_ANGLE")

# Process: Add Attribute Index
arcpy.AddIndex_management(Output_Feature_Class, "NEAR_FID", "", "NON_UNIQUE", "NON_ASCENDING")

# Process: Add Join
arcpy.AddJoin_management(Output_Layer, "FID", Thals_DEM_shp, "NEAR_FID", "KEEP_COMMON")

# Process: Feature To Point
arcpy.FeatureToPoint_management(stmnt_basin_intersect_Layer, SBI_CS_ONLY, "CENTROID")

# Process: Select Layer By Location
arcpy.SelectLayerByLocation_management(Strmnt_basinsplitter_s_Layer, "INTERSECT", SBI_CS_ONLY, "", "NEW_SELECTION")
```

```
# Process: Symmetrical Difference
arcpy.SymDiff_analysis(BUFFERED_STREAM_NETWORK, Output_Layer_Name, Strmnt_Bas_buf3_shp, "ALL", "")

# Process: Multipart To Singlepart (3)
arcpy.MultipartToSinglepart_management(Strmnt_Bas_buf3_shp, StrmBas_bufseg_s_shp)

# Process: Clip
arcpy.Clip_analysis(StrmBas_bufseg_s_shp, AVON_Marsh, AV_StrmBas_bufseg_clipped_shp, "")

# Process: Clip (2)
arcpy.Clip_analysis(BUFFERED_STREAM_NETWORK, AVON_Marsh, AV_StrmBas_bufseg_clipped_shp__2_, "")
```

***Create polyline for channel width***

```
# ---------------------------------------------------------------------------
# ChannelWidth.py
# Created on: 2012-10-30 04:55:56.00000
#   (generated by ArcGIS/ModelBuilder)
#       Usage: ChannelWidth <Input__DEM_Thalweg> <Input__Adjusted_profiles> <Input__Flood_surface_multipatch> <Output__Bankfull_Intersection_Points> <Output__Bankfull_segmented_cross-section> <BANKFULL_WIDTH> <Width_segDEM_shp>
# Description:
# Calculates channel width at bankfull elevation and channel segment lengths need to calculate cross-section geometry
# ---------------------------------------------------------------------------

# Set the necessary product code
# import arcinfo


# Import arcpy module
import arcpy

# Check out any necessary licenses
arcpy.CheckOutExtension("3D")

# Script arguments
Input__DEM_Thalweg = arcpy.GetParameterAsText(0)
if Input__DEM_Thalweg == '#' or not Input__DEM_Thalweg:
    Input__DEM_Thalweg = "C:\\Users\\Jennie Graham\\Documents\\SMU\\RDT V3\\Thalwegs\\Thals_DEM.shp" # provide a default value if unspecified

Input__Adjusted_profiles = arcpy.GetParameterAsText(1)
if Input__Adjusted_profiles == '#' or not Input__Adjusted_profiles:
    Input__Adjusted_profiles = "COG_CreekTrans2011" # provide a default value if unspecified
```

```
Input__Flood_surface_multipatch = arcpy.GetParameterAsText(2)
if Input__Flood_surface_multipatch == '#' or not Input__Flood_surface_multipatch:
    Input__Flood_surface_multipatch = "C:\\Users\\Jennie Graham\\Documents\\SMU\\RDT V3\\Flood\\COG_floodsurface.shp" # provide a default value if unspecified

Output__Bankfull_Intersection_Points = arcpy.GetParameterAsText(3)
if Output__Bankfull_Intersection_Points == '#' or not Output__Bankfull_Intersection_Points:
    Output__Bankfull_Intersection_Points = "C:\\Users\\Jennie Graham\\Documents\\SMU\\RDT V3\\Geometry\\Win1DEM_pts.shp" # provide a default value if unspecified

Output__Bankfull_segmented_cross-section = arcpy.GetParameterAsText(4)
if Output__Bankfull_segmented_cross-section == '#' or not Output__Bankfull_segmented_cross-section:
    Output__Bankfull_segmented_cross-section = "C:\\Users\\Jennie Graham\\Documents\\SMU\\RDT V3\\Geometry\\Intermediate\\FullLine.shp" # provide a default value if unspecified

BANKFULL_WIDTH = arcpy.GetParameterAsText(5)
if BANKFULL_WIDTH == '#' or not BANKFULL_WIDTH:
    BANKFULL_WIDTH = "C:\\Users\\Jennie Graham\\Documents\\SMU\\RDT V3\\Geometry\\Win1\\WidthDEM.shp" # provide a default value if unspecified

Width_segDEM_shp = arcpy.GetParameterAsText(6)
if Width_segDEM_shp == '#' or not Width_segDEM_shp:
    Width_segDEM_shp = "C:\\Users\\Jennie Graham\\Documents\\SMU\\RDT V3\\Geometry\\Win1\\Width_segDEM.shp" # provide a default value if unspecified

# Local variables:
Output_Layer = Output__Bankfull_segmented_cross-section
v_name__tot_Layer = Output_Layer
Intersection_Count = Input__Flood_surface_multipatch

# Process: Intersect 3D Line With Multipatch
arcpy.Intersect3DLineWithMultiPatch_3d(Input__Adjusted_profiles,
Input__Flood_surface_multipatch, "ALL", Output__Bankfull_Intersection_Points,
Output__Bankfull_segmented_cross-section)

# Process: Make Feature Layer
arcpy.MakeFeatureLayer_management(Output__Bankfull_segmented_cross-section,
Output_Layer, "", "", "FID FID VISIBLE NONE;Shape Shape VISIBLE NONE;Bnk_T Bnk_T VISIBLE NONE;ID ID VISIBLE NONE;Shape Shape VISIBLE NONE;Bnk_T Bnk_T VISIBLE NONE;ID ID VISIBLE NONE;LINE_OID LINE_OID VISIBLE NONE;FROM_MP_ID FROM_MP_ID VISIBLE NONE;TO_MP_ID TO_MP_ID VISIBLE NONE;DIST_3D DIST_3D VISIBLE NONE;LENGTH_3D LENGTH_3D VISIBLE NONE")
```

```
# Process: Select Layer By Location (2)
arcpy.SelectLayerByLocation_management(Output_Layer,  "INTERSECT",  Input__DEM_Thalweg,
"", "NEW_SELECTION")

# Process: Feature To Line
arcpy.FeatureToLine_management("FullLine_Layer", BANKFULL_WIDTH, "", "ATTRIBUTES")

# Process: Split Line At Vertices
arcpy.SplitLine_management(BANKFULL_WIDTH, Width_segDEM_shp)
```

***Create polyline for cross section geometry***

```
# ---------------------------------------------------------------------------
# XSGeometry.py
# Created on: 2012-10-30 05:20:49.00000
#   (generated by ArcGIS/ModelBuilder)
#       Usage:       XSGeometry       <Output__XS_geometry>       <Segmented_Bankfull_width>
<Dissolve_Field_s_> <Hydraulic_Radius> <W_D_Ratio>
# Description:
# Calculates Cross-section geometry and adds fields for upstream length, tidal prism, etc
# ---------------------------------------------------------------------------

# Import arcpy module
import arcpy

# Check out any necessary licenses
arcpy.CheckOutExtension("3D")

# Script arguments
Output__XS_geometry = arcpy.GetParameterAsText(0)
if Output__XS_geometry == '#' or not Output__XS_geometry:
   Output__XS_geometry       =       "C:\\Users\\Jennie       Graham\\Documents\\SMU\\RDT
V3\\Geometry\\SC_XSgeometryRTK.shp" # provide a default value if unspecified

Segmented_Bankfull_width = arcpy.GetParameterAsText(1)
if Segmented_Bankfull_width == '#' or not Segmented_Bankfull_width:
   Segmented_Bankfull_width = "SCWidth_seg" # provide a default value if unspecified

Dissolve_Field_s_ = arcpy.GetParameterAsText(2)
if Dissolve_Field_s_ == '#' or not Dissolve_Field_s_:
   Dissolve_Field_s_ = "PnID" # provide a default value if unspecified

Hydraulic_Radius = arcpy.GetParameterAsText(3)
if Hydraulic_Radius == '#' or not Hydraulic_Radius:
   Hydraulic_Radius = "[SUM_XSA]/ [MIN_LENGTH]" # provide a default value if unspecified

W_D_Ratio = arcpy.GetParameterAsText(4)
```

```
if W_D_Ratio == '#' or not W_D_Ratio:
   W_D_Ratio = "[Width] / [MeanDepth]" # provide a default value if unspecified

# Local variables:
Add_US_Flow_length = Output__XS_geometry
Add_Marsh_US_Flow_length = Add_US_Flow_length
Add_XS_Flow_length = Add_Marsh_US_Flow_length
Add_Marsh_XS_Flow_length = Add_XS_Flow_length
Add_US_Drainage_area = Add_Marsh_XS_Flow_length
Add_Marsh_US_Drainage_area = Add_US_Drainage_area
Add_Thalweg_Depth_field = Add_Marsh_US_Drainage_area
Add_Hydraulic_radius_field = Add_Thalweg_Depth_field
Add_Mean_Depth_field = Add_Hydraulic_radius_field
Add_W_D_Ratio_field = Add_Mean_Depth_field
Add_XS_TP = Add_W_D_Ratio_field
Add_US_TP = Add_XS_TP
Add_XS_drainage_area = Add_US_TP
Add_Width_field = Add_XS_drainage_area
Calculate_width = Add_Width_field
Depth_Calculated = Calculate_width
Caculate_mean_depth = Depth_Calculated
calculate_W_D_Ratio = Caculate_mean_depth
XSgeometry = calculate_W_D_Ratio
Width_segDEM_shp__2_ = Segmented_Bankfull_width
H1 = Width_segDEM_shp__2_
H2 = H1
SegLngth = H2
A1 = SegLngth
A2 = A1
XSA = A2
H1_ = XSA
H2_ = XSA
SegLngth_ = XSA
A1_ = XSA
A2_ = XSA
XSA_ = XSA

# Process: Add Z Information
arcpy.AddZInformation_3d(Segmented_Bankfull_width,
"Z_MIN;Z_MAX;LENGTH_3D;MIN_SLOPE", "NO_FILTER")

# Process: Add Field (3)
arcpy.AddField_management(Width_segDEM_shp__2_,    "H1",    "FLOAT",    "",    "",    "",    "",
"NON_NULLABLE", "NON_REQUIRED", "")

# Process: Add Field (5)
```

```
arcpy.AddField_management(H1, "H2", "FLOAT", "", "", "", "", "NON_NULLABLE", "NON_REQUIRED", "")

# Process: Add Field (6)
arcpy.AddField_management(H2, "SegLngth", "FLOAT", "", "", "", "", "NON_NULLABLE", "NON_REQUIRED", "")

# Process: Add Field (4)
arcpy.AddField_management(SegLngth, "A1", "FLOAT", "", "", "", "", "NON_NULLABLE", "NON_REQUIRED", "")

# Process: Add Field
arcpy.AddField_management(A1, "A2", "FLOAT", "", "", "", "", "NON_NULLABLE", "NON_REQUIRED", "")

# Process: Add Field (7)
arcpy.AddField_management(A2, "XSA", "FLOAT", "", "", "", "", "NON_NULLABLE", "NON_REQUIRED", "")

# Process: Calculate Field (2)
arcpy.CalculateField_management(XSA, "H1", "[Bnk_T] - [Z_Max]", "VB", "")

# Process: Calculate Field (3)
arcpy.CalculateField_management(XSA, "H2", "[Z_Max] - [Z_Min]", "VB", "")

# Process: Calculate Field (4)
arcpy.CalculateField_management(XSA, "SegLngth", "!shape.length@meters!", "PYTHON_9.3", "")

# Process: Calculate Field (5)
arcpy.CalculateField_management(XSA, "A1", "[H1] * [SegLngth]", "VB", "")

# Process: Calculate Field (6)
arcpy.CalculateField_management(XSA, "A2", "[H2] * [SegLngth] *0.5", "VB", "")

# Process: Calculate Field (7)
arcpy.CalculateField_management(XSA, "XSA", "[A1] + [A2]", "VB", "")

# Process: Dissolve
arcpy.Dissolve_management(XSA_, Output__XS_geometry, Dissolve_Field_s_, "Z_Min MIN;LENGTH_3D MIN;Z_Max MAX;XSA SUM;Bnk_T MIN;Min_Slope MAX;Min_Slope MEAN;Z_Min MEAN", "MULTI_PART", "DISSOLVE_LINES")

# Process: Add Field (8)
arcpy.AddField_management(Output__XS_geometry, "US_FlwLng", "FLOAT", "", "", "", "", "NON_NULLABLE", "NON_REQUIRED", "")
```

```
# Process: Add Field (18)
arcpy.AddField_management(Add_US_Flow_length, "MUS_FlwLng", "FLOAT", "", "", "", "",
"NON_NULLABLE", "NON_REQUIRED", "")

# Process: Add Field (10)
arcpy.AddField_management(Add_Marsh_US_Flow_length, "XS_FlwLng", "FLOAT", "", "", "", "",
"NON_NULLABLE", "NON_REQUIRED", "")

# Process: Add Field (19)
arcpy.AddField_management(Add_XS_Flow_length, "MXS_FlwLng", "FLOAT", "", "", "", "",
"NON_NULLABLE", "NON_REQUIRED", "")

# Process: Add Field (12)
arcpy.AddField_management(Add_Marsh_XS_Flow_length, "US_Area", "FLOAT", "", "", "", "",
"NON_NULLABLE", "NON_REQUIRED", "")

# Process: Add Field (20)
arcpy.AddField_management(Add_US_Drainage_area, "MUS_Area", "FLOAT", "", "", "", "",
"NON_NULLABLE", "NON_REQUIRED", "")

# Process: Add Field (14)
arcpy.AddField_management(Add_Marsh_US_Drainage_area, "ThalDepth", "FLOAT", "", "", "",
"", "NON_NULLABLE", "NON_REQUIRED", "")

# Process: Add Field (16)
arcpy.AddField_management(Add_Thalweg_Depth_field, "HydRadius", "FLOAT", "", "", "", "",
"NON_NULLABLE", "NON_REQUIRED", "")

# Process: Add Field (17)
arcpy.AddField_management(Add_Hydraulic_radius_field, "MeanDepth", "FLOAT", "", "", "", "",
"NON_NULLABLE", "NON_REQUIRED", "")

# Process: Add Field (15)
arcpy.AddField_management(Add_Mean_Depth_field, "WD_Ratio", "FLOAT", "", "", "", "",
"NON_NULLABLE", "NON_REQUIRED", "")

# Process: Add Field (11)
arcpy.AddField_management(Add_W_D_Ratio_field, "XS_TP", "FLOAT", "", "", "", "",
"NON_NULLABLE", "NON_REQUIRED", "")

# Process: Add Field (13)
arcpy.AddField_management(Add_XS_TP, "US_TP", "FLOAT", "", "", "", "", "NON_NULLABLE",
"NON_REQUIRED", "")

# Process: Add Field (9)
```

```
arcpy.AddField_management(Add_US_TP, "MXS_Basin", "FLOAT", "", "", "", "", "NON_NULLABLE", "NON_REQUIRED", "")

# Process: Add Field (2)
arcpy.AddField_management(Add_XS_drainage_area, "Width", "FLOAT", "", "", "", "", "NON_NULLABLE", "NON_REQUIRED", "")

# Process: Calculate Field
arcpy.CalculateField_management(Add_Width_field, "Width", "!shape.length@meters!", "PYTHON_9.3", "")

# Process: Calculate Field (9)
arcpy.CalculateField_management(Calculate_width, "ThalDepth", "[MIN_Bnk_T] - [MIN_Z_Min]", "VB", "")

# Process: Calculate Field (11)
arcpy.CalculateField_management(Depth_Calculated, "MeanDepth", "[MIN_Bnk_T]-[MEAN_Z_Min]", "VB", "")

# Process: Calculate Field (10)
arcpy.CalculateField_management(Caculate_mean_depth, "WD_Ratio", W_D_Ratio, "VB", "")

# Process: Calculate Field (8)
arcpy.CalculateField_management(calculate_W_D_Ratio, "HydRadius", Hydraulic_Radius, "VB", "")
```

***Delineate cross-section drainage area, flow length and Tidal Prism***

```
# ---------------------------------------------------------------------------
# XSChannel.py
# Created on: 2012-10-30 05:21:26.00000
#   (generated by ArcGIS/ModelBuilder)
# Usage: XSChannel <INPUT__DEM_Thalweg> <INPUT__Buffered_streamnet_semented_by_basin_boundaries_and_clipped_to_Marsh_extent> <INPUT__Marsh_basins> <INPUT__Segmented_stream_network> <INPUT__Cross-section_geometry_polyline> <OUTPUT__XS_Drainage_basin_to_marsh_extent> <OUTPUT__XS_Flowlength_to_marsh_extent> <Statistic_field__XS_Drainage_Area> <Statistics_Field__Cross-section_upstream_flowlength>
# Description:
# ---------------------------------------------------------------------------

# Import arcpy module
import arcpy

# Load required toolboxes
arcpy.ImportToolbox("Model Functions")
```

```
# Script arguments
INPUT__DEM_Thalweg = arcpy.GetParameterAsText(0)
if INPUT__DEM_Thalweg == '#' or not INPUT__DEM_Thalweg:
    INPUT__DEM_Thalweg = "CogRes_Thal" # provide a default value if unspecified

INPUT__Buffered_streamnet_semented_by_basin_boundaries_and_clipped_to_Marsh_extent =
arcpy.GetParameterAsText(1)
if INPUT__Buffered_streamnet_semented_by_basin_boundaries_and_clipped_to_Marsh_extent
==                    '#'                    or                    not
INPUT__Buffered_streamnet_semented_by_basin_boundaries_and_clipped_to_Marsh_extent:

INPUT__Buffered_streamnet_semented_by_basin_boundaries_and_clipped_to_Marsh_extent =
"CogRes_StrmBas_bufseg_clipped" # provide a default value if unspecified

INPUT__Marsh_basins = arcpy.GetParameterAsText(2)
if INPUT__Marsh_basins == '#' or not INPUT__Marsh_basins:
    INPUT__Marsh_basins = "mb9" # provide a default value if unspecified

INPUT__Segmented_stream_network = arcpy.GetParameterAsText(3)
if INPUT__Segmented_stream_network == '#' or not INPUT__Segmented_stream_network:
    INPUT__Segmented_stream_network = "CogRes_strmnt_seg" # provide a default value if
unspecified

INPUT__Cross-section_geometry_polyline = arcpy.GetParameterAsText(4)
if INPUT__Cross-section_geometry_polyline == '#' or not INPUT__Cross-
section_geometry_polyline:
    INPUT__Cross-section_geometry_polyline = "Cog2011_XSgeometry" # provide a default value
if unspecified

OUTPUT__XS_Drainage_basin_to_marsh_extent = arcpy.GetParameterAsText(5)
if OUTPUT__XS_Drainage_basin_to_marsh_extent == '#' or not
OUTPUT__XS_Drainage_basin_to_marsh_extent:
    OUTPUT__XS_Drainage_basin_to_marsh_extent = "C:\\Users\\Jennie
Graham\\Documents\\SMU\\RDT V3\\Basin\\XS\\AVBasin_%value%.shp" # provide a default
value if unspecified

OUTPUT__XS_Flowlength_to_marsh_extent = arcpy.GetParameterAsText(6)
if OUTPUT__XS_Flowlength_to_marsh_extent == '#' or not
OUTPUT__XS_Flowlength_to_marsh_extent:
    OUTPUT__XS_Flowlength_to_marsh_extent = "C:\\Users\\Jennie
Graham\\Documents\\SMU\\RDT V3\\strmnt_wrk\\XS\\AVFlwLng_%value%.shp" # provide a
default value if unspecified

Statistic_field__XS_Drainage_Area = arcpy.GetParameterAsText(7)
if Statistic_field__XS_Drainage_Area == '#' or not Statistic_field__XS_Drainage_Area:
    Statistic_field__XS_Drainage_Area = "Area SUM" # provide a default value if unspecified
```

```
Statistics_Field__Cross-section_upstream_flowlength = arcpy.GetParameterAsText(8)
if Statistics_Field__Cross-section_upstream_flowlength == '#' or not Statistics_Field__Cross-section_upstream_flowlength:
    Statistics_Field__Cross-section_upstream_flowlength = "LENGTH SUM" # provide a default value if unspecified

# Local variables:
Selected_Features = INPUT__DEM_Thalweg
Output_Layer_Name__6_ = Selected_Features
Cog2011_XSgeometry = Output_Layer_Name__6_
AV_XSgeometry__2_ = Cog2011_XSgeometry
XS_geometry_-_FlowLngth__TP__drainage_area = AV_XSgeometry__2_
Output_Layer_Name__7_ = Selected_Features
Output_Layer_Name__8_ = Output_Layer_Name__7_
Output_Layer_Name__9_ = Output_Layer_Name__7_
Value = INPUT__DEM_Thalweg
Value__5_ = OUTPUT__XS_Flowlength_to_marsh_extent
Value__4_ = OUTPUT__XS_Drainage_basin_to_marsh_extent

# Process: Iterate Feature Selection
arcpy.IterateFeatureSelection_mb(INPUT__DEM_Thalweg, "", "false")

# Process: Select Layer By Location (6)
arcpy.SelectLayerByLocation_management(INPUT__Cross-section_geometry_polyline, "INTERSECT", Selected_Features, "", "NEW_SELECTION")

# Process: Select Layer By Location (7)
arcpy.SelectLayerByLocation_management(INPUT__Buffered_streamnet_semented_by_basin_boundaries_and_clipped_to_Marsh_extent, "INTERSECT", Selected_Features, "", "NEW_SELECTION")

# Process: Select Layer By Location (8)
arcpy.SelectLayerByLocation_management(INPUT__Marsh_basins, "INTERSECT", Output_Layer_Name__7_, "", "NEW_SELECTION")

# Process: Dissolve (5)
arcpy.Dissolve_management(Output_Layer_Name__8_, OUTPUT__XS_Drainage_basin_to_marsh_extent, "", Statistic_field__XS_Drainage_Area, "MULTI_PART", "DISSOLVE_LINES")

# Process: Get Field Value (3)
arcpy.GetFieldValue_mb(OUTPUT__XS_Drainage_basin_to_marsh_extent, "SUM_Area", "String", "0")

# Process: Calculate Field (3)
```

```
arcpy.CalculateField_management(Output_Layer_Name__6_, "MXS_Basin", Value__4_, "VB", "")

# Process: Select Layer By Location (9)
arcpy.SelectLayerByLocation_management(INPUT__Segmented_stream_network, "INTERSECT", Output_Layer_Name__7_, "", "NEW_SELECTION")

# Process: Dissolve (4)
arcpy.Dissolve_management(Output_Layer_Name__9_, OUTPUT__XS_Flowlength_to_marsh_extent, "", Statistics_Field__Cross-section_upstream_flowlength, "MULTI_PART", "DISSOLVE_LINES")

# Process: Get Field Value (4)
arcpy.GetFieldValue_mb(OUTPUT__XS_Flowlength_to_marsh_extent, "SUM_LENGTH", "String", "0")

# Process: Calculate Field (4)
arcpy.CalculateField_management(Cog2011_XSgeometry, "MXS_FlwLng", Value__5_, "VB", "")

# Process: Calculate Field (5)
arcpy.CalculateField_management(AV_XSgeometry__2_, "XS_TP", "[MXS_FlwLng] * [SUM_XSA]", "VB", "")
```

***Delineate upstream drainage area, flowlength and Tidal Prism***

```
# ---------------------------------------------------------------------------
# USChannel.py
# Created on: 2012-10-30 05:22:01.00000
#   (generated by ArcGIS/ModelBuilder)
# Usage: USChannel <INPUT__Stream_network_and_basin_boundary_intersection_points_near_Thalwegs> <INPUT__DEM_Thalweg_points> <INPUT__Buffered_stream_network> <INPUT__Cross-section_polyline> <INPUT__Segmented_stream_network> <INPUT__Drainage_Basins> <INPUT__Thalweg_with_XS_geometry_attributes> <OUTPUT__Upstream_buffer> <OUTPUT__Upstream_Drainage_Basin> <OUTPUT__Upstream_Flow_Length> <OUTPUT__Upstream_tidal_prism> <Distance__value_or_field_> <INPUT__Streamnetwork-Basin_intersection_polygon> <OUTPUT__Marsh_Upstream_buffer__2_> <INPUT__Marsh_Basins> <INPUT__Buffered_stream_network_clipped_to_Marsh_extent> <OUTPUT__Marsh_Upstream_Flow_Length> <OUTPUT__Marsh_Upstream_Basin_Area>
# Description:
# ---------------------------------------------------------------------------

# Set the necessary product code
# import arcinfo
```

```
# Import arcpy module
import arcpy

# Load required toolboxes
arcpy.ImportToolbox("Model Functions")

# Script arguments
INPUT__Stream_network_and_basin_boundary_intersection_points_near_Thalwegs = arcpy.GetParameterAsText(0)
if INPUT__Stream_network_and_basin_boundary_intersection_points_near_Thalwegs == '#' or not INPUT__Stream_network_and_basin_boundary_intersection_points_near_Thalwegs:
    INPUT__Stream_network_and_basin_boundary_intersection_points_near_Thalwegs = "AV_SBint_XSonly" # provide a default value if unspecified

INPUT__DEM_Thalweg_points = arcpy.GetParameterAsText(1)
if INPUT__DEM_Thalweg_points == '#' or not INPUT__DEM_Thalweg_points:
    INPUT__DEM_Thalweg_points = "AV_Thals" # provide a default value if unspecified

INPUT__Buffered_stream_network = arcpy.GetParameterAsText(2)
if INPUT__Buffered_stream_network == '#' or not INPUT__Buffered_stream_network:
    INPUT__Buffered_stream_network = "AV_strmnt_buf" # provide a default value if unspecified

INPUT__Cross-section_polyline = arcpy.GetParameterAsText(3)
if INPUT__Cross-section_polyline == '#' or not INPUT__Cross-section_polyline:
    INPUT__Cross-section_polyline = "AV_XSgeometry" # provide a default value if unspecified

INPUT__Segmented_stream_network = arcpy.GetParameterAsText(4)
if INPUT__Segmented_stream_network == '#' or not INPUT__Segmented_stream_network:
    INPUT__Segmented_stream_network = "AV_strmnt_seg" # provide a default value if unspecified

INPUT__Drainage_Basins = arcpy.GetParameterAsText(5)
if INPUT__Drainage_Basins == '#' or not INPUT__Drainage_Basins:
    INPUT__Drainage_Basins = "Basins_AVON" # provide a default value if unspecified

INPUT__Thalweg_with_XS_geometry_attributes = arcpy.GetParameterAsText(6)
if INPUT__Thalweg_with_XS_geometry_attributes == '#' or not INPUT__Thalweg_with_XS_geometry_attributes:
    INPUT__Thalweg_with_XS_geometry_attributes = "AV_Thals_join" # provide a default value if unspecified

OUTPUT__Upstream_buffer = arcpy.GetParameterAsText(7)
if OUTPUT__Upstream_buffer == '#' or not OUTPUT__Upstream_buffer:
    OUTPUT__Upstream_buffer = "C:\\Users\\Jennie Graham\\Documents\\SMU\\RDTV3\\strmnt_wrk\\US\\AVbuf_%value%_s.shp" # provide a default value if unspecified
```

```
OUTPUT__Upstream_Drainage_Basin = arcpy.GetParameterAsText(8)
if OUTPUT__Upstream_Drainage_Basin == '#' or not OUTPUT__Upstream_Drainage_Basin:
  OUTPUT__Upstream_Drainage_Basin = "C:\\Users\\Jennie Graham\\Documents\\SMU\\RDT V3\\Basin\\US\\AV_USB_%value%.shp" # provide a default value if unspecified

OUTPUT__Upstream_Flow_Length = arcpy.GetParameterAsText(9)
if OUTPUT__Upstream_Flow_Length == '#' or not OUTPUT__Upstream_Flow_Length:
  OUTPUT__Upstream_Flow_Length = "C:\\Users\\Jennie Graham\\Documents\\SMU\\RDT V3\\strmnt_wrk\\US\\AV_USF%value%.shp" # provide a default value if unspecified

OUTPUT__Upstream_tidal_prism = arcpy.GetParameterAsText(10)
if OUTPUT__Upstream_tidal_prism == '#' or not OUTPUT__Upstream_tidal_prism:
  OUTPUT__Upstream_tidal_prism = "C:\\Users\\Jennie Graham\\Documents\\SMU\\RDT V3\\strmnt_wrk\\USTP\\AV_USTP_%value%.shp" # provide a default value if unspecified

Distance__value_or_field_ = arcpy.GetParameterAsText(11)
if Distance__value_or_field_ == '#' or not Distance__value_or_field_:
  Distance__value_or_field_ = "AV_Thals_4" # provide a default value if unspecified

INPUT__Streamnetwork-Basin_intersection_polygon = arcpy.GetParameterAsText(12)
if INPUT__Streamnetwork-Basin_intersection_polygon == '#' or not INPUT__Streamnetwork-Basin_intersection_polygon:
  INPUT__Streamnetwork-Basin_intersection_polygon = "AV_StrmBasin_splitter_s" # provide a default value if unspecified

OUTPUT__Marsh_Upstream_buffer__2_ = arcpy.GetParameterAsText(13)
if OUTPUT__Marsh_Upstream_buffer__2_ == '#' or not OUTPUT__Marsh_Upstream_buffer__2_:
  OUTPUT__Marsh_Upstream_buffer__2_ = "C:\\Users\\Jennie Graham\\Documents\\SMU\\RDT V3\\strmnt_wrk\\US\\MAVbuf_%value%_s.shp" # provide a default value if unspecified

INPUT__Marsh_Basins = arcpy.GetParameterAsText(14)
if INPUT__Marsh_Basins == '#' or not INPUT__Marsh_Basins:
  INPUT__Marsh_Basins = "AVON_Marsh" # provide a default value if unspecified

INPUT__Buffered_stream_network_clipped_to_Marsh_extent = arcpy.GetParameterAsText(15)
if INPUT__Buffered_stream_network_clipped_to_Marsh_extent == '#' or not INPUT__Buffered_stream_network_clipped_to_Marsh_extent:
  INPUT__Buffered_stream_network_clipped_to_Marsh_extent = "AV_strmnt_buf_marsh" # provide a default value if unspecified

OUTPUT__Marsh_Upstream_Flow_Length = arcpy.GetParameterAsText(16)
if OUTPUT__Marsh_Upstream_Flow_Length == '#' or not OUTPUT__Marsh_Upstream_Flow_Length:
```

```
  OUTPUT__Marsh_Upstream_Flow_Length = "C:\\Users\\Jennie Graham\\Documents\\SMU\\RDT V3\\strmnt_wrk\\US\\AV_MUSF%value%.shp" # provide a default value if unspecified

OUTPUT__Marsh_Upstream_Basin_Area = arcpy.GetParameterAsText(17)
if OUTPUT__Marsh_Upstream_Basin_Area == '#' or not OUTPUT__Marsh_Upstream_Basin_Area:
  OUTPUT__Marsh_Upstream_Basin_Area = "C:\\Users\\Jennie Graham\\Documents\\SMU\\RDT V3\\Basin\\US\\AV_MUSB_%value%.shp" # provide a default value if unspecified

# Local variables:
SBint_XSonly_Buffer1 = Distance__value_or_field_
Output_Layer_Name__2_ = SBint_XSonly_Buffer1
Output_Layer_Name__3_ = Output_Layer_Name__2_
Output_Layer_Name__4_ = Output_Layer_Name__3_
Output_Layer_Name__5_ = Output_Layer_Name__3_
Output_Layer_Name__7_ = Output_Layer_Name__3_
Output_Layer_Name__6_ = Output_Layer_Name__2_
AV_XSgeometry = Output_Layer_Name__6_
COMPLETED_CROSS_SECTIONAL_GEOMETRY__5_ = AV_XSgeometry
AV_XSgeometry__2_ = COMPLETED_CROSS_SECTIONAL_GEOMETRY__5_
XSgeometry__2_ = AV_XSgeometry__2_
FINAL_DEM_XS_GEO = XSgeometry__2_
Output_Layer_Name__8_ = Output_Layer_Name__2_
Output_Layer_Name__9_ = Output_Layer_Name__8_
Output_Layer_Name__10_ = Output_Layer_Name__8_
Output_Layer = OUTPUT__Upstream_buffer
Value__2_ = OUTPUT__Upstream_Flow_Length
Value__3_ = OUTPUT__Upstream_Drainage_Basin
Value__4_ = OUTPUT__Upstream_tidal_prism
Selected_Features = INPUT__Stream_network_and_basin_boundary_intersection_points_near_Thalwegs
SCStrmBasin_splitter_s = Selected_Features
US_buf_shp = SCStrmBasin_splitter_s
MUS_buf_shp = SCStrmBasin_splitter_s
Value = INPUT__Stream_network_and_basin_boundary_intersection_points_near_Thalwegs
Output_Layer__2_ = OUTPUT__Marsh_Upstream_buffer__2_
Value__5_ = OUTPUT__Marsh_Upstream_Flow_Length
Value__6_ = OUTPUT__Marsh_Upstream_Basin_Area

# Process: Iterate Feature Selection
arcpy.IterateFeatureSelection_mb(INPUT__Stream_network_and_basin_boundary_intersection_points_near_Thalwegs, "", "false")

# Process: Buffer
```

```
arcpy.Buffer_analysis(Selected_Features, SBint_XSonly_Buffer1, Distance__value_or_field_, "FULL", "ROUND", "NONE", "")

# Process: Select Layer By Location (2)
arcpy.SelectLayerByLocation_management(INPUT__DEM_Thalweg_points, "INTERSECT", SBint_XSonly_Buffer1, "", "NEW_SELECTION")

# Process: Select Layer By Location (6)
arcpy.SelectLayerByLocation_management(INPUT__Cross-section_polyline, "INTERSECT", Output_Layer_Name__2_, "", "NEW_SELECTION")

# Process: Select Layer By Location
arcpy.SelectLayerByLocation_management(INPUT__Streamnetwork-Basin_intersection_polygon, "INTERSECT", Selected_Features, "", "NEW_SELECTION")

# Process: Symmetrical Difference (2)
arcpy.SymDiff_analysis(INPUT__Buffered_stream_network_clipped_to_Marsh_extent, SCStrmBasin_splitter_s, MUS_buf_shp, "ALL", "")

# Process: Multipart To Singlepart (2)
arcpy.MultipartToSinglepart_management(MUS_buf_shp, OUTPUT__Marsh_Upstream_buffer__2_)

# Process: Make Feature Layer (2)
arcpy.MakeFeatureLayer_management(OUTPUT__Marsh_Upstream_buffer__2_, Output_Layer__2_, "", "", "FID FID VISIBLE NONE;FID_AV_str FID_AV_str VISIBLE NONE;Shape Shape VISIBLE NONE;Id Id VISIBLE NONE;FID_AV_S_1 FID_AV_S_1 VISIBLE NONE;FID_honeyc FID_honeyc VISIBLE NONE;LEFT_FID LEFT_FID VISIBLE NONE;RIGHT_FID RIGHT_FID VISIBLE NONE;BUFF_DIST BUFF_DIST VISIBLE NONE;FID_AV_s_2 FID_AV_s_2 VISIBLE NONE;Id_1 Id_1 VISIBLE NONE;ORIG_FID ORIG_FID VISIBLE NONE")

# Process: Select Layer By Location (8)
arcpy.SelectLayerByLocation_management(Output_Layer__2_, "INTERSECT", Output_Layer_Name__2_, "", "NEW_SELECTION")

# Process: Select Layer By Location (9)
arcpy.SelectLayerByLocation_management(INPUT__Segmented_stream_network, "INTERSECT", Output_Layer_Name__8_, "", "NEW_SELECTION")

# Process: Dissolve (5)
arcpy.Dissolve_management(Output_Layer_Name__9_, OUTPUT__Marsh_Upstream_Flow_Length, "", "LENGTH SUM", "MULTI_PART", "DISSOLVE_LINES")

# Process: Get Field Value (4)
```

```
arcpy.GetFieldValue_mb(OUTPUT__Marsh_Upstream_Flow_Length, "SUM_LENGTH", "String", "0")

# Process: Calculate Field (4)
arcpy.CalculateField_management(Output_Layer_Name__6_, "MUS_FlwLng", Value__5_, "VB", "")

# Process: Symmetrical Difference
arcpy.SymDiff_analysis(INPUT__Buffered_stream_network, SCStrmBasin_splitter_s, US_buf_shp, "ALL", "")

# Process: Multipart To Singlepart
arcpy.MultipartToSinglepart_management(US_buf_shp, OUTPUT__Upstream_buffer)

# Process: Make Feature Layer
arcpy.MakeFeatureLayer_management(OUTPUT__Upstream_buffer, Output_Layer, "", "", "FID FID VISIBLE NONE;FID_AV_str FID_AV_str VISIBLE NONE;Shape Shape VISIBLE NONE;Id Id VISIBLE NONE;FID_AV_S_1 FID_AV_S_1 VISIBLE NONE;FID_honeyc FID_honeyc VISIBLE NONE;LEFT_FID LEFT_FID VISIBLE NONE;RIGHT_FID RIGHT_FID VISIBLE NONE;BUFF_DIST BUFF_DIST VISIBLE NONE;FID_AV_s_2 FID_AV_s_2 VISIBLE NONE;Id_1 Id_1 VISIBLE NONE;ORIG_FID ORIG_FID VISIBLE NONE")

# Process: Select Layer By Location (3)
arcpy.SelectLayerByLocation_management(Output_Layer, "INTERSECT", Output_Layer_Name__2_, "", "NEW_SELECTION")

# Process: Select Layer By Location (5)
arcpy.SelectLayerByLocation_management(INPUT__Segmented_stream_network, "INTERSECT", Output_Layer_Name__3_, "", "NEW_SELECTION")

# Process: Dissolve (2)
arcpy.Dissolve_management(Output_Layer_Name__5_, OUTPUT__Upstream_Flow_Length, "", "LENGTH SUM", "MULTI_PART", "DISSOLVE_LINES")

# Process: Get Field Value
arcpy.GetFieldValue_mb(OUTPUT__Upstream_Flow_Length, "SUM_LENGTH", "String", "0")

# Process: Calculate Field
arcpy.CalculateField_management(AV_XSgeometry, "US_FlwLng", Value__2_, "VB", "")

# Process: Select Layer By Location (10)
arcpy.SelectLayerByLocation_management(INPUT__Marsh_Basins, "INTERSECT", Output_Layer_Name__8_, "", "NEW_SELECTION")

# Process: Dissolve (6)
```

```
arcpy.Dissolve_management(Output_Layer_Name__10_,
OUTPUT__Marsh_Upstream_Basin_Area, "", "Area SUM", "MULTI_PART", "DISSOLVE_LINES")

# Process: Get Field Value (5)
arcpy.GetFieldValue_mb(OUTPUT__Marsh_Upstream_Basin_Area, "SUM_Area", "String", "0")

# Process: Calculate Field (5)
arcpy.CalculateField_management(COMPLETED_CROSS_SECTIONAL_GEOMETRY__5_,
"MUS_Area", Value__6_, "VB", "")

# Process: Select Layer By Location (4)
arcpy.SelectLayerByLocation_management(INPUT__Drainage_Basins,                "INTERSECT",
Output_Layer_Name__3_, "", "NEW_SELECTION")

# Process: Dissolve (3)
arcpy.Dissolve_management(Output_Layer_Name__4_,    OUTPUT__Upstream_Drainage_Basin,
"", "Area SUM", "MULTI_PART", "DISSOLVE_LINES")

# Process: Get Field Value (2)
arcpy.GetFieldValue_mb(OUTPUT__Upstream_Drainage_Basin, "SUM_Area", "String", "0")

# Process: Calculate Field (2)
arcpy.CalculateField_management(AV_XSgeometry__2_, "US_area", Value__3_, "VB", "")

# Process: Select Layer By Location (7)
arcpy.SelectLayerByLocation_management(INPUT__Thalweg_with_XS_geometry_attributes,
"INTERSECT", Output_Layer_Name__3_, "", "NEW_SELECTION")

# Process: Dissolve (4)
arcpy.Dissolve_management(Output_Layer_Name__7_,    OUTPUT__Upstream_tidal_prism,    "",
"XS_TP SUM", "MULTI_PART", "DISSOLVE_LINES")

# Process: Get Field Value (3)
arcpy.GetFieldValue_mb(OUTPUT__Upstream_tidal_prism, "SUM_XS_TP", "String", "0")

# Process: Calculate Field (3)
arcpy.CalculateField_management(XSgeometry__2_, "US_TP", Value__4_, "VB", "")
```

***Calculate creek sinuosiity, order, and longitudinal slopes***

```
# ---------------------------------------------------------------------------
# Sinuosity.py
# Created on: 2012-10-30 05:22:38.00000
#   (generated by ArcGIS/ModelBuilder)
# Usage: Sinuosity <INPUT__Ordered_Stream_Network_Polyline> <INPUT__DEM> <OUTPUT__Z-
aware_Stream_Network_Polyline>                <INPUT__Coss-section_Geometry_Polyline>
```

```
<OUTPUT__Completed_Cross-section_Geometry_Polyline> <Win2Straight_shp>
<Win2Strmnt_BEpts_shp> <Sinuosity_Field_Name> <Expression>
# Description:
# ---------------------------------------------------------------------------

# Set the necessary product code
# import arcinfo


# Import arcpy module
import arcpy

# Check out any necessary licenses
arcpy.CheckOutExtension("3D")

# Script arguments
INPUT__Ordered_Stream_Network_Polyline = arcpy.GetParameterAsText(0)
if INPUT__Ordered_Stream_Network_Polyline == '#' or not
INPUT__Ordered_Stream_Network_Polyline:
  INPUT__Ordered_Stream_Network_Polyline = "Win2_strmnt_ordr" # provide a default value
if unspecified

INPUT__DEM = arcpy.GetParameterAsText(1)
if INPUT__DEM == '#' or not INPUT__DEM:
  INPUT__DEM = "Win2DEM" # provide a default value if unspecified

OUTPUT__Z-aware_Stream_Network_Polyline = arcpy.GetParameterAsText(2)
if OUTPUT__Z-aware_Stream_Network_Polyline == '#' or not OUTPUT__Z-
aware_Stream_Network_Polyline:
  OUTPUT__Z-aware_Stream_Network_Polyline = "C:\\Users\\Jennie
Graham\\Documents\\SMU\\RDT V3\\Thalwegs\\Win2_strmnt_ordr_z.shp" # provide a default
value if unspecified

INPUT__Coss-section_Geometry_Polyline = arcpy.GetParameterAsText(3)
if INPUT__Coss-section_Geometry_Polyline == '#' or not INPUT__Coss-
section_Geometry_Polyline:
  INPUT__Coss-section_Geometry_Polyline = "XSgeometry" # provide a default value if
unspecified

OUTPUT__Completed_Cross-section_Geometry_Polyline = arcpy.GetParameterAsText(4)
if OUTPUT__Completed_Cross-section_Geometry_Polyline == '#' or not
OUTPUT__Completed_Cross-section_Geometry_Polyline:
  OUTPUT__Completed_Cross-section_Geometry_Polyline = "C:\\Users\\Jennie
Graham\\Documents\\SMU\\RDT V3\\Geometry\\Win2_XSgeometry_final.shp" # provide a
default value if unspecified
```

```
Win2Straight_shp = arcpy.GetParameterAsText(5)
if Win2Straight_shp == '#' or not Win2Straight_shp:
  Win2Straight_shp = "C:\\Users\\Jennie Graham\\Documents\\SMU\\RDT V3\\Sinuosity\\Win2Straight.shp" # provide a default value if unspecified

Win2Strmnt_BEpts_shp = arcpy.GetParameterAsText(6)
if Win2Strmnt_BEpts_shp == '#' or not Win2Strmnt_BEpts_shp:
  Win2Strmnt_BEpts_shp = "C:\\Users\\Jennie Graham\\Documents\\SMU\\RDT V3\\Sinuosity\\Win2Strmnt_BEpts.shp" # provide a default value if unspecified

Sinuosity_Field_Name = arcpy.GetParameterAsText(7)
if Sinuosity_Field_Name == '#' or not Sinuosity_Field_Name:
  Sinuosity_Field_Name = "Win2_strmnt_ordr_z.Sinuosity" # provide a default value if unspecified

Expression = arcpy.GetParameterAsText(8)
if Expression == '#' or not Expression:
  Expression = "[Win2_strmnt_ordr_z.Length_T] / [Win2Straight.Length_S]" # provide a default value if unspecified

# Local variables:
win1_dem_InterpolateShape = OUTPUT__Z-aware_Stream_Network_Polyline
Win1_strmnt_ordr_z_shp__3_ = win1_dem_InterpolateShape
Win1_strmnt_ordr_z_shp__4_ = Win1_strmnt_ordr_z_shp__3_
Win1_strmnt_ordr_z_shp__7_ = Win1_strmnt_ordr_z_shp__4_
Output_Layer = Win1_strmnt_ordr_z_shp__7_
Win1_strmnt_ordr_z_Layer = Output_Layer
KEN_strmnt_ordr_z4_Layer = Win1_strmnt_ordr_z_Layer
Straight_shp__2_ = Win2Straight_shp
Straight_shp__4_ = Straight_shp__2_
Straight_shp__3_ = Straight_shp__4_

# Process: Interpolate Shape
arcpy.InterpolateShape_3d(INPUT__DEM, INPUT__Ordered_Stream_Network_Polyline, OUTPUT__Z-aware_Stream_Network_Polyline, "", "1", "BILINEAR", "DENSIFY", "0")

# Process: Add Z Information
arcpy.AddZInformation_3d(OUTPUT__Z-aware_Stream_Network_Polyline, "Z_MIN;Z_MAX;LENGTH_3D;MIN_SLOPE;MAX_SLOPE;AVG_SLOPE", "NO_FILTER")

# Process: Add Field
arcpy.AddField_management(win1_dem_InterpolateShape, "Length_T", "FLOAT", "", "", "", "", "NON_NULLABLE", "NON_REQUIRED", "")

# Process: Calculate Field
```

```
arcpy.CalculateField_management(Win1_strmnt_ordr_z_shp__3_, "Length_T", "!shape.length@meters!", "PYTHON_9.3", "")

# Process: Add Field (3)
arcpy.AddField_management(Win1_strmnt_ordr_z_shp__4_, "Sinuosity", "FLOAT", "", "", "", "", "NON_NULLABLE", "NON_REQUIRED", "")

# Process: Make Feature Layer
arcpy.MakeFeatureLayer_management(Win1_strmnt_ordr_z_shp__7_, Output_Layer, "", "", "FID FID VISIBLE NONE;Shape Shape VISIBLE NONE;ARCID ARCID VISIBLE NONE;GRID_CODE GRID_CODE VISIBLE NONE;FROM_NODE FROM_NODE VISIBLE NONE;TO_NODE TO_NODE VISIBLE NONE;Z_Min Z_Min VISIBLE NONE;Z_Max Z_Max VISIBLE NONE;Length3D Length3D VISIBLE NONE;Min_Slope Min_Slope VISIBLE NONE;Max_Slope Max_Slope VISIBLE NONE;Avg_Slope Avg_Slope VISIBLE NONE;Length_T Length_T VISIBLE NONE;Sinuosity Sinuosity VISIBLE NONE")

# Process: Feature Vertices To Points
arcpy.FeatureVerticesToPoints_management(win1_dem_InterpolateShape, Win2Strmnt_BEpts_shp, "BOTH_ENDS")

# Process: Points To Line
arcpy.PointsToLine_management(Win2Strmnt_BEpts_shp, Win2Straight_shp, "ORIG_FID", "", "NO_CLOSE")

# Process: Add Field (2)
arcpy.AddField_management(Win2Straight_shp, "Length_S", "FLOAT", "", "", "", "", "NON_NULLABLE", "NON_REQUIRED", "")

# Process: Calculate Field (2)
arcpy.CalculateField_management(Straight_shp__2_, "Length_S", "!shape.length@meters!", "PYTHON_9.3", "")

# Process: Add Attribute Index
arcpy.AddIndex_management(Straight_shp__4_, "ORIG_FID", "", "NON_UNIQUE", "NON_ASCENDING")

# Process: Add Join
arcpy.AddJoin_management(Output_Layer, "FID", Straight_shp__3_, "ORIG_FID", "KEEP_ALL")

# Process: Calculate Field (3)
arcpy.CalculateField_management(Win1_strmnt_ordr_z_Layer, Sinuosity_Field_Name, Expression, "VB", "")

# Process: Spatial Join
```

```
arcpy.SpatialJoin_analysis(INPUT__Coss-section_Geometry_Polyline,
KEN_strmnt_ordr_z4_Layer, OUTPUT__Completed_Cross-section_Geometry_Polyline,
"JOIN_ONE_TO_ONE", "KEEP_ALL", "", "INTERSECT", "", "")
```